HIPPOCAMPAL CIRCADIAN RHYTHMS IN TEMPORAL LOBE EPILEPSY

By

DAVID ARTHUR STANLEY

A DISSERTATION PRESENTED TO THE GRADUATE SCHOOL
OF THE UNIVERSITY OF FLORIDA IN PARTIAL FULFILLMENT
OF THE REQUIREMENTS FOR THE DEGREE OF
DOCTOR OF PHILOSOPHY

UNIVERSITY OF FLORIDA

2013

To my parents, Jan and Leonard, and my brother, Geoffrey

ACKNOWLEDGMENTS

First and foremost, I would like to thank my mentors, Dr. Paul Carney, Dr. William Ditto, and Dr. Sachin Talathi. They provided me with guidance throughout my studies and were fully dedicated to enabling me to succeed as a researcher. They held me to the highest standards of scholarly work. For the phone calls, Skype meetings, and passionate scientific debates, many of which carried on late into the evenings, I am most sincerely grateful. I also wish to acknowledge my committee members and collaborators at Arizona State University and the University of Florida who provided outstanding feedback and advice throughout my PhD: Dr. Kevin Bennett, Dr. John Harris, Dr. Leonidas Iasemidis, Dr. Pramod Khargonekar, Dr. Mark L. Spano, and Dr. Stephen Helms Tillery.

I have many people to thank for where I am today. My elementary school friend Carson Mok encouraged me to become interested in mathematics at a young age. Mr. Colin Wackett, my Grade 8 teacher at Mount Albert, was very inspirational and instilled in me a love of learning. I have to thank my subsequent math and science teachers at Dr. John M. Denison for their instruction and for organizing the Math and Science Olympics teams, including Mrs. S. Dalrymple, Mrs. C. MacIsaac, Mr. Olav Randoja, Mr. Churchill, Mr. Law, and Mr. Darren Lluoma. I am also indebted to Mr. Oberfrank for his guidance throughout OAC English.

I had several mentors at the University of Toronto, including Dr. Peter H. Backx, who took me into his top caliber cardiac electrophysiology lab when I was still a high school student and who exposed me to scientific research for the first time. I also must thank Dr. Mark Jellinek and Dr. Nazir P. Kherani for inviting me into their labs and for providing me with further early exposure to scientific research. Dr. Mark Jellinek supervised my research on the physics of viscous mixing during the summer of 2004. Dr. Nazir Kherani supervised my Engineering Science Bachelor's thesis research, and helped me prepare and publish my first research paper. I am also very grateful for my opportunity to work

with Dr. Martin Renqiang Min. He taught me what I know about machine learning, and I deeply enjoyed our collaboration. Finally, I owe sincerest gratitude to my Master's advisor, Dr. Berj Bardakjian, for encouraging me to enter the field of computational neuroscience. While I was always interested in the brain, his animated classroom lectures revealed the beautiful mathematics that underlie its function. He has been a superb teacher, mentor and friend.

While I was at the University of Toronto, my friend Ernest Ho was completing his PhD in neuroscience and taught me many important lessons during our dinnertime conversations. He also provided valuable feedback on my work and inspired much of my writing style for this thesis – I will pay homage where possible. Of my many Canadian friends, Shawn Brown, Grisha Boyko-Vekin, Lorne Chi, Sinisa Colic, Josh Dian, Saigin Govender, Cynthia Long, Kirk Hooper, Jerome Hu, Stephen Hutchison, Sara Krowicki, Ryan Janzen, Michael Simmonds, and Trista Hurley-Waxali have all shaped this work in specific ways. Despite my leaving Canada, I am very grateful that you have remained in touch and have supported me throughout my PhD. I also wish to acknowledge my close friends from Arizona State University, Anna Dari, Behnam Kia, David Guffrey, and Srinidhi Kuntaegowdanahalli, for their support, advice, and wit. Very special thanks go to Pengpeng Cao for being an amazing friend and for always being there (especially with our "interlibrary loans").

Following my move to the University of Florida, I found a new home amongst a new group of colleagues. I wish to thank Eric Bennett, Fernando Delgado, Francisco Casanova, Rob Castellucci, Sonam Chheda, Diana Gu, Maria Houria, Svetlana Kantorovich, Qianying Lin, Gowri Natarajan, Mansi Parekh, Ali Piracha, Stefano Re Fraschini, Matt Shore, Deguang Wang, Rabia Zafar, Rujuta Munje, Claire Cox, A. M. Merel Boers, and Junli Zhou for their friendship and advice. Also, special thanks to Mansi for her help and tutelage with MRI analysis, Eric for helping me get set up in

Gainesville, and Tifiny McDonald for surmounting all the barriers to my transferring to UF.

Finally, this work would have not been possible without the support of my family. My spectacular mother, Janet, spent countless hours exposing me at a young age to myriad math problems, brain teasers, puzzles, and literary works. She also did her best to educate me musically by teaching me piano, and continues to edit my papers to this day. My father, Leonard, helped me pursue my childhood passion for disassembling various electronic devices, which I suspect relates to my interest in dynamical systems. He has always kept a watchful eye on the big picture and has provided me with insightful guidance throughout my life. To Uncle Steve, thank you for your support and encouragement, for sharing your love of puzzles, and for “taking me to school” me at cards. To my grandparents, Sally and Jim, you gave me a great childhood and inspired me to live a fulfilling and balanced life according to strong core values. It is for you that I will “believe in all I can achieve.” I have come to realize that it largely traces back to my late Grandpa Stan that I am now pursuing an academic career. I am grateful to my late Grandma Barbara for all her kindness and for the value she placed on education. My late Grandpa Art had epilepsy himself. Although I did not know him, he has largely shaped who I am today. Finally, to my brother Geoffrey, you think deeply and you are bound to accomplish great things. I can always depend on you and look forward to the future and all its adventures. Let’s “try for the sun.”

In addition to my friends and mentors, none of this work would have been possible without funding. I am deeply grateful to the funding agencies who supported my PhD studies, in particular, the National Sciences and Engineering Research Council of Canada (NSERC), the National Institutes of Health (NIH), and the Office of Naval Research (ONR). Additionally, both the Queen Elizabeth II Aiming for the Top Scholarship and the Heart and Stroke Foundation helped to fund my exposure to research prior to beginning my PhD.

Research in many biological fields involves the use and sacrifice of animals, and ethical arguments can be made both for and against animal experimentation. This work did not involve the direct sacrifice of animals; however, it did benefit from data collected in previous animal studies. I am grateful to those who provided me with experimental data, including Daniel Cordiner, Dr. Dong-Uk Hwang, Dr. Wendy Norman, Dr. Mansi Parekh, Dr. Sachin S. Talathi, and Dr. Junli Zhou, and I am respectful for the animals sacrificed to provide this data.

Much of the modeling work done in this thesis was made possible by the open-source GENESIS software package developed by Dave Beeman and James Bower. This thesis is typeset in LaTeX2ϵ. References were imported to BibTex using BIBTEXFORMAT, an incredibly useful tool written by Ben Bulheller. Images were processed using GIMP. Will M. D. Foe provided the LaTeXtemplate that is used in writing this thesis.

TABLE OF CONTENTS

LIST OF TABLES

LIST OF FIGURES

Abstract of Dissertation Presented to the Graduate School
of the University of Florida in Partial Fulfillment of the
Requirements for the Degree of Doctor of Philosophy

HIPPOCAMPAL CIRCADIAN RHYTHMS IN TEMPORAL LOBE EPILEPSY

By

David Arthur Stanley

August 2013

Chair: Paul R. Carney
Cochair: Sachin S. Talathi
Major: Biomedical Engineering

For over a century epileptic seizures have been known to cluster at specific times of the day. Recent studies have suggested that the circadian regulatory system may become permanently altered in epilepsy, but little is known about how this affects neural activity and the daily patterns of seizure recurrence. To investigate, we tracked long-term changes in the rate of spontaneous hippocampal EEG spikes (SPKs) in a rat model of temporal lobe epilepsy. In healthy animals, SPKs oscillated with near 24-hour period; however, following injury by status epilepticus (SE), a persistent phase shift of approximately 12 hours emerged in animals that later went on to develop chronic spontaneous seizures. Additional measurements showed that this phase shift affected other features of hippocampal activity, including 24-hour modulation of gamma- and beta-frequency rhythms, but did not affect global 24-hour rhythms, including core body temperature and theta state transitions. Based on this, we hypothesized that the phase shift might be due to locally impaired circadian input to the hippocampus. This was investigated using a biophysical computer model in which we showed that subtle changes in the relative strengths of circadian inputs could produce a phase shift in hippocampal neural activity. Additional EEG analysis provided evidence for altered circadian input strengths by showing that the amplitude of 24-hour modulation of certain EEG rhythms, particularly hippocampal theta, was attenuated following SE injury. Furthermore, MRI provided evidence that the medial septum, a putative circadian

relay center, exhibited signs of damage and therefore could contribute to local circadian impairment. Our results suggest that balanced circadian input is critical to maintaining natural circadian phase in the hippocampus, and that damage to the medial septum may disrupt this balance.

CHAPTER 1
INTRODUCTION

"Now sailors all take my advice — Let steamships be your motta — And never go to sea again — In the sailing ship Calcutta!" This was written by John Fisher at age 14, a midshipman-to-be aboard the Calcutta. During the course of his life (1841-1920) seafaring vessels experienced a monumental transformation, from wooden ships propelled by sails to steel-hulled ships driven by steam turbines. The British Navy of the time, being an old and immensely successful organization, was highly resistant to such change; indeed, a standard navy instruction book states: "There is no greater fallacy than to suppose that ships can be navigated on long voyages without masts and sails" [Nares, 1868].

For Fisher, however, it was a time of innovation. He felt no nostalgia for the sailing ships of Nelson's time, and instead sought to leverage the technological advances of the industrial revolution to their fullest potential. He proposed using the internal combustion engine, as opposed to steam boilers, to power ship turbines. He predicted the importance (and threat) of submarine technology, which was perceived by his contemporaries as "underhanded, unfair, and damned un-English" [Morris, 2010]. Early in his career, he published a paper on electric torpedo guidance [Fisher, 1871]. He was an enthusiast for aviation and the father of the 1906 Dreadnought, which set the template for 20th century battleship design. He envisioned an oil pipeline under the English channel, a project that came to fruition in 1944 when it was used to supply troops in Normandy.[1]

The revolution in naval architecture during Fisher's time mirrors the connection often seen in the sciences, whereby scientific discoveries are linked to advances in equipment

[1] An engaging account of Admiral John Fisher's life, beyond his technical work, is provided by Morris [2010].

or technique. Classical examples include Galileo's telescope, which led to the discovery of Jupiter's moons, and Ramon y Cajal's employment of silver staining, which yielded the fundamental tenets of neuroscience. Fisher himself understood the disruptive nature of technology and the danger of resisting change. He is remembered today as perhaps the second most important figure in British naval history, after Lord Nelson. Importantly, despite reaching the highest ranks of the admiralty, his renown is not for his role in naval engagements, but rather for his forward-thinking reforms. This underscores the importance of his role as an early promoter of technical innovation.

Presently, the field of neuroscience is entering a period of diversification. Its mainstay technique of electrophysiological recording has remained relatively unchanged for over 50 years, with the notable exception of patch clamping developments in the 1980s. Now however, with advances in cell biology, new suites of optical and molecular techniques are enabling the study of neurons with greater resolution and specificity than previously possible. The burgeoning field of synthetic biology is hoped to present sophisticated ways to interact with neurons on cellular and molecular levels.[2] Ambitious hardware projects seek to engineer high density electrode recording arrays. Non-invasive brain imaging is improving rapidly, and has shown a trend of doubling its resolution every twelve months [Kurzweil, 2005]. These developments have necessitated the creation of new mathematical models [Truccolo et al., 2005] and have refined existing models by allowing improved measurement of model parameters [Gerstner and Naud, 2009]. Together, these advances have recently prompted both

[2] Synthetic biology, which aims to develop standardized methods and components for constructing biological systems, has been compared to the development of standardized parts and processes that occurred, for example, during the industrial revolution and, more recently, during the semiconductor revolution [Baker et al., 2006]. With such aspirations, the 21st century has been optimistically dubbed the "century of biology," following of the century of chemistry (19th century) and the century of physics (20th century). The historical origin of these terms is discussed by Hingston et al. [2008].

American and European initiatives to better understand the brain and neurological disease. Like the industrial revolution of Fisher's time, these novel techniques are greatly transforming the field of neuroscience.

The research presented in this dissertation follows the theme of leveraging new technology. As we have witnessed over the last decade, improvements in computer processing power and storage capacity have been impressive, and this has made it feasible to collect and analyze vast amounts of neural data. In fact, it is now possible to track millisecond timescale action potentials, the fundamental units of neural activity, continuously over days and even weeks. This makes slow timescale processes, such as 24-hour circadian rhythms, attractive targets of study. Slow rhythms have been examined extensively in isolation, but relatively little is known about how they interact with other brain functions, especially in relation to disease. In this thesis we will examine 24-hour oscillations in the brain, and we will study them within the context of epilepsy, a pathology that exhibits both rapid electroencephalogram abnormalities and also slow timescale evolution. It is our modest hope that this work will encourage further exploration of slow timescale processes, alongside those more traditionally studied in neuroscience, leading to an improved understanding of the relationship between these vastly different timescales. More generally, we hope that this work will convey to the reader a sense of excitement for the potential of technology to extend the frontiers of neuroscience research in the coming years.

CHAPTER 2
BACKGROUND AND HYPOTHESIS

2.1 Why Study Epilepsy?

Epilepsy is one of the oldest diseases known to humanity, having been described over 2000 years ago in Babylonian stone tablet inscriptions [Reynolds and Wilson, 2008, Wilson and Reynolds, 1990].[1] These tablets are part of a series called the *Sakikku*, an anthology of disease that dates as early as 718 B.C.E. The script on these tablets provides a rigorous description of many classical symptoms of epilepsy, including paranoia, hallucinations, and mood disorders. In addition, these scripts attempt to explain the underlying source of the epileptic attacks, attributing them to demons and other supernatural forces. Many ancient Greeks shared this belief about the mystical nature of epilepsy, and referred to it as the "sacred disease." However, a refutation of this mysticism is provided by a treatise in the Hippocratic Corpus:

> "Men regard its nature and cause as divine from ignorance and wonder, because it is not at all like to other diseases. And this notion of its divinity is kept up by their inability to comprehend it ... But if it is reckoned divine because it is wonderful, instead of one there are many diseases which would be sacred; for, as I will show, there are others no less wonderful and prodigious, which nobody imagines to be sacred." [2]

Importantly, it has been argued that this refutation may be one of the earliest recorded distinctions between mysticism and science [Riggs and Riggs, 2005].

[1] Parts of this chapter are in press with the Journal of Neurophysiology: Stanley, D.A., Talathi, S.S., Parekh, M.B., Cordiner, D., Zhou, J., Mareci, T.H., Ditto, W.L., Carney, P.R. Local phase shift in the 24-hour rhythm of hippocampal EEG spiking activity in a rat model of temporal lobe epilepsy [Stanley et al., 2013].

[2] From *On the Sacred Disease*, a part of the Hippocratic Corpus, translated by Francis Adams and published by Kaplan [Fischer, 2008].

It is appropriate that epilepsy was at the centre of this early debate on the distinction between mysticism and science. Indeed, it is still a matter of debate today as to whether operations of the brain, particularly the generation of the conscious experience, is within the scope of scientific theory. It seems difficult to imagine how a collection of atoms obeying the laws of physics could give rise to the subjective experience [Ho, 2011].[3] While research on the neural basis of consciousness is progressing,[4] this is still very much an open question. Epilepsy is often referred to as the model disease to study for purposes of understanding the brain. In particular, research into the loss of consciousness accompanying certain types of epileptic seizures may yield critical insights to these questions.

In addition to the desire to understand the brain, many scientists choose to study epilepsy due to the demand for treatment. Epilepsy is the third most common neurological disorder after stroke and Alzheimer's disease [Hirtz et al., 2007], with one in 26 people developing epilepsy at some point in their lives, and one in 10 people experiencing a seizure. Overall, approximately 30-40% of epilepsy cases are refractory to present pharmacological therapy [Kwan and Brodie, 2000]. For those patients that are successfully treated, there are numerous side effects with which they must contend. Epileptics are more likely to suffer from mental and cognitive deficits, and can also experience sleep disorders and other comorbidities that diminish their quality of life.

It is difficult to assess and quantify the societal impacts of epilepsy. One approach is to examine the direct and indirect monetary costs associated with the disease. A major study by Begley et al. [2000] estimates the projected annual cost of epilepsy in the US

[3] Chalmers [1995] comments that any physical explanation for an experience, for example, of the colour red, suffers the criticism that such a physical process could also occur in the absence of such an experience.

[4] Nobel laureate Francis Crick dedicated much of his later life to developing a framework for studying consciousness [Crick and Koch, 2003].

is in excess of $12.5 billion. Importantly, indirect costs, such as comorbid diseases and socioeconomic effects, including foregone earnings, house care, and unemployment, account for 85% of these costs.[5] Given the magnitude of these indirect costs, even therapies that do not outright cure the seizures, but rather make them more manageable or mitigate treatment side effects, can have a large impact on reducing expenditures and on improving quality of life.

The research presented in this dissertation focuses on the fundamental mechanisms associated with epilepsy. While this work may someday be important for developing a cure, the more immediate implications will be for tackling these indirect costs and side effects, such as improving seizure predictability. A detailed discussion of implications of this work will be provided in subsequent chapters.

2.2 Epilepsy Overview

2.2.1 Seizure Types

Epilepsy is a neurological disorder characterized by recurrent spontaneous seizures. A seizure is defined as an abnormal synchronous discharge of neural activity in the brain. Epileptic seizures may be either partial (also known as focal) or generalized. Partial seizures exhibit a localized site of onset, whereas generalized seizures are distributed. Partial seizures can be either simple or complex, depending whether or not a loss of consciousness occurs. They may also exhibit secondary generalization, progressing to involve the whole cortex.

2.2.2 Classification of Epilepsies

The most common epilepsy classification scheme was proposed by the International League Against Epilepsy (ILEA) in 1981 [ILEA, 1981]. This scheme involves classifying

[5] Lower percentages for indirect costs have been reported outside of the US. Strzelczyk et al. [2008] have compiled the results of 22 studies from a variety of geographic regions.

epilepsy syndromes based on seizure localization, specifically whether the seizure is localized (partial, focal seizures) or generalized. A third category is reserved for seizures that are unclassified, either because of inadequate data, or because of some attributes that defy classification into either of the two aforementioned groups. This classification was revised by ILEA in 1989 into a dual-axis classification scheme, with one axis describing localization, as above, and the other axis describing etiology [ILEA, 1989]. For the first axis, an epileptic syndrome may be either 1) localization-related (local, partial, or focal), 2) generalized, 3) special (such as situation-related seizures), or 4) undetermined whether focal or generalized. For the second axis, an epileptic syndrome may be A) idiopathic (age-related, usually of genetic inheritance), B) symptomatic involving a known injury, or C) cryptogenic. Cryptogenic epilepsies are epilepsies for which the etiology is unknown. They are presumed to be symptomatic, but they are also age-related. Localization-related symptomatic epilepsies (category 1-B) include common epilepsy syndromes such as temporal, parietal, frontal, and occipital lobe epilepsies. Absence epilepsies typically fall into category 2-A, generalized idiopathic syndromes. Certain instances of Lennox-Gastaut syndrome are considered cryptogenic [ILEA, 1989].

2.2.3 Etiology

The underlying etiology of epilepsy is varied. Hereditary epilepsies have been associated with specific protein mutations, including individual voltage-gated and ligand-gated channels [Biervert et al., 1998, Meisler et al., 2005]. These mutations alter neuronal properties, often making them hyperexcitable. On the other hand, approximately 40% of epilepsies are acquired through injury to the nervous system [Hauser and Hesdorffer, 1990, Raza et al., 2004]. In such cases the brain enters a silent period lasting months or years following the initial insult [Angeleri et al., 1999, Aroniadou-Anderjaska et al., 2008]. This is referred to as the *latency* period of epilepsy. During this time seizures do not occur but underlying pathological processes are at

work, eventually culminating in the emergence of recurrent spontaneous seizures. Following injury and throughout the latency period, the brain is said to be in a state of *epileptogenesis*. Epileptogenic processes may continue to occur even after the beginning of chronic seizures.

The precise mechanisms that cause the healthy brain to transition to the epileptic state are unknown. On a most general level, epileptic seizures are thought to result from an imbalance between excitation and inhibition [El-Hassar et al., 2007, Sloviter, 2005].[6] This imbalance may result from a number of mechanisms, for example, sprouting of recurrent excitatory connections, loss of inhibitory cells, disinhibition (i.e. inhibition of inhibitory cells), changes in receptor density, and inhibitory-driven hyper-synchrony. These concepts are summarized in detail in a number of review articles [Briggs and Galanopoulou, 2011, Dudek and Spitz, 1997]. Epileptic seizures may be dependent not only on local changes in excitability, but also on interaction amongst many distant brain regions. For example, it has been proposed that, even in the case of epilepsies classified as focal, multiple disparate brain regions must be connected for the seizure to occur [Bertram, 2009]. This involvement of multiple sites may explain the recurrence of seizures years later following resection of what was once considered the primary seizure focus.

2.2.4 Temporal Lobe Epilepsy

Temporal Lobe Epilepsy (TLE) is the most common type of localization-related epilepsy [Wiebe, 2000] and is also among the most refractory to present medical treatment [Engel, 2001]. TLE patients exhibit simple partial seizures, complex partial seizures, and also secondary generalized seizures. Seizures may occur in clusters,

[6] This imbalance need not necessarily be excitatory. For example, it has been suggested that enhanced inhibition may in fact contribute to the epileptogenic process through inhibition-induced synchrony [Dudek and Spitz, 1997].

in intervals, or in isolation. TLE can be divided into two types: mesial TLE, which involves the hippocampus, parahippocampal gyrus, and/or amygdala; and lateral TLE, which involves the temporal lobe of the neocortex. As a symptomatic epilepsy, TLE results from specific brain insults, such as traumatic brain injury, infection, stroke, and prolonged seizure (status epilepticus), and emerges following a latency period [Aroniadou-Anderjaska et al., 2008]. A classical hallmark of TLE is the interictal spike [Buzsaki et al., 1991, Leung, 1988], a pathological population discharge that appears spontaneously in pathological EEG. High frequency oscillations (HFOs) (80-500 Hz) are also associated with pathological activity in TLE [Bragin et al., 1999, Staba et al., 2002]. Given the prevalence of TLE and also its relative intractability, TLE will be the epilepsy syndrome that is the focus of this dissertation.

2.3 Hippocampal Electroencephalogram

During the natural course of its operation, the brain exhibits many patterns of activity. In addition to the firing of individual neurons that accounts for most information processing, the combined activity of many neurons forms regular patterns that can be detected and classified into several specific states. Measurement of this activity is typically performed by electroencephalography (EEG). This involves using scalp or depth electrodes[7] to detect the electric fields produced by hundreds of surrounding neurons. Patterns of activity picked up by the EEG are typically associated with the behavioural state of the organism. These patterns can be grouped into two categories: 1) EEG rhythms, which are recurrent oscillations in the EEG signal with well-defined frequency ranges and 2) EEG spikes, which are high-amplitude transients in the EEG signal that reflect the synchronous discharge of large populations of neurons. Below we will review the major patterns of activity specific to the hippocampus.

[7] In our studies, depth electrodes are used to record EEG from within the hippocampus.

2.3.1 Hippocampal Gamma and Theta Rhythms

Within the hippocampus, the two main types of rhythms are hippocampal theta and gamma rhythms. The theta rhythm (5-10 Hz) is continually present during states of arousal, particularly awake mobility and exploration, and also during REM sleep. It is a highly pervasive oscillation, encompassing the entire hippocampus and extending to other connected structures, including the entorhinal cortex, the medial septum and the supramammillary nucleus [Buzsáki, 2002]. It has been associated primarily with encoding and retrieval of memory [Hasselmo, 2005] and also spatial positioning [O'Keefe and Recce, 1993]. Initiation of the theta rhythm is controlled by neuromodulatory input from the ascending arousal centres of the brainstem, which project to the hippocampus and septal areas [Vertes et al., 1993]. These inputs promote the circuitry of the hippocampus and connected structures to enter into theta frequency oscillations. The actual mechanism by which these theta oscillations are generated is thought to depend critically on interaction between the hippocampus and the medial septum, as studies have shown that lesioning the septum abolishes hippocampal theta [Petsche et al., 1962].[8] In particular, resonant interactions amongst GABAergic interneurons in the hippocampus and medial septum have been shown using computer models to reproduce theta-frequency oscillations [Hajos et al., 2004, Wang, 2002]. However, recent *in vitro* studies have shown that it is also possible to reproduce theta oscillations in hippocampal slice without septal input, suggesting that the hippocampus alone possesses the necessary circuitry to generate hippocampal theta [Goutagny et al., 2009].

[8] There are multiple cell types present in the medial septum that could contribute to hippocampal theta generation. The two main types are cholinergic and GABAergic cells. Studies have shown that selective pharmacological lesioning of septal cholinergic cells reduces, but does not eliminate, the theta rhythm. This suggests septal GABAergic cells are sufficient to maintain the theta oscillation, and that septal cholinergic cells regulate the theta rhythm's magnitude [Lee et al., 1994].

Gamma rhythms (25-140 Hz) are also present in the hippocampus. Unlike the theta rhythm, which is sustained throughout specific behaviours, gamma rhythms tend to occur in short transient bursts of only several cycles [Buzsaki, 2009]. Gamma rhythms can occur at specific times in the theta cycle and also outside of theta. They are believed to play a role in binding together cell assemblies for information processing. Two main mechanisms are involved with the generation of hippocampal gamma oscillations: interneuron network gamma (ING) and pyramidal interneuronal network gamma (PING). For ING, the gamma oscillation is generated entirely by inhibitory interactions amongst interneurons, as has been demonstrated in interneuron-only network models [Wang and Buzsaki, 1996]. While ING is often studied in *in vitro* preparations, it likely does not occur in isolation *in vivo*. Pyramidal cell involvement is demonstrated by PING, in which pyramidal cells provide fast excitation to inhibitory neurons to modulate their excitation and therefore contribute to their synchronization. Details of these mechanisms are provided by a number of reviews [Buzsáki and Wang, 2012, Whittington et al., 2000].

2.3.2 Hippocampal Sharp Waves and Interictal Spikes

When the hippocampus is not in the theta state, it can exhibit several other modes of activity, the predominant one being large amplitude irregular activity (LIA) [Ho, 2011]. Superimposed on this LIA can emerge hippocampal population discharges called sharp waves (SPWs). They appear as short (30-120 ms) high amplitude transients in the EEG signal [Buzsaki, 1986]. SPWs are thought to be important for memory consolidation and the transfer of information between the hippocampus and the neocortex [Buzsaki, 1996]. They are formed by recurrent circuitry of the hippocampal CA3 regions, and it is thought that perisomatic-targeting interneurons play a central role in their initiation [Ellender et al., 2010]. Interictal spikes (IS) are similar to SPWs and are associated with pathological brain changes seen in epilepsy. SPWs and IS occur during the non-theta state, which includes the behaviours such as awake immobility and slow-wave sleep

[Kramis et al., 1975]. Awake immobility refers to activities such as drinking, eating, and grooming [Suzuki and Smith, 1987]. While SPWs occur exclusively in non-theta states, IS can also occur in the theta state, although their rate is severely depressed [Buzsaki et al., 1991, Leung, 1988, Suzuki and Smith, 1987]. In this dissertation, we will refer to spiking events such as SPWs and IS collectively as hippocampal EEG spikes (SPKs).

2.4 On Seizures and Cycles

Epilepsy is fundamentally linked to brain rhythms. Like brain rhythms, epileptic seizures are a product of underlying neural activity and are dependent on the synchronization of large numbers of neurons. Just as neuromodulatory inputs associated with specific behavioural states control the emergence of certain rhythms, so too can behavioural states promote neuromodulatory conditions favourable for the emergence of seizures. For example, an experimental study in rats showed that temporal lobe seizures were reduced during episodes of theta activity, suggesting that the theta state is unfavourable for the formation of seizures [Colom et al., 2006].[9] Similarly, state changes associated with different stages of sleep can also affect the emergence of epileptic seizures [Malow et al., 1997].

The focus of this dissertation, however, is on the relationship between epilepsy and rhythms that have much larger time scales, on the order of 24-hours. Prior studies have shown that there is actually a bidirectional relationship between epileptic seizures and 24-hour rhythms, with seizures showing 24-hour patterns of recurrence, and also epilepsy affecting the 24-hour rhythms of biological processes. These relationships are reviewed in the following sections.

[9] This reduction was observed for three different cases: for spontaneous episodes of theta, for pharmacologically indued theta (carbachol), and also for theta induced by tail pinch. This suggests that the seizure reduction is dependent on the presence of theta state, regardless of its mechanism of induction [Colom et al., 2006].

2.4.1 Effect of 24-Hour Rhythms on Seizures

It has long been known that, although epileptic seizures appear to be random and spontaneous events, they actually show predictable patterns when studied over very long timescales. This was first documented in the late 19th century by Sir William Gowers, who grouped epileptic ”fits” by their tendency to occur most frequently either during the day, during the night, or diffusely throughout both the day and night [Gowers and Schlesinger, 1885]. This was one of the first indications of a connection between epileptic seizures and daily rhythms. Since then, the 24-hour rhythm of seizures has been classified in a variety of epilepsy syndromes, including TLE [Hofstra and de Weerd, 2009, Hofstra et al., 2010].

There are many daily rhythms present in the body. Their origin and function can be traced to the extrinsic 24-hour light-dark cycle, which determines optimal times for resting, feeding, and procreating. Most organisms on the planet entrain to this daily cycle. Mammals show 24-hour rhythms in their globally regulated functions, including digestive activity, wake-sleep state, rest-activity cycle, and core body temperature [Beersma and Gordijn, 2007]. Correspondingly, to generate these global rhythms, basic physiological processes, including neural activity, metabolic activity, gene transcription, and hormone secretion, must also be regulated on a 24-hour cycle. Together, these rhythms are coordinated to a large extent by the circadian timing system, a hierarchy of entrainable 24-hour clocks that oscillate even in the absence of external cues.

Although sleep and circadian rhythms are closely related, there are important differences between them as well. They are controlled by different (although interconnected) brain regions and utilize different neuromodulators and neurohormones. While they are usually coupled, in cases such as jet lag, they can become misaligned.[10] The

[10] Forced desynchrony protocols can separate the endogenous circadian rhythm from other 24-hour rhythms in the body [Cambras et al., 2007, Carskadon et al., 1999].

wake-sleep cycle is sometimes used as a surrogate marker for circadian rhythms, but it is often desirable to differentiate between the two, especially when trying to elucidate underlying mechanisms. Additional details on mechanisms underlying circadian and wake-sleep regulation are provided in Chapter 3.

While there is strong evidence that wake-sleep state can influence epileptiform activity [Malow et al., 1997], a number of lines of evidence suggest that the 24-hour pattern of seizures is driven primarily by circadian rhythms. First, it has been shown in an animal model of limbic epilepsy that the 24-hour rhythm of seizures appears for both animals kept in a controlled light-dark environment, and also for those kept in constant darkness [Quigg et al., 2000]. Additionally, a recent clinical study examined a human patient with two separate epileptic foci, one limbic and one parietal. This investigation showed that, although seizures from both foci showed 24-hour rhythms, these rhythms were out of phase with each other, with temporal seizures peaking near noon and parietal seizures peaking in the early morning hours [Quigg and Straume, 2000]. Finally, studies have compared human mesial TLE to a similar epilepsy model in rats. It was shown that the 24-hour seizure rhythms in rats and humans were in phase, both peaking in the early afternoon, despite the fact that humans are diurnal (sleeping at night) and rats are nocturnal [Quigg et al., 1998]. Although wake-sleep cycle is inverted across nocturnal and diurnal organisms, 24-hour rhythms of the circadian system are phase-conserved across these species. For example, melatonin, one of the primary hormonal outputs of the circadian system, is secreted at night for both nocturnal and diurnal organisms [Quigg, 2000]. These findings suggest that the primary driver

---

Another important difference between circadian rhythms and the wake-sleep cycle is that circadian rhythms are true rhythms, whereas the wake-sleep cycle is a series of discrete transitions between wakefulness and stages of sleep.

of seizure 24-hour rhythms for TLE may not be the wake-sleep cycle, but rather the circadian system.

Despite the evidence for the involvement of the circadian system in the regulation of 24-hour rhythms, little is known about mechanisms underlying this regulation. Traditionally it is thought that the 24-hour seizure rhythms result from modulation of the epileptic brain region by neuromodulators and/or neurohormones that are released with 24-hour rhythmicity [Quigg, 2000]. Thus, similar to how certain behavioural states exhibit favourable conditions for seizure formation, certain times of day may also contain levels of neuromodulators that promote the epileptic brain to be most prone to seize. It is well established that the release of many neuromodulators and neurohormones is regulated on a 24-hour basis; additionally, many of these also have the ability to promote or inhibit epileptic seizures. An example of such a neurohormone is melatonin, which is released primarily at night. Although it is a putative anticonvuslant, it has also been shown to promote epileptiform activity in slice [Musshoff and Speckmann, 2003]. Furthermore, as mentioned above, melatonin is a hormone that is phase-conserved across nocturnal and diurnal species. Other compounds, such as vasopressin and hormones of the hypothalamic/pituitary/adrenal axis have been proposed to play roles in the 24-hour rhythm of seizures [Quigg, 2000]. More recent studies have also hypothesized that molecular mechanisms might play a similar role [Cho et al., 2012]. However, as of yet, a causal linkage between these neuromodulators, neural activity, and seizure 24-hour rhythms has not been demonstrated.

2.4.2 Effect of Epilepsy on 24-Hour Rhythms

A fundamental question in circadian research is how certain diseases affect the circadian system and impair its ability to coordinate 24-hour rhythms. Studies suggest that severe neurodegenerative disorders, including Alzheimer's disease, Huntington's disease, Parkinson's disease, and multiple sclerosis, affect brain regions associated with sleep and circadian rhythms and this results in disrupted 24-hour

rhythms [Barnard and Nolan, 2008, Wulff et al., 2010]. Interest in this is motivated by the fact that such disrupted daily rhythms can have extensive pathological implications, including emotional disorders, cognitive deficiency, impaired resistance to disease, and increased risks of cardiovascular disease and cancer [Hastings et al., 2003, Wulff et al., 2010]. Studies on shift workers have shown increased risk of diabetes, ulcers, cancer and cardiovascular diseases, and chronic jet lag has been demonstrated to produce temporal lobe atrophy and cognitive defects [Cho, 2001, Cho et al., 2000].

Evidence is growing for the case that epilepsy, too, might affect the circadian system. There are two distinct avenues by which 24-hour rhythms might become disturbed in epilepsy. First, the acute effects of epileptic seizures might promote transient 24-hour rhythm perturbations. This is supported by a study showing that daily rhythms of core body temperature experience slight and transient phase shifts following seizures [Quigg et al., 2001]. Secondly, it has been proposed that permanent structural changes in the brain associated with the chronic epilepsy state may block or impair circadian rhythms [Quigg, 2000]. This is supported by a number of studies on globally regulated functions, which have shown abnormalities of the wake-sleep cycle [Bastlund et al., 2005, Shouse et al., 1996], increased variability in core body temperature (CBT) 24-hour rhythms [Quigg et al., 1999], and altered melatonin release [Hofstra and de Weerd, 2009, Quigg, 2000]. One study also reported altered 24-hour behavioural rhythms, but suggested that these might be caused by postictal hyperactivity [Stewart and Leung, 2003]. A variety of brain regions have been proposed to underlie these changes. For example, reported cell loss in the dorsomedial hypothalamus, a region relevant for sleep regulation, has been suggested as the cause for abnormalities in wake-sleep cycle [Bastlund et al., 2005]. Likewise, changes in the medial preoptic nucleus reported by [Quigg et al., 1999], may underlie the increased complexity in core body temperature rhythms. There are likely other brain structures involved in the regulation of circadian rhythms may be altered in the epileptic state and that remain to

be identified. In summary, preliminary evidence supports the notion that the circadian system is altered in epilepsy; however, unlike the case for neurodegenerative diseases, it is not clear exactly which mechanisms and brain regions are involved. This results partly from the large number of epilepsy syndromes, and also from epilepsy's nature of affecting a wide range of brain structures [Parekh et al., 2010].

2.5 Motivation

Thus far, we have outlined a dual relationship between epilepsy and 24-hour rhythms: first, the pattern of recurrence of epileptic seizures is modulated on a 24-hour cycle; second, epilepsy can affect the circadian regulatory system to alter the expression of 24-hour rhythms. While these phenomena have been characterized by a number of studies, much work remains to be done to elucidate the underlying mechanisms. As we have discussed, descriptions are still largely phenomenological and based on system-level studies; few studies on this topic delve into performing long-term neural- or molecular-level measurements during epilepsy.[11] Such measurements, however, will constrain the set of potential phenomenological models and also yield data that can guide future quantitative modeling efforts. This work will ultimately suggest future experimental studies to confirm specific mechanisms for both seizure 24-hour rhythms and for the circadian disruption seen in epilepsy.

From a more practical perspective, a better understanding of the relationship between epilepsy and 24-hour rhythms will be beneficial for a number of reasons. First, by revealing how daily changes in the brain affect seizure likelihood, it will yield a better understanding for the brain naturally regulates seizures. This knowledge will then be useful for developing new pharmacological therapies to inhibit epileptic seizures.

[11] An exception to this is the study by Matzen et al. [2012], which characterizes changes in excitation and inhibition through single and paired pulse electrophysiological measurements.

Secondly, being able to understand and predict daily seizure rhythms will allow for optimization of existing epilepsy therapies. For example, chronotherapies, such as differential dosing of antiepileptic drugs according to the time-of-day, optimization of sleep schedules, improvement of sleep hygiene, and daily modulation of electrical treatments such as vagal nerve stimulation could all improve seizure control and reduce treatment side effects. Third, as mentioned above, clinical studies have shown that, in focal epilepsy, the time of peak seizure occurrence is dependent on the location of the seizure focus. By mining large amounts of EEG data, it may be possible to optimize epilepsy diagnosis by incorporating information on seizure 24-hour rhythms. Fourth, seizure prediction strategies, which aim to give advanced warning of when epileptic seizures will occur, could benefit from incorporating time of day information. These and other chronotherapy strategies are reviewed in detail by Loddenkemper et al. [2011]. As mentioned above, there are also many negative side effects and disease risks associated with disorganized sleep and circadian rhythms. A better understanding of the ways in which these rhythms are altered is the first step towards treating the sleep and circadian disorders that epileptics often experience.

2.6 Hypotheses

In this dissertation, we will investigate 24-hour rhythms of hippocampal neural activity in a rat model of TLE. Our approach will consist of biophysical computer modeling, analysis of large neural data sets,[12] and MRI analysis.

Based on the current state of the literature, we formulate the following hypotheses:

1. Features of hippocampal neural activity, including EEG rhythms and population spiking events, will show 24-hour rhythmicity in their activity.

2. These rhythms will be disrupted in epileptic animals.

[12] Long-term neural recordings were collected by Talathi et al. [2009].

3. Altered 24-hour rhythms can be linked to structural damage in the circadian system.

4. Structural damage will be detectable using MRI analysis.

By beginning with long-term neural measurements, our approach will complement existing systems-level studies, elucidating how 24-hour rhythms are altered on a neural level. Should hypothesis #2 be shown true, and 24-hour neural rhythms become disrupted in epilepsy, it is possible that the associated change in homeostasis could influence the emergence of seizures. In this case, circadian disruption and seizure 24-hour rhythms, two aspects of epilepsy that are normally studied independently, may in fact be related. Such a finding could shape the paradigm of future studies, shifting away from the idea that seizure 24-hour rhythms are passively entrained to normal circadian rhythms, and towards the idea that circadian abnormalities encourage the emergence of seizures. More generally, our neural-level approach will lead to the development of more mechanistic theories for the relationship between circadian rhythms and epilepsy and, hopefully, have impacts ranging from the development of chronotherapies to improved fundamental understanding of the disease.

2.7 Organization of this Dissertation

This dissertation aims to provide a complete investigation of 24-hour rhythms in spontaneous neural activity, derived from previously collected long-term neural recordings. Following our analysis of this data, we will propose specific mechanisms to explain our results and test these by developing a biophysical computer model. This will lead to further hypotheses, which will be tested through subsequent EEG and MRI data analysis.

Prior to presenting these results, however, some additional background on the circadian system is required. This is presented in Chapter 3. Chapter 4 outlines the general methods used in this study that are relevant to subsequent chapters. Chapters 5-8 address our specific hypotheses stated above. Results of our analysis

of neural data, with specific focus on EEG spiking events, are presented in Chapter 5. In this chapter, we demonstrate that, for epileptic animals, a phase shift emerges in the 24-hour rhythm of EEG spiking events (Hypotheses #1 and #2). Based on this, we propose that certain brain regions responsible for providing circadian regulation become dysfunctional. We test this proposed mechanism in Chapter 6 by designing a neural network model of 24-hour rhythms and using it to demonstrate how structural changes, in particular to the medial septum, can reproduce observed circadian anomalies (Hypothesis #3). This leads to investigations of structural changes in the medial septum in Chapter 7 and of functional changes in the theta rhythm in Chapter 8. Specifically, Chapter 7 uses *in vivo* and excised MRI to measure changes in the septum in epileptic animals (Hypothesis #4). Chapter 8 returns to Hypotheses #1 and #2 by showing that the amplitudes of EEG rhythms are modulated on a 24-hour time scale and, furthermore, the modulation of certain rhythms (beta and gamma) experience a phase shift following injury. Chapter 8 also provides evidence that there are multiple circadian inputs that may be altered following injury (Hypothesis #3). Finally, we discuss implications of the collective findings presented in this work in Chapter 9, specifically in relation to seizure 24-hour rhythms. The material presented in Chapters 5, 6, and 7 is derived from our in press manuscript titled “Local phase shift in the 24-hour rhythm of hippocampal EEG spiking activity in a rat model of temporal lobe epilepsy.”

CHAPTER 3
THE MAMMALIAN CIRCADIAN SYSTEM

3.1 Overview

There primary goal of this chapter is to provide readers with the necessary and sufficient background information about the circadian regulatory system in order to interpret results presented in subsequent chapters of this dissertation.[1] We will review what is known about the structural organization of the circadian system and focus specifically on how this can influence neural activity in the brain.

3.2 A Hierarchy of Oscillators

Circadian rhythms are 24-hour oscillations that are ubiquitous in biological systems, ranging from bacteria to the human brain. Coordination of circadian rhythms is achieved by the circadian timing system, which consists of three general components: an input, a pacemaker, and an output [Loddenkemper et al., 2011, Ohdo, 2010]. In mammals, the primary circadian pacemaker is located in the suprachiasmatic nucleus (SCN) [Gerstner and Yin, 2010]. We shall discuss the SCN and also the other components of the circadian system in the following paragraphs.

There are several important inputs to the circadian system. A primary input arises from the photoreceptors in the retina, which transmit information about the environmental light-dark cycle. These photoreceptors include both conventional rods and cones and also retinal ganglion cells (RGCs), which serve as the non-image forming photoreceptors for the brain. They project directly to the SCN and also to many other brain structures. They respond primarily to blue light, as opposed to green or violet light [Vandewalle et al., 2007]. RGCs, rods, and cones traverse the retinohypothalamic

[1] Parts of this chapter are in press with the Journal of Neurophysiology: Stanley, D.A., Talathi, S.S., Parekh, M.B., Cordiner, D., Zhou, J., Mareci, T.H., Ditto, W.L., Carney, P.R. Local phase shift in the 24-hour rhythm of hippocampal EEG spiking activity in a rat model of temporal lobe epilepsy [Stanley et al., 2013].

tract to reach the SCN, where their input acts to entrain SCN cells to the environmental light-dark cues. Additional important inputs to the SCN arise from the intergeniculate leaet (IGL), from the raphe nuclei, and from several other sites in the brain that transmit non-photic information to the SCN about feeding and temperature patterns [Ohdo, 2010].

The SCN consists of approximately 20,000 neurons. In slice, intact SCN tissue has been shown to be intrinsically oscillatory, exhibiting sustained 24-hour rhythms of neural firing activity in isolation of other inputs. These 24-hour oscillations are not an emergent property of the network, as isolated SCN cells in culture have also shown sustained 24-hour rhythms [Hastings et al., 2003]. Rather, SCN firing activity oscillations are thought to be generated by 24-hour oscillations in gene transcription. Clock genes, including *Per*, *Cry*, and *Rev-erb* α, have been shown to participate in a feedback circuit that oscillates with near-24-hour period [Ko and Takahashi, 2006, Shearman et al., 2000]. This molecular clock machinery is not present in all SCN cells, but only in certain "clock" cells. These cells possess 24-hour rhythms of firing activity, and also exhibit unique electrophysiological properties. The daily changes in their electrical behaviour may be linked to molecular 24-hour oscillations through modulation of specific potassium currents [Belle et al., 2009].

While the SCN serves as the master clock of the circadian system, it does not exhibit a great many efferent projections. Rather, the circadian system relies on a number of intermediary nuclei that are organized into a hierarchical-type network (Figure 3-1) [Gerstner and Yin, 2010].[2] These nuclei receive the SCN's clock signal, integrate it with other information, and then transmit it throughout the body. A standard example

[2] This hierarchical network includes both feedforward and feedback connections. Additionally, a number of recent studies have identified independent peripheral circadian oscillators that form part of the circadian network and that, like the SCN, maintain 24-hour oscillations in isolation [Guilding and Piggins, 2007, Ko and Takahashi, 2006].

is the circuit that controls the release of melatonin. While melatonin is a principal output of the circadian system, it is produced by the pineal gland and its release is indirectly controlled by the SCN. Specifically, SCN relies on a polysynaptic pathway via the paraventricular nucleus (PVN) and the superior cervical ganglion (SCG) to finally reach the pineal gland [Richter et al., 2004]. Melatonin then is released into the bloodstream to exert effects throughout the body and also to exert a feedback effect on the SCN itself [Saper et al., 2005].

3.3 Circadian Regulation of the Wake-Sleep Cycle

Another important function of the circadian system is the regulation of the wake-sleep cycle. The circuit controlling sleep and wakefulness provides an important example of how the SCN signal is integrated with other information. Specifically, the wake-sleep circuit consists of contrasting brain centres promoting arousal and sleep, respectively. Key arousal areas are monoaminergic nuclei, such as the locus coeruleus (LC), the raphe nuclei, and the tuberomammillary nucleus (TMN); these are activated in part by orexin containing cells (ORX) of the lateral hypothalamic area (LHA). The main sleep-promoting region is the ventrolateral pre-optic nucleus (VLPO). A detailed review this architecture is provided by Saper et al. [2005] but, essentially, these two regions are mutually inhibitory and function as a flip-flop switch. Many of these nuclei, such as the VLPO and the ORX cells receive input from the SCN [Abrahamson et al., 2001, Deurveilher et al., 2005, Loddenkemper et al., 2011]. However, while the SCN exerts an influence, the switch does not strictly follow the SCN's 24-hour rhythm. Rather, wake-sleep transitions respond to many additional factors, including homeostatic drive (extended periods of sleep will follow deprivation) and also external stimulation. In this manner, the wake-sleep circuit integrates the SCN clock signal with many other inputs, allowing it to respond dynamically to a breadth of demands.

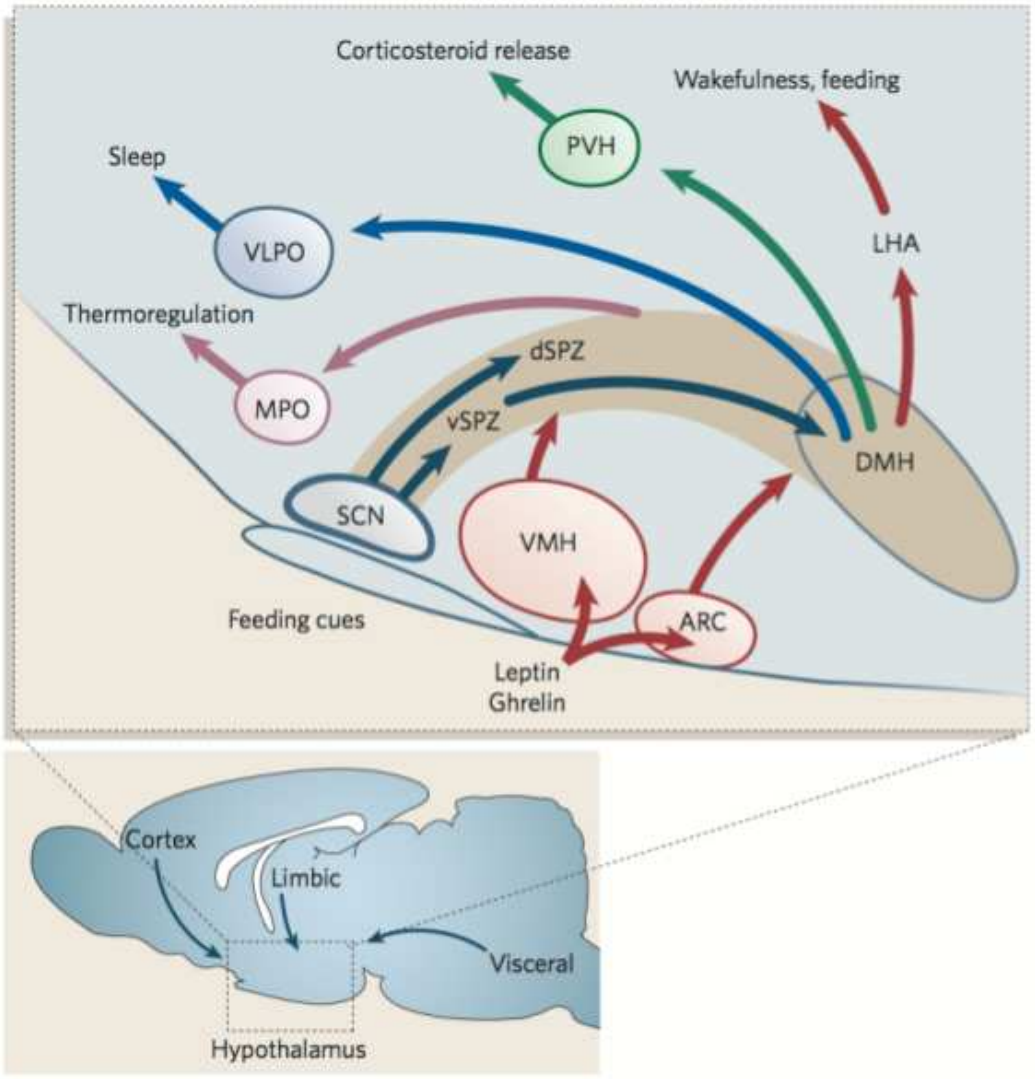

Figure 3-1. A summary of the hierarchical arrangement of the mammalian circadian system. The SCN does not directly control 24-hour rhythms in the body, but acts through a number of intermediary nuclei that transmit the clock signal whilst integrating it with other information. The majority of SCN output traverses the ventral and dorsal subparaventricular zone (vSPZ and dSPZ). dSPZ neurons project to the medial preoptic nucleus (MPO) to regulate 24-hour rhythms of body temperature. vSPZ neurons pass to the dorsomedial nucleus of the hypothalamus (DMH). The DMH then projects to the ventrolateral hypothalamic nucleus (VLPO), the lateral hypothalamic area (LHA), and the paraventricular nucleus of the hypothalamus (PVH) to influence, respectively, sleep, arousal, and release of corticosteroids and melatonin. A number of additional nuclei and circadian-regulated functions, such as feeding and thyroid release, are not shown, but are reviewed elsewhere [Gerstner and Yin, 2010, Loddenkemper et al., 2011]. Reproduced with permission from Saper et al. [2005].

3.4 24-Hour Rhythms in the Brain

The hierarchical structure of the circadian system allows for the regulation of 24-hour rhythms pervasively throughout the body. It has recently been estimated that more than 10% of genes are subject to circadian regulation in mammalian peripheral tissue[Storch et al., 2002]. In the brain, circadian regulation is highly pervasive as well, and 24-hour rhythms of neural activity can be detected at most recording sites using a variety of recording techniques. A summary of publications describing brain 24-hour rhythms is presented Table 3-1. In this table, we did not include data on the hippocampus, which is instead presented in the next section.

3.5 24-Hour Rhythms in the Hippocampus

Investigations on the relationship between 24-hour rhythms and epilepsy in this dissertation will focus specifically on temporal lobe epilepsy (TLE) in the hippocampus. This makes the hippocampus an important structure upon which to focus in our review of the circadian literature. Fortunately, as an important site for the formation of learning and memory, the hippocampus has been of interest for numerous circadian studies. This interest arises mainly from the observation that many behaviours, particularly those involving memory and cognitive performance, show time-of-day dependency [Barnes et al., 1977, Gerstner and Yin, 2010]. We have presented detailed summary of studies on hippocampal 24-hour rhythms in Table 3-2. It is important to note that, while there are numerous studies on 24-hour rhythms in the hippocampus, there is a paucity of studies that have examined these rhythms in the diseased state.

3.6 Circadian Inputs to the Hippocampus

From Table 3-2, it is clear that multiple measures of hippocampal neural activity show 24-hour rhythms, including both spontaneous and evoked activity. Evidence from a subset of these studies [Chaudhury et al., 2005, Wang et al., 2009, West and Deadwyler, 1980] suggests that these rhythms are, in part, truly circadian - that is,

Table 3-1. Brain regions exhibiting 24-hour rhythms *in vivo*

Brain Region	Measurement[a]	Species	Reference
Accumbens nucleus	MUA	Hamster	Yamazaki et al. [1998]
Anterior Hypothalamus	Hist.	Rats	Mochizuki et al. [1992] [b]
Caudate nucleus	MUA	Rat	Inouye and Kawamura [1979]
	5-HT, Hist., NE	Rat	Friedman and Walker [1968, 1969]
Caudate putamen	MUA	Hamster	Yamazaki et al. [1998]
Lateral hypothalamic area	MUA	Rat	Inouye [1983]
Lateral septum	MUA	Hamster	Yamazaki et al. [1998]
Locus coeruleus	SUA	Rat	Aston-Jones et al. [2001]
	5-HT, NE	Rat	Agren et al. [1986]
Medial and dorsal raphe	MUA	Rat	Inouye and Kawamura [1979]
	5-HT	Rat	Pinato et al. [2004][c]
	5-HT, NE	Rat	Agren et al. [1986]
Medial preoptic region	MUA	Hamster	Yamazaki et al. [1998]
Medial septum	MUA	Hamster	Yamazaki et al. [1998]
Mid-brain	5-HT, Hist., NE	Rat	Friedman and Walker [1968, 1969]
Midbrain reticular formation	MUA	Rat	Inouye and Kawamura [1979]
Preoptic area	MUA	Rat	Inouye [1983]
Reticular formation	MUA	Rat	Inouye [1983]
Stria medullaris	MUA	Hamster	Yamazaki et al. [1998]
Substantia Nigra	MUA	Rat	Inouye [1983]
Suprachiasmatic nucleus	MUA	Rat	Inouye and Kawamura [1979]
	MUA	Rat	Inouye [1983]
	MUA	Hamster	Yamazaki et al. [1998]
Thalamus	MUA	Rat	Inouye [1983]
Ventrolateral thalamic nucleus	MUA	Hamster	Yamazaki et al. [1998]
Ventromedial hypothalamic nucleus	MUA	Rat	Inouye [1983]
		Hamster	Yamazaki et al. [1998]
Visual cortex	MUA	Rat	Inouye and Kawamura [1979]

[a] MUA = multiunit activity, SUA = single unit activity, 5-HT = serotonin, NE = norepinephrine, Hist. = histamine

[b] Histaminergic neurons in the brain are located in the tuberommaillary nucleus of the posterior hypothalamus. However, the anterior hypothalamic area contains the highest concentration of histaminergic fibres.

[c] Variation was bimodal.

independent of behavioural or light-dark cycle changes. This raises a fundamental question: how do these rhythms arise?

While there are no direct projections from the SCN and the hippocampus, there are numerous indirect pathways by which circadian signals may be relayed to the hippocampus. Unfortunately, however, there is little evidence as to which of these pathways are most relevant. We have conducted a detailed literature search of these potential pathways and have grouped them into three categories. First, the hippocampus receives afferent synaptic projections from many brain regions and most of these regions show 24-hour rhythms (Table 3-1). Thus, these brain regions could potentially be relevant for driving hippocampal 24-hour rhythms. Major hippocampal afferents that show 24-hour rhythmicity are summarized in Table 3-3[3] . Second, neurons in the hippocampus have receptors for many neurohormones that are modulated on a 24-hour cycle, such as melatonin and adenosine [Liu et al., 2000, Wan et al., 1999]. These could also influence hippocampal neural activity; the action of such neurohormones is summarized in Table 3-4. Third, a number of recent studies have shown that molecular clocks present in hippocampal neurons might influence synaptic activity [Valnegri et al., 2011, Wang et al., 2009]. Taken together, it is clear that there are many possible pathways by which 24-hour rhythms can propagate to the hippocampus. However, it is not clear which of these pathways are *functionally* relevant for generating hippocampal 24-hour rhythms. In order to answer such a question, additional experimental studies, specifically those quantifying the effects of lesioning putative circadian pathways, are needed. Unfortunately, although such studies have been conducted for the primary

[3] The majority of these afferents arrive in the hippocampus via two routes, one dorsal, one ventral. The dorsal route traverses the fimbria-fornix, cingulum, whereas the ventral route traverses the amygdala [Da Silva et al., 1990, Mongeau et al., 1997]

outputs of the SCN [Inouye and Kawamura, 1979], very little is known about the functional circadian inputs to the hippocampus.

Despite the paucity of direct evidence through lesioning experiments, there exist some studies that provide indirect indications of which pathways might be most relevant for generating hippocampal 24-hour rhythms. As suggested by Tables 3-1 and 3-3, the septum may be an important relay centre between the SCN and the hippocampus. Multiunit recordings have shown that the septum possesses a robust circadian rhythm that persists in the absence of external light/dark cues [Yamazaki et al., 1998]. Furthermore, it is well established from tracing studies that the septum, unlike the hippocampus, receives heavy innervation from the SCN [Morin et al., 1994]. In turn, the medial septum is perhaps the most critical subcortical input to the hippocampus. A recent study on hippocampal dependent learning suggested that the septum may play a functional role in regulating hippocampal circadian rhythms [Ruby et al., 2008]. Specifically, the authors showed that hamsters with arrhythmic SCN displayed impaired hippocampal learning. They proposed that this may result from chronic inhibition of the septum by the arrhythmic SCN, since pharmacological inhibition of the septum had similar effects on learning. Such chronic inhibition of the septum could produce these effects through suppression of septal excitation of the hippocampus.

Another study investigated the effects of melatonin on synaptic transmission and LTP in the hippocampus, comparing control mice to melatonin knockouts [Chaudhury et al., 2005]. They found that melatonin knockout altered, but did not eliminate 24-hour rhythms of synaptic transmission. This suggests that 24-hour rhythms in the hippocampus are generated by the overlapping influence of multiple circadian inputs, of which melatonin is one.

A study on hippocampal place cell activity has shown that, although hippocampal place cell firing exhibits 24-hour patterns, these patterns are not phase-locked to the day-night cycle. Rather, it was proposed that they are entrained to other external cues,

such as food availability. Therefore, it was proposed that a food entrainable 24-hour oscillator outside the SCN might also be a relevant circadian input to the hippocampus [Munn and Bilkey, 2012]. Finally, a number of other functionally relevant pathways have been proposed, such as hypothalamic-regulated hormone release [Matzen et al., 2012] and indirect input from the orexin-secreting cells in the lateral hypothalamus [Gerstner and Yin, 2010]. However, at present, there is little direct evidence for their functional relevance.

In summary, we have provided a review of the literature concerning 24-hour rhythms in the hippocampus. We have also conducted a detailed literature survey on the possible input pathways that could lead to the generation of these 24-hour rhythms. Although there is little evidence for which of these pathways are strongest and most functionally relevant, preliminary studies have suggested that both melatonin and input from the medial septum may play important roles in generation of hippocampal 24-hour rhythms. The notion that multiple circadian inputs may contribute to the generation of hippocampal 24-hour rhythms is consistent with the requirement that the circadian hierarchy must dynamically regulate 24-hour rhythms to respond to a variety of external cues.

Table 3-2. Experimental measurement of hippocampal 24-hour rhythms

Study	Stimulation site	Recording site	Species	Quantity[a] Measured	Comments[b]
Barnes et al. [1977]	Perforant path	Dentate granule cells	Rat, Squirrel monkey *in vivo*	fEPSP, PS amplitude	Peak fEPSP occurred out of phase for rat (nocturnal) and monkey (diurnal)
West and Deadwyler [1980]	Perforant path	Dentate granule layer	Rat *in vivo*	fEPSP, PS amplitude	Circadian rhythm of PS, peaking at night, independent of behaviour, light, or corticosterone. No differences in fEPSP.
Cauller et al. [1985]	Perforant path (angular bundle)	Dentate hilus	Rat *in vivo*	fEPSP slope, PS amplitude	fEPSP peaks during night, PS during day
Harris and Teyler [1983]	Dentate stratum moleculare	Dentate granule cells	Rat slice	LTP of PS amp.	LTP peaks in night in dentate
	CA1 stratum radiatum	CA1 stratum pyramidale			LTP peaks in night in CA1
Dana and Martinez [1984]	Perforant path	Dentate hilus	Rat *in vivo*	LTP of PS amp.	LTP peaks at night in controls, peaks during day in adrenalectomized rats
Brunel and de Montigny [1987]	No stim.	CA3 pyramidal cells	Rat *in vivo*	Single cell firing rate (spontaneous)	Peak firing rate in the morning, with seasonal dependence
Raghavan et al. [1999]	CA3 stratum radiatum	CA1 pyramidal	Syrian hamster slice	LTP of PS after tetanus	Slices prepared during day and tested at night have highest LTP

[a] fEPSP = field excitatory postsynaptic potential (evoked), PS = population spike (evoked), VC = voltage clamp, LTP = long-term potentiation, HVA = high-voltage-activated, s/mAHP = slow/medium afterhyperpolarization, ADP = afterdepolarization.

[b] For each study, 24-hour variation in measured quantities implied unless otherwise stated.

Table 3-2. Continued

Study	Stimulation site	Recording site	Species	Quantity Measured	Comments
Kole et al. [2001]	CA3 pyramidal cells	CA3 pyramidal cells	Rat slice	HVA Ca^{2+} currents, mAHP, sAHP, ADP during VC	Ca^{2+} currents greatest after onset of dark phase. mAHP reduced and ADP increased at night; no change sAHP. Spike frequency accommodation reduced at night.
Chaudhury et al. [2005]	CA1 stratum radiatum	CA1 pyramidal layer	Mouse slice	LTP of fEPSP slope	LTP decays more slowly during night
		CA1 dendritic layer		LTP of PS slope	LTP of PS greater at night
		CA1 pyramidal layer		PS amplitude	No difference for control mice, but greater at night for melatonin knockout

Table 3-3. Synaptic inputs to the hippocampus from brain regions showing 24-hour modulation

Brain region	Neurotransmitter	Reference
Hypothalamus	Multiple	Pasquier and Reinoso-Suarez [1978]
Locus coeruleus	Norepinephrine	Gage et al. [1983], Haring and Davis [1985], Pasquier and Reinoso-Suarez [1978]
Medial septum	Acetylcholine, GABA	Gage et al. [1983], Peterson et al. [1987b]
Raphe nuclei	Serotonin	Azmitia and Segal [1978], Pasquier and Reinoso-Suarez [1978]
Substantia nigra	Dopamine	Scatton et al. [1980]
Tuberomammillary nuclei	Histamine	Panula et al. [1989]
Ventral tegmental area	Dopamine	Scatton et al. [1980]

Table 3-4. Non-synaptic inputs to the hippocampus showing 24-hour modulation

Modulator	Species preparation	Peak Release	Effect	Reference
Adenosine	Rat slice	Night	Inhibitory (inhib. of glutamate release)	Liu et al. [2000]
BDNF	Rat slice	No data	BDNF potentiates synaptic response	Kang and Schuman [1995]
BDNF	Rat slice	Night	24-hour rhythm, peaking at night, in dentate and CA3. No change in CA1	Schaaf et al. [2000]
Melatonin	Rat slice	Night	Attenuates GABAergic currents	Wan et al. [1999]
Melatonin	Rat slice	Night	1μM mel. increases neuron firing rate	Musshoff et al. [2002]
Melatonin	Rat slice	Night	1μM mel. increases epileptiform activity	Musshoff and Speckmann [2003]
Melatonin	Rat slice	Night	Melatonin-associated reduction in LTP	Ozcan et al. [2006]

CHAPTER 4
GENERAL METHODS

4.1 Overview

This chapter describes the experimental methods that are general to Chapters 5, 7 and 8.[1] This includes a complete description of how the three main experimental datasets used in this dissertation were collected. The first is the Evolution into Epilepsy EEG dataset, which was collected over multiple years by Dr. Dong-Uk Hwang, Dr. Sachin S. Talathi, Dr. Junli Zhou, and others. The second data set is the core body temperature (CBT) data, collected by Daniel Cordiner. The third is the MRI data, collected by Mansi B. Parekh. Additionally, this chapter will describe general data analysis methods that are used in Chapters 5 and 8.

4.2 Animal Husbandry

Animal studies were conducted on 2-month-old male Sprague Dawley rats weighing 200-265g. Protocols were approved by the University of Floridas Institutional Animal Care and Use Committee (IACUC protocol number D710). All animals were housed in a 24 h symmetric light-dark (LD) environment with light stage centered at 12:00 noon and with constant temperature and humidity levels. Animals were provided with food, water, and cleaning at regular intervals and monitored with continuous time-locked video. Injury was induced using a well-characterized model for chronic temporal lobe epilepsy (TLE) [Lothman et al., 1989, 1990, Sanchez et al., 2006], in which electrical induction of SE is used to bring about a state of recurrent spontaneous seizures after a latency period of 2–4 weeks. Animals were monitored during pre-injury, latency, and spontaneously seizing stages of epileptogenesis. The latency period was included in

[1] Parts of this chapter are in press with the Journal of Neurophysiology: Stanley, D.A., Talathi, S.S., Parekh, M.B., Cordiner, D., Zhou, J., Mareci, T.H., Ditto, W.L., Carney, P.R. Local phase shift in the 24-hour rhythm of hippocampal EEG spiking activity in a rat model of temporal lobe epilepsy [Stanley et al., 2013].

this analysis because spontaneous seizures have been previously shown to promote transient perturbations to circadian rhythms [Quigg et al., 2001]. The beginning of the spontaneously seizing stage was marked by the first recorded grade 3 or greater seizure.

4.3 Long-Term Data Collection

EEG and CBT Data were continuously collected from animals throughout epileptogenesis. Due to the experimental demands of continuous longitudinal recording, it was necessary to use a low number of animals for EEG and CBT rhythm analysis. However, each animal provided many circadian cycles of data (>3 weeks per animal), which allowed for clear reconstruction of 24-hour rhythms and highly confident estimations of phase. The experimental timeline is supplied in Figure 4-1.

Surgical, electrophysiological, and data analysis techniques are described below.

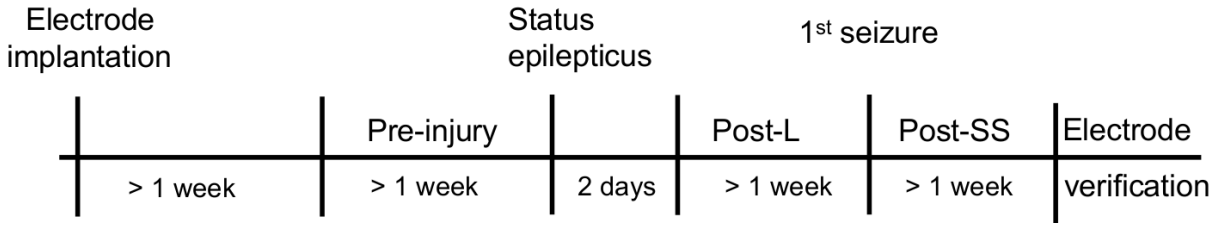

Figure 4-1. Experimental timeline for EEG and core body temperature (CBT) recordings. For EEG, data were split into pre-injury (Pre), post-injury latency (Post-L) and post-injury spontaneously seizing (Post-SS) stages. The beginning of the Post-SS stage was defined as following the first spontaneous grade 3 or greater seizure. Since CBT recordings did not include simultaneous EEG due to interference from the CBT transponder, we did not attempt to split post-injury data in to latency and spontaneously seizing stages.

4.4 Surgical Methods

Prior to all surgeries, rats were anesthetized by subcutaneous injection of 10 mg/kg xylazine (Webster Veterinary) and maintained anesthetized by 1.5% isoflurane (Akron Inc.). All rats were stereotaxically implanted in the right ventral hippocampus (5.3 mm caudal to Bregma, 4.9 mm lateral (right) of Bregma, and 5 mm ventral from dura) with a Teflon-coated bipolar twisted electrode (330 m diameter), which was later used for

induction of SE. Additionally, for collection of EEG data, sixteen channel Omnetics based microwire recording electrode arrays (Tucker Davis Technologies, Alachua, FL) were implanted bilaterally into the dentate gyrus and CA1 regions (Figure 4-2). Electrodes were made of tungsten with polyimide insulation, had 2mm tip length, and were 50m in diameter. The microwire array was anchored to the skull with four 0.8 mm stainless steel screws. Two were AP 2 mm to the bregma and bilateral 2 mm, and two were AP -2 mm to the lambdoidal suture and bilateral 2 mm. These two pairs served as the ground and reference, respectively. Electrode placement was verified using MRI after brains had been excised (see below). For CBT recording, a radio-frequency TA E-Mitter transponder was inserted in the abdominal cavity and powered by a ER4000 Energizer/Receiver unit (both from Mini Mitter Co., Bend, OR) that was placed underneath the cages.

4.5 Induction of Self-Sustaining Status Epilepticus

To induce SE, 10-second pulse trains were applied to the bipolar twisted stimulating electrodes using a Model 2100 Stimulator (A-M Systems, Sequim, WA), consisting of biphasic square waves with frequency 50 Hz, pulse duration 1 ms, and amplitude 250-400 A, with 2-second intervals between trains [Lothman et al., 1989, 1990, Sanchez et al., 2006]. The protocol for varying the stimulus current amplitude was as follows: The initial stimulus current was 50 A. This was increased in 25 A increments until either three consecutive grade 5 seizures were observed or until the upper limit stimulus current of 600 A was reached. The stimulation applied to all spontaneously seizing animals fell within the range of 250-400 A. Animals demonstrated wet dog shakes and seizures throughout the duration of the stimulation procedure, which lasted for 60-90 mins. Upon termination of stimulation, EEG recordings documented intermittent, self-sustaining 30-60 s seizures and interictal 2-5 Hz EEG activity lasting for 24 hours. Following a latency period of 2-4 weeks, rats developed spontaneous recurrent limbic seizures. Recordings of the latency period began 2 days following SE stimulus. For EEG

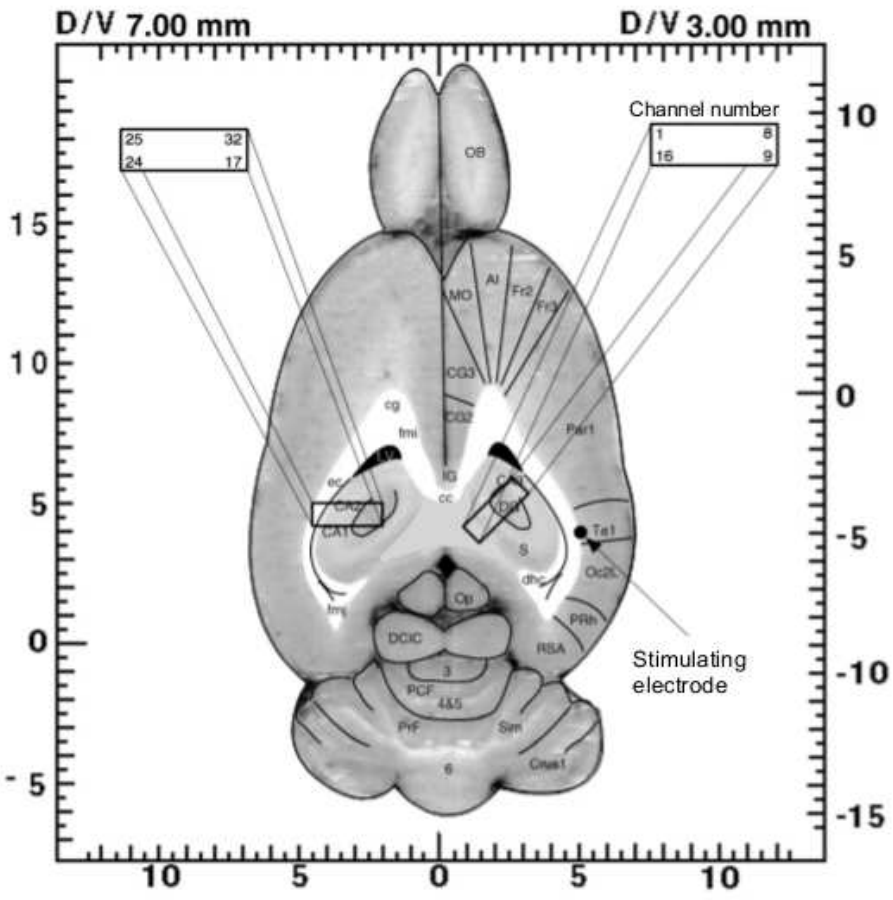

Figure 4-2. Placement of stimulating and recording electrodes. Channel number 2, corresponding to the ipsilateral CA1 region, was used for EEG analysis in this study.

recordings, a total of N=6 animals were stimulated. These were divided into two groups: those that exhibited spontaneous seizures (N=3) and those that did not exhibit seizure activity for at least 4 weeks following stimulus (N=3). For CBT and MRI analysis, only rats that developed spontaneous seizures were analyzed.

4.6 Seizure Detection

An in-house seizure detection system [Talathi et al., 2008] was used to scan EEG data sets to identify potential seizure epochs. These data sets were then visually scored by an expert epileptologist (PRC). The Racine grades of the seizures were confirmed from video recordings [Racine, 1972]. Seizure information was used to assess the

beginning of the spontaneously seizing stage of epileptogenesis, which was marked by the first recorded grade 3 or greater seizure.

4.7 EEG and CBT Data Acquisition

The EEG data from the recording electrodes was channeled through a 16-channel commutator to a pair of 16 channel RA16PA Medusa PreAmps with frequency response between 1.5 Hz and 7.5 Hz (Tucker Davis Technologies, Alachua, FL). The EEG signal was digitized at the rate of 12 kHz and passed onto the digital signal processing (DSP) unit, the Pentusa RX-5 acquisition board (Tucker Davis Technologies, Alachua, FL). The data from the DSP unit were streamed onto a PC and stored for further processing. CBT data were streamed through the ER4000 receiver and stored on a PC using Vital View software (Mini Mitter Co., Bend OR) at a sampling rate of one data point per second. Due to interference from the E-Mitter transponder in the hippocampal EEG recordings, it was necessary to collect EEG and CBT data independently from separate sets of animals.

4.8 Theta Epoch Detection

Theta-activity in the hippocampus is distributed throughout the wake-sleep cycle. Given the fact that theta-state transitions can affect the occurrence of many hippocampal activities, including SPWs, IS, and gamma rhythms [Buzsaki et al., 1991, Leung, 1988, Suzuki and Smith, 1987], we sought to quantify the distribution of theta activity throughout the day. Epochs of hippocampal theta activity were identified using an automated routine [Belluscio et al., 2012, Csicsvari et al., 1998]. We calculated the ratio of the power in theta (6 – 10 Hz) to the power in delta (1 – 6 Hz) in 2-second epochs and classified data as predominantly theta when this ratio exceeded a specified threshold. The threshold was 2.0 by default, although the sensitivity of our results to a range of threshold values between 1.0 and 3.0 in steps of 1.0 was examined. Similarly, our results were found to be insensitive to other common choices of theta and delta bands, such as 5 – 10 Hz and 2 – 4 Hz, respectively.

4.9 Data Analysis

4.9.1 Smoothing and Detrending

For purposes of analyzing 24-hour rhythms in SPK rate, EEG rhythms power, theta epoch occurrence, and CBT time series, all time series were all treated in a similar manner. First, time series data were pooled into 1 h non-overlapping time bins and the average value for each 1 h time bin was calculated. Data were then smoothed using 6-hour, 90%-overlapping moving average windows. We observed that, for some time series, data values would drift over the course of days or weeks. This was particularly the case for SPK rates, as was previously investigated [Talathi et al., 2009], and we refer to this as baseline drift. To detrend data by removing these long-timescale changes, we estimated the baseline drift by averaging data within a 1-day moving window. Then, we subtracted these baseline values from the original data. In figures where detrended (baseline-subtracted) data are shown, we use the symbol Δ to denote that the plotted value is a deviation from baseline. We also explored the use of alternative window sizes and overlap values for smoothing and baseline calculations, and found these changes had minimal effect on the results.

4.9.2 Cosinor Analysis

To obtain phase information, the detrended time series data were then compressed into a single 24-hour time window. This was achieved by applying the mapping $T_n \rightarrow T_n$ modulo 24 hours, where T_n is the time point in hours associated with each data value X_n in the detrended time series. Data were then fitted to sinusoidal functions of the form $f = A \times cos(2\pi(T - T_0)/24)$ using least-squares minimization. To confirm that the data were indeed sinusoidal, we conducted the zero-amplitude test [Nelson et al., 1979]. The 95% confidence intervals associated with phase estimates were estimated as previously described [Nelson et al., 1979].

CHAPTER 5
HIPPOCAMPAL EEG SPIKES: 24-HOUR RHYTHM PHASE SHIFT

5.1 Overview

To study 24-hour rhythms of neural activity, we obtained *in vivo* EEG recordings that were performed continuously throughout the pre-injury, latency, and chronic stages of a rat temporal lobe epilepsy (TLE) model.[1] [2] From this data, we extracted spontaneous large-amplitude EEG events or SPKs, which included both sharp waves (SPWs) and interictal spikes (IS) [Buzsaki et al., 1983, Suzuki and Smith, 1987]. Together, SPWs and IS have previously been used to quantify 24-hour rhythms of hippocampal neural activity [Talathi et al., 2009]. Due to their generation within the hippocampus (Buzski 1986) and the similarities in their underlying mechanisms of generation [Buzsaki et al., 1991, Leung, 1988, Suzuki and Smith, 1987], they are an ideal marker for spontaneous neural activity originating within the hippocampus. In the following sections, we report our analysis of 24-hour rhythms of these hippocampal SPKs.

5.2 Methods

5.2.1 Animal Methods and Data Collection

Animal methods, experimental timelines, and procedures for acquisition of raw data are described in the General Methods chapter (Chapter 4). An experimental timeline is supplied in Figure 4-1 of the General Methods. Our procedures for fitting of 24-hour

[1] Parts of this chapter are in press with the Journal of Neurophysiology: Stanley, D.A., Talathi, S.S., Parekh, M.B., Cordiner, D., Zhou, J., Mareci, T.H., Ditto, W.L., Carney, P.R. Local phase shift in the 24-hour rhythm of hippocampal EEG spiking activity in a rat model of temporal lobe epilepsy [Stanley et al., 2013].

[2] This work involved analysis of the Evolution into Epilepsy EEG datasets, which were collected over multiple years by Dr. Dong-Uk Hwang, Dr. Sachin S. Talathi, Dr. Junli Zhou, and other experimentalists who previously worked with Dr. Carney. Dr. Talathi also supplied code for extraction and sorting of spike data. Daniel Cordiner collected CBT data.

rhythm data to cosine functions and for extraction of theta epochs are also discussed in that chapter.

For *in vivo* EEG recordings, a total of N=5 animals were used for for EEG recording (3 spontaneously seizing, 2 stimulated but non-seizing). Additionally, N=3 rats were used for CBT recording (all spontaneously seizing).

5.2.2 Spike (SPK) Detection

From EEG data, we extracted large-amplitude EEG events, which included both hippocampal sharp waves (SPWs) and interictal spikes (IS) [Buzsaki et al., 1983, Suzuki and Smith, 1987]. We shall refer to SPWs and IS collectively as hippocampal EEG spikes (SPKs). Our procedure for identifying and sorting SPKs is detailed previously [Talathi et al., 2009]. Briefly, data from a single microwire channel in CA1 were divided into 1-hour non-overlapping epochs. High-amplitude events were detected when the signal exceeded a threshold of 5σ, where σ is the standard deviation of the data in the epoch. Events were centered and normalized within a 0.45 s window and were then input into a customized version of an established spike clustering algorithm [Fee et al., 1996]. This algorithm ensured spikes with consistent waveform were tracked throughout the experiment (Figure 5-1).

Subsequent smoothing of data and measurement of 24-hour rhythms is as described in Section 4.9 of Chapter 4.

5.2.3 Statistics

All statistical tests reported are paired-samples t tests, unless otherwise specified. In all cases, significance is considered to be $p<0.05$. Error bars represent standard error of the mean (SEM) unless otherwise stated.

5.3 Results

5.3.1 Phase Shift in 24-Hour Rhythm of EEG SPKs

Spontaneous hippocampal EEG SPKs were tracked continuously throughout the day for the pre-injury, latency, and chronic stages of TLE model rats. This was performed

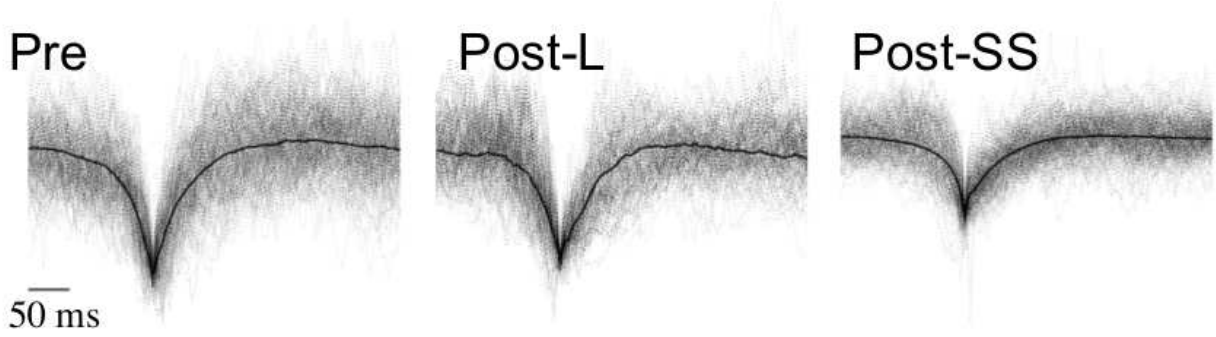

Figure 5-1. EEG spike (SPK) profiles for pre-injury (Pre), latency (Post-L) and spontaneously seizing (Post-SS) stages of epileptogenesis. Solid line shows mean shape profile and dotted lines are 200 randomly selected SPKs from a 24-hour interval.

for each animal, and data were analyzed longitudinally. SPK rates in each animal showed distinct 24-hour oscillations (Figure 5-2 A). However, following injury, a phase shift emerged of 12 h (Figure 5-2 B). This phase shift was statistically significant and persisted throughout the latency period ($p=0.010$, N=3 rats) and after the advent of spontaneous seizures (Figure 5-2 C,D) ($p=0.0078$, N=3 rats). Going from pre-injury to latency periods, the phase shifts experienced by these three animals were 11.9 ± 1.4, 9.1 ± 1.1, and 9.0 ± 0.7 hours (mean $\pm$ 95% confidence). A similar phase shift was reported previously [Talathi et al., 2009]; however, the origin of the phase shift was not clear and, furthermore, it was not clear whether the phase shift was related to the emergence of seizures. Therefore, we also analyzed SPK rates in animals that were stimulated into SE, but that did not successfully exhibit chronic spontaneous seizures. These animals were monitored for at least 4 weeks following initial SE to confirm the absence of seizures. We found that, although there was some drift in the phase, it was much less severe than for the seizing animals (Figure 5-2 E,F). Specifically, the phase shifts observed for the two non-seizing animals were 5.6 ± 2.3 and 2.5 ± 1.5 hours (mean $\pm$ 95% confidence). These data suggest that the phase shift is correlated with the

emergence of seizures following SE stimulation; however, further tests need to be done to determine whether the phase shift plays a causal role in the emergence of seizures.

While the aforementioned analysis was based on a low sample size (N=3 seizing, N=2 non-seizing animals), the results were consistent in that each of the three seizing animals showed a phase shift between 9 and 12 hours. Since phases were estimated over many circadian cycles from baseline-subtracted data, it was possible to obtain highly confident estimates of phase for each animal; the 95% confidence intervals associated with acrophase estimates were at most $\pm$1.3 hours for seizing animals, and all reported animals passed the zero-amplitude test with $p < 0.0001$ [Nelson et al., 1979]. Thus, we can be confident of the robust appearance of a phase shift in each of the three animals examined.

5.3.2 Core Body Temperature Analysis

Given that the master circadian clock in the SCN plays a central role in entraining 24-hour rhythms throughout the body, we tracked daily rhythms of CBT, a well-validated biomarker for SCN rhythms [Hofstra and de Weerd, 2008]. Overall, the phase of CBT circadian rhythms did not shift significantly during the epileptogenic period (Figure 5-3) (p=0.68, N=3 rats), although the variability in the signal did increase, as has been previously reported Quigg et al. [1999]. This suggests that the SPK phase shift cannot be attributed to a phase shift in the SCN master circadian clock.

5.3.3 Theta Activity Analysis

Perturbations to activity rhythms and sleep architecture have been reported in animal and human epilepsy [Bastlund et al., 2005, Shouse et al., 1996, Stewart and Leung, 2003], and might also contribute to the SPK phase shift. Activity and sleep state can influence SPKs by affecting the transition of the hippocampus between theta (activated) and non-theta (deactivated) states (Buzski 1996). The theta state occurs during awake mobility and rapid eye movement (REM) sleep, while the non-theta state occurs during awake immobility and slow-wave sleep [Kramis et al., 1975]. It is well

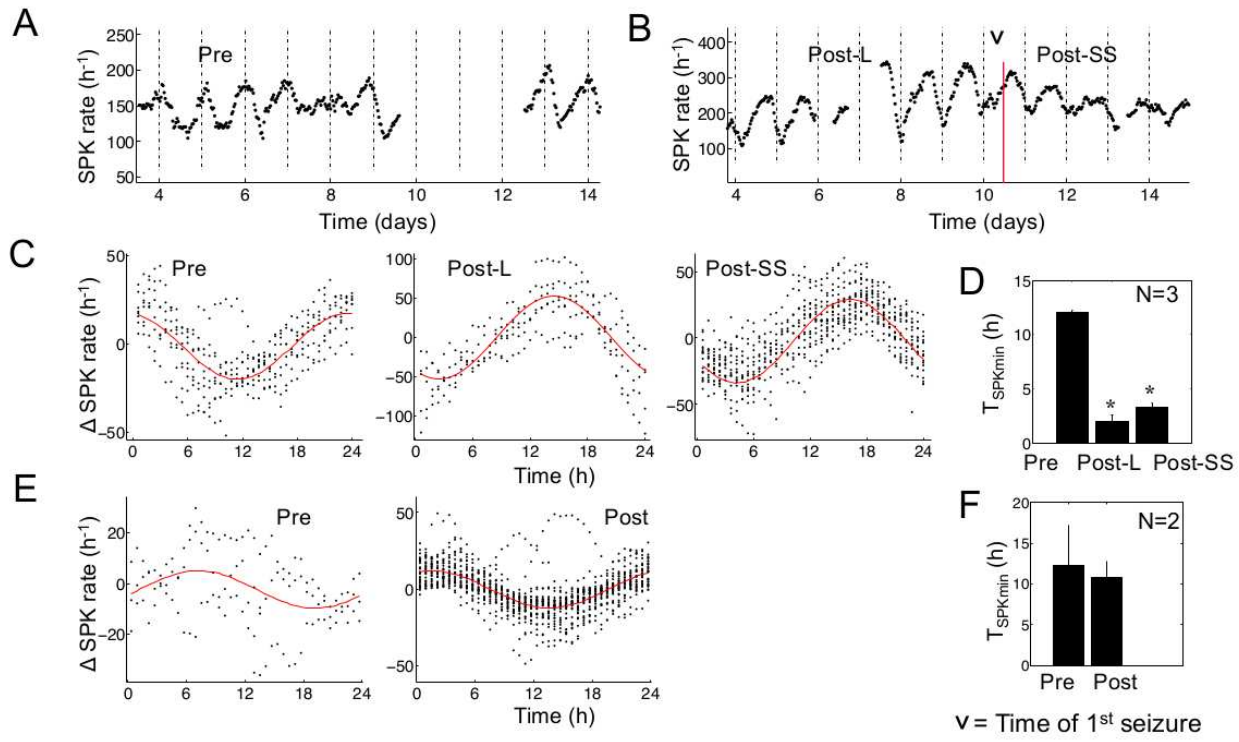

Figure 5-2. Phase shift in the 24-hour rhythm of spontaneous hippocampal EEG spikes (SPKs). (A,B) Chronic tracking of SPK rates for pre-injury (Pre), latency (Post-L), and spontaneously seizing (Post-SS) stages of epileptogenesis for a single rat. Days are marked from the start of pre-injury recording in (A) and from the day of status epilepticus in (B). Red vertical line indicates the first spontaneous seizure and dotted vertical lines correspond to 00:00 (midnight). The gaps in the traces reflect missing data due to technical problems. (C) The baseline drift in SPK rate was subtracted out and the resulting detrended time series was combined into a 24-hour time window (modulo 24). This was done for Pre, Post-L, and Post-SS stages of epileptogenesis. Cosine fits (red) reveal a phase shift post-injury. (D) Estimating the average time of minimum SPK activity across all animals showed a statistically significant phase shift during Post-L and Post-SS stages. The time of minimum SPK activity was measured to avoid the discontinuity between 23:59 and 00:00. (E) SPK rates are shown from a rat that was stimulated into status epilepticus, but that did not successfully develop spontaneous seizures following four weeks of monitoring. Pre-injury (Pre) and post-injury (Post) stages are shown. Cosine fits (red) show a slight drift in phase following injury. (F) For animals that did not develop spontaneous seizures, the phase shift post-injury did not reach significance. Values are mean $\pm$ SEM. *p $<$ 0.05 by t test.

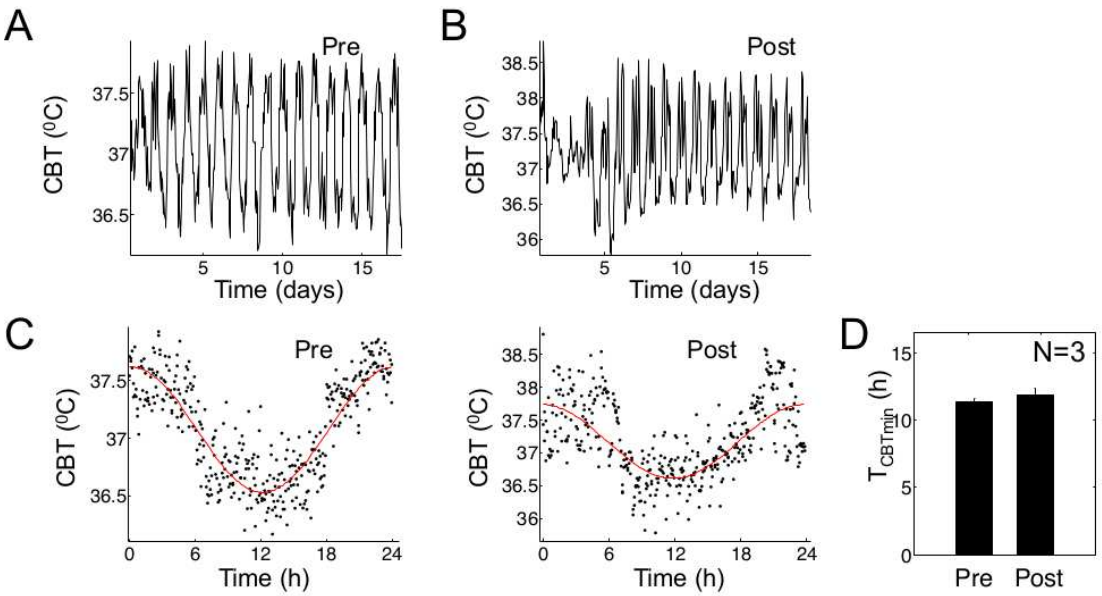

Figure 5-3. Circadian phase of core body temperature (CBT) rhythm is unperturbed following injury. (A,B) Tracking of 24-hour rhythms of CBT is shown for a single spontaneously seizing rat, pre- and post-injury, respectively. Days are marked from the start of pre-injury recording in (A) and from the day of status epilepticus in (B). (C) Data were compressed into single 24-hour time windows as in previous figures. There was no observed phase shift following injury, although the variability of the signal did increase. (D) The lack of phase shift in CBT activity following injury was consistent across rats examined. Values are mean ± SEM.

established that SPWs are absent during theta and that IS rates are substantially reduced during theta [Buzsaki et al., 1991, Leung, 1988, Suzuki and Smith, 1987]. Therefore, suppression of SPKs can emerge at different times of day resulting from activities that promote hippocampal theta.

To investigate whether hippocampal theta is altered in such a way that could affect the daily pattern of SPKs, we measured changes in the average time spent in the theta state throughout the circadian cycle. Theta was distinguished from non-theta based on the ratio between the power in the theta band (6 – 10 Hz) and the power in the delta band (1 – 6 Hz) in 2-second epochs of data [Belluscio et al., 2012, Csicsvari et al., 1998] (see Materials and Methods). Example traces of each EEG state are shown in Figure 5-4. We observed that the distribution of theta activity over the circadian cycle showed

a 24-hour rhythm that did not shift phase following injury (Figure 5-5 A–C), a result that was consistent across all rats examined (Figure 5-5 D) (p=0.71 and p=0.31 for latency and spontaneously seizing stages, respectively; N=3 rats). This suggests that the SPK phase shift is not driven by a phase shift in the daily distribution of hippocampal theta. Similar findings were obtained when varying the ratio for theta detection between 1.0 and 3.0.

SPKs may include both SPWs and IS and, as discussed above, while SPWs are absent during theta, IS can occur during theta states [Buzsaki et al., 1991, Leung, 1988, Suzuki and Smith, 1987]. Therefore, we hypothesized that the emergence of IS could contribute to the phase shift by promoting the emergence of SPKs during times of day when theta is prevalent. To investigate this, we tracked the rate of SPKs occurring exclusively in the non-theta state (Figure 5-5 E,F). Still, a phase shift of 12 hours appeared, a result that was consistent across all rats examined (p=0.0073 and p=0.00094 for latency and spontaneously seizing stages, respectively; N=3 rats). This suggests that the phase shift is not dependent on IS occurring during the theta state and, in general, is not due to the occurrence of theta state transitions.

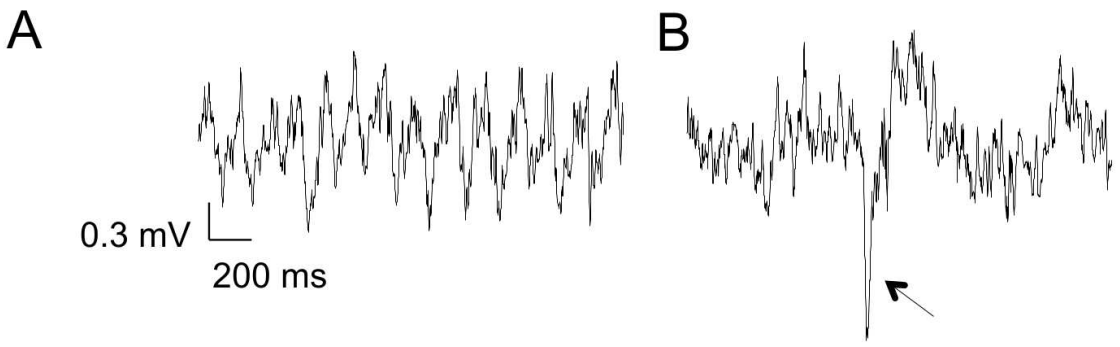

Figure 5-4. Extracted 2-second epochs of theta activity and non-theta, respectively. SPK event is indicated by arrow. Ratio of theta to delta power is 3.28 in theta (A) and 0.09 in non-theta (B).

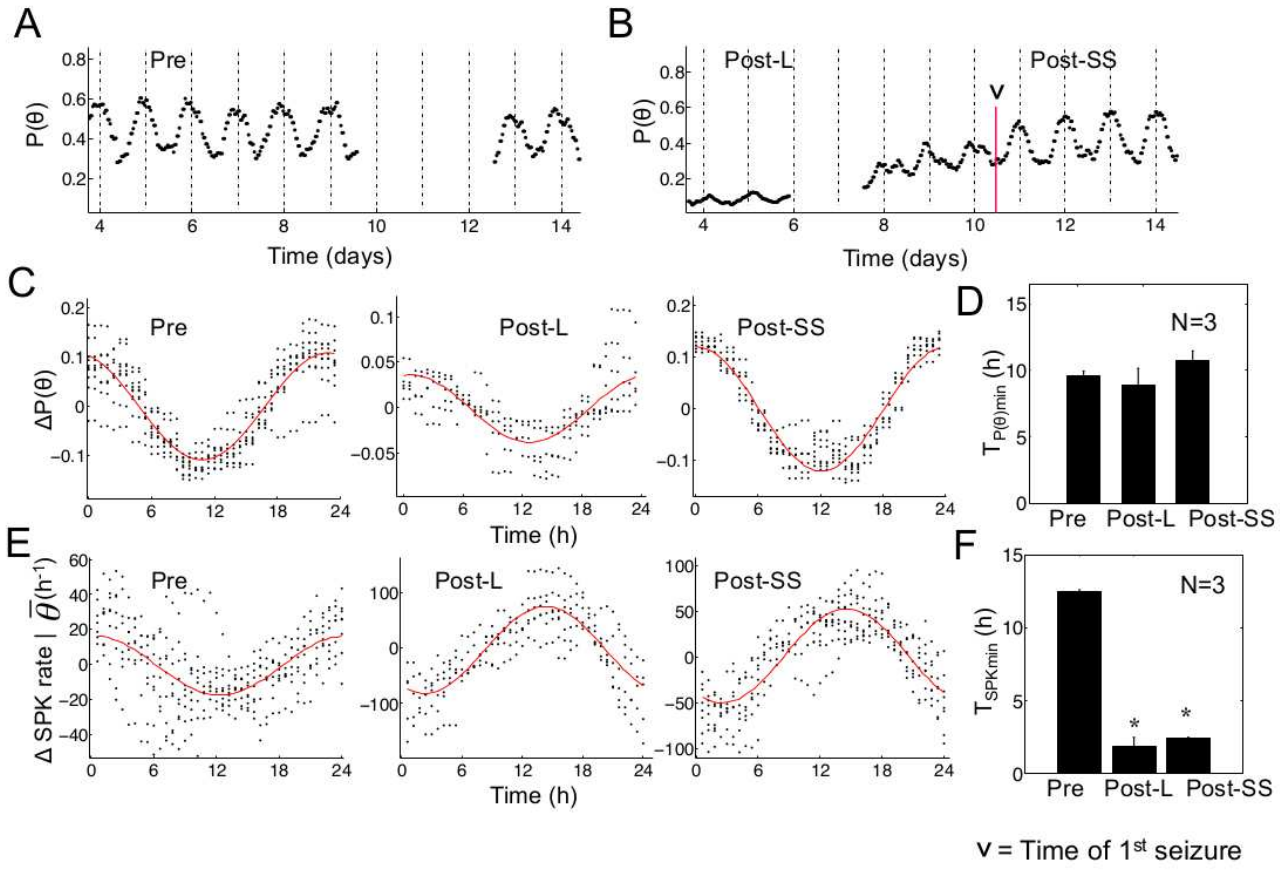

Figure 5-5. Interaction of SPKs with the 24-hour rhythm of theta activity cannot explain SPK phase shift. (A,B) Fraction of time spent in theta state for pre-injury (Pre), latency (Post-L), and spontaneously seizing (Post-SS) stages of epileptogenesis for a single rat. Days are marked from the start of pre-injury recording in (A) and from the day of status epilepticus in (B). Red vertical line marks the first spontaneous seizure. The gaps in the traces reflect missing data due to technical problems. (C) Data were compressed into a single 24-hour time window as described in previous figures. The theta activity trends show a 24-hour rhythm that does not shift phase between Pre, Post-L, and Post-SS stages. Cosine fits are indicated by solid red lines. (D) Examining the time of minimum theta activity across all rats showed that there was no significant change in the theta rhythms 24-hour oscillation. (E) Examination of SPKs exclusively in the non-theta state allowed for tracking of SPK rates independent of transitions between theta and non-theta states. As before, a phase shift was observed following injury. (F) This analysis was repeated for all rats and we observed a statistically significant phase shift between the pre-injury and post-injury stages of epileptogenesis. Values are mean $\pm$ SEM. *p $<$ 0.05 by t test.

5.4 Discussion

5.4.1 Summary of Results

We have shown that there emerges a phase shift of 12 hours in the 24-hour rhythm of hippocampal spikes in an animal model of limbic epilepsy. This phase shift was evident in all seizing animals examined, and was severely reduced in animals that were stimulated but that did not develop spontaneous seizures. We measured this phase shift relative to both the CBT rhythm and the 24-hour rhythm of hippocampal theta activity, and found that neither of these rhythms exhibited a phase shift sufficient to account for the changes in hippocampal SPKs.

5.4.2 Variability of Data in Pre-Injury Time Period of Non-Seizing Animals

It was noted that pre-injury data for the non-seizing animals showed a significant amount of variability, as evidenced by the size of the error bar in Figure 5-2 F. This may have resulted in part from the fact that technical difficulties prevented the full seven days of pre-injury data from being collected for one of these non-seizing animals. The data from the animal in question are shown as an example in Figure 5-2 E. Although this animal still passed the zero-amplitude test ($p=0.000096$), the paucity of data increased the confidence interval of this animals T_{SPKmin} to ± 2.3 hours (95% confidence interval); this is almost twice the largest confidence interval for the seizing animals, ± 1.3 hours. While the paucity of data was one factor contributing to the variability of the pre-injury data, another contributing factor may be the presence of a circadian driver that entrains not to the day-night cycle, but to another cycle in the environment. It has previously been proposed that entry into a new environment and associated food availability could affect a putative food-entrainable circadian oscillator [Munn and Bilkey, 2012]. The influence of such a circadian driver could contribute to variability in the SPK acrophase in the pre-injury period. Further tests need to be done to determine whether such variability in the pre-injury acrophase affects the likelihood of developing spontaneous seizures following SE.

5.4.3 Interictal Spikes as a Driver for the Phase Shift

To summarize our analysis of the SPK phase shift in relation to theta rhythms, we observed the following: 1) that theta rhythms do not shift phase following injury; and 2) that SPK activity exclusively within the non-theta state exhibits a phase shift. While the second point discounts the possibility that IS may contribute to the phase shift by leaking into the theta state following injury, there is yet another mechanism by which IS could be responsible for the phase shift. Specifically, it is possible that the phase shift could simply be due to an increase in the overall frequency of IS following injury, provided that these IS occur at a different circadian phase than the SPWs. Unfortunately, this possibility cannot be confirmed or denied without direct measurement of SPWs and IS. However, for several reasons, we propose that both SPWs and IS together shift towards peaking during the day post-injury. First, given the similarities in SPW and IS mechanisms of generation [Buzsaki, 1986, Suzuki and Smith, 1987], it is most likely that they are affected by circadian drivers in a similar manner and, therefore, exhibit similar circadian phases. Secondly, our analysis of EEG rhythms has shown that circadian modulation of EEG rhythm amplitude in the beta and low gamma frequency ranges also exhibits a phase shift following injury (Chapter 8). Therefore, this identification of a secondary EEG feature that also phase shifts suggests that processes other than simply the emergence of IS are involved.

CHAPTER 6
MECHANISMS FOR CIRCADIAN RHYTHM PHASE SHIFTING

6.1 Overview

In this chapter, we develop a detailed computer model incorporating realistic circadian inputs in order to explain our experimental observations.[1] These observations are outlined in the previous chapter, in which we report a phase shift in the 24-hour rhythm of hippocampal spiking activity in epileptic rats. We also found that the circadian phases of CBT and hippocampal theta activity rhythms stationary, suggesting that the phase shift did not result from alteration to the SCN rhythm or wake-sleep cycle. Therefore, we here investigate alternate mechanisms that could account for the SPK phase shift. As discussed earlier, the circadian system is organized into a hierarchy of relay centers. While the SCN itself does not project directly to the hippocampus, the hippocampus receives circadian input from many other relay centers. It is possible that permanent damage to these centers, as has been hypothesized to occur in multiple types of epilepsy [Quigg, 2000], could contribute to the experimentally observed phase shift. The ideas in this chapter were initially presented at OCNS 2011 [Stanley et al., 2011a].

6.2 Methods

6.2.1 Modeling Overview

To investigate this hypothesis, we implemented a detailed computer model of circadian regulation in a hippocampal neural network. Three types of hippocampal neurons were modeled, namely, pyramidal cells, basket cells, and O-LM cells (Figure 6-2A). In addition, we included a population of MSG neurons. The models parameters

[1] Parts of this chapter are in press with the Journal of Neurophysiology: Stanley, D.A., Talathi, S.S., Parekh, M.B., Cordiner, D., Zhou, J., Mareci, T.H., Ditto, W.L., Carney, P.R. Local phase shift in the 24-hour rhythm of hippocampal EEG spiking activity in a rat model of temporal lobe epilepsy [Stanley et al., 2013].

and network connectivity were based on the CA3 network (Figure 6-1), which controls the initiation of the CA1 SPKs [Buzsaki, 1986, Ellender et al., 2010].

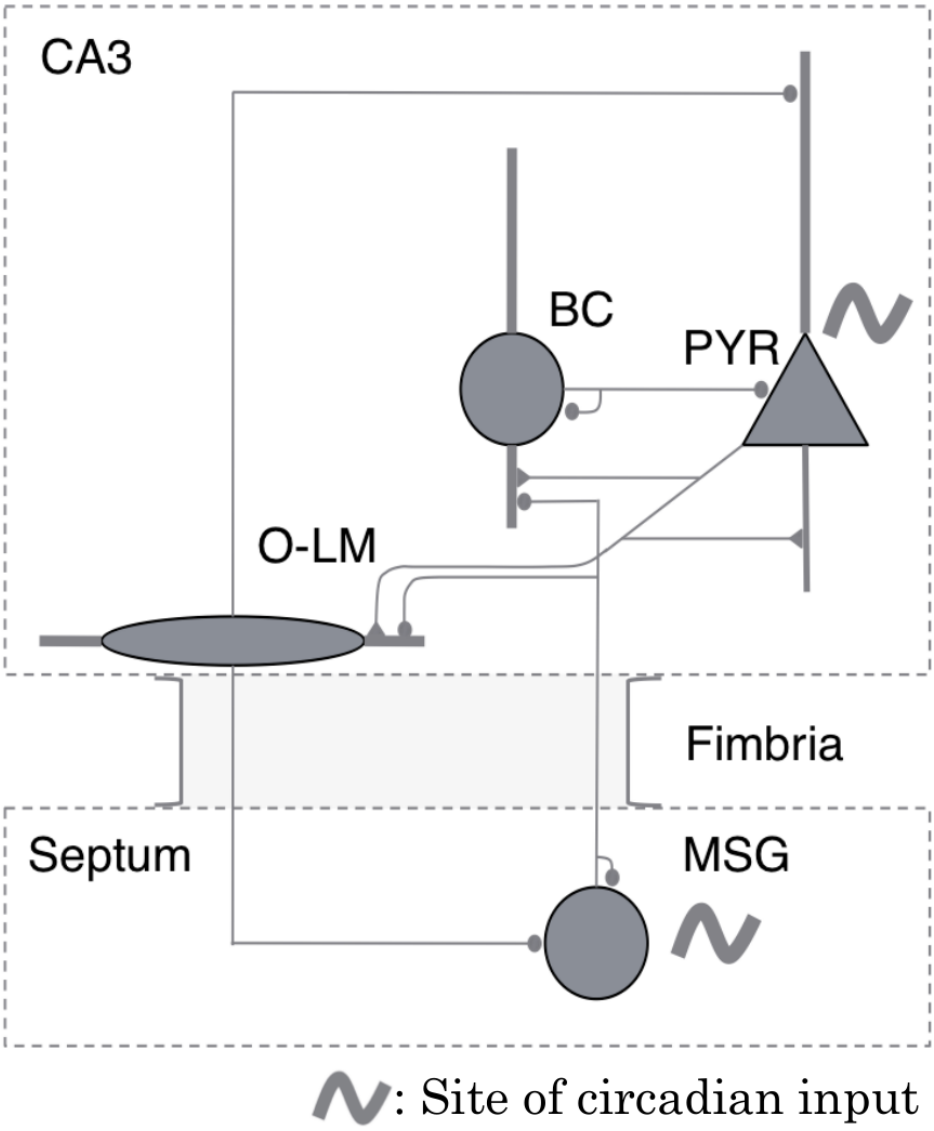

Figure 6-1. Network connectivity in the neural network model. Sites of circadian input to region CA3 and to the medial septum are indicated by tilde marks. Additionally, all GABAergic synapses are subject to circadian modulation by melatonin. BC=basket cells; MSG=medial septal GABAergic interneurons; O-LM=stratum oriens interneurons projecting into lacunosum moleculare; PYR=pyramidal neuron.

Representation of circadian input in the model was based on evidence that multiple sources of circadian drive interact in the hippocampus to produce an overall 24-hour

rhythm. For example, it was recently shown that daily variations in CA1 evoked responses are altered but not eliminated by melatonin knock out [Chaudhury et al., 2005], suggesting the overlapping influence of multiple circadian factors. Three circadian inputs were modeled: circadian modulation of medial septum neural activity, nighttime release of melatonin, and diurnal modulation of hippocampal pyramidal cells. These inputs are based on known physiology and the model was validated to reproduce findings from several experimental studies: rhythmic cycling of pyramidal cell firing rate, peaking during the day [Brunel and de Montigny, 1987]; increased nighttime inhibitory drive following SE injury [Matzen et al., 2012]; and also increased neural activity in response to elevated melatonin [Musshoff et al., 2002].

6.2.2 CA3 Network Model

Our in vivo analysis tracked 24-hour oscillations in the rate of spontaneous hippocampal SPKs. The SPKs recorded experimentally in CA1 are known to originate as a result of synchronous population bursts in CA3 circuitry [Buzsaki, 1986]. Therefore, modeling efforts were focused on circadian regulation of neural activity in region CA3. The network model contained 200 CA3 pyramidal cells, 25 basket cells, and 25 stratum oriens interneurons that project into the lacunosum moleculare (O-LM). In addition, to represent circadian input from the medial septum, we also included a population of medial septal GABAergic (MSG) neurons. We focused specifically on septal GABAergic rather than septal cholinergic input because pharmacological [Buzsaki, 1986, Suzuki and Smith, 1988b] and lesioning [Lee et al., 1994] studies have shown little cholinergic effect on SPK rates in vivo.

The pyramidal neuron model was comprised of 19 compartments, with 8 compartments for the basal dendrites, 10 for the apical dendrites, and a single somatic compartment [Traub et al., 1991]. Each compartment contained active and passive channel conductances [Hodgkin and Huxley, 1952] and was connected to other compartments by passive

resistances [Rall, 1962]. The cable equations for the membrane voltage, V_i, in compartment i are described below.

$$C_{m,i}\frac{dV_i}{dt} = \sum_{j=1}^{19} G_{i,j}(V_j - V_i) - I_{int,i} - I_{syn,i} - I_{leak,i} + I_{inj,i} \tag{6–1}$$

$$I_{int,i} = I_{Na} + I_{K_{DR}} + I_{Ca} + I_{K_{AHP}} + I_{K_C} + I_{K_A} \tag{6–2}$$

In these equations, $G_{i,j}$ is the specific axial conductance between compartments i and j ($G_{i,j} = 0$ for unconnected compartments; $G_{i,i} = 0$ for all i) and $C_{m,i}$ is the specific membrane capacitance. $I_{int,i}$ represents the sum of the following intrinsic ionic currents: sodium (Na); delayed rectifier potassium (K_{DR}); A-type transient potassium (K_A); calcium (Ca); calcium-dependent potassium (K_{AHP}); and calcium- and voltage-dependent potassium (K_C). These currents are described by the Hodgkin-Huxley formalism, $I_k = \bar{g}_k g_k (V - E_k)$, where $\bar{g}_k$ and E_k are ion channel maximal conductance and reversal potential, respectively. g_k is a product of Hodgkin-Huxley type gating variables x with first order kinetics of the form $dx(V,t)/dt = \alpha(V)(1-x) - \beta(V)x$. $\alpha(V)$ and $\beta(V)$ are derived from empirical fits to experimental data [Traub et al., 1991]. Similarly, I_{syn} represents the sum of all synaptic currents, $I_{syn} = \sum_k \bar{g}_{syn,k} s_k (V - E_{syn,k})$. Each term in this sum reflects a specific presynaptic neuron and network properties are provided in the following section. Variables $\bar{g}_{syn,k}$ and $E_{syn,k}$ are channel maximal conductance and reversal potential, respectively. The gating variable for the synapse, s_k, is calculated by the *synchan* object in GENESIS [Bower and Beeman, 2003], and uses the impulse response function $A(e^{-t/\tau_1} - e^{-t/\tau_2})/(\tau_1 - \tau_2)$. In this equation, A is a normalizing factor and τ_1 and τ_2 are synaptic time constants. They are specific to the type of synapse and are described in the section below. $I_{leak,i}$ represents leak through the compartment's membrane and $I_{inj,i}$ is direct current injection applied to the soma and was set to 500 pA.

All biophysical parameters, including values for rate constants, maximal conductances, reversal potentials, calcium accumulation, and compartmental geometries, are taken directly from the GENESIS implementation of Traub et al. [1991].

For all interneurons, we used a single compartment to represent the cell. Basket cells are based on Wang and Buzsaki [1996], while O-LM and MSG cells are based on Wang [2002]. Code for all interneurons was derived from the implementation by Hajos et al. [2004], which is available on ModelDB (accession number 116567) [Hines et al., 2004, Migliore et al., 2003]. The voltage equation for all interneuron types assumes the form below.

$$C_{m,i}\frac{dV_i}{dt} = -I_{int} - I_{syn} - I_{leak} + I_{inj} \tag{6–3}$$

Intrinsic currents, I_{int}, are specific to each interneuron type as follows: basket $I_{int} = I_{Na}+I_{K_{DR}}$; O-LM $I_{int} = I_{Na}+I_{K_{DR}}+I_H+I_{CA}+I_{K_{Ca}}$; MSG $I_{int} = I_{Na}+I_{K_{DR}}+I_{K_S}$. Here, Na and K_{DR} are sodium and delayed-rectifier potassium, respectively, while Ca is high-voltage activated calcium, K_{Ca} is calcium-dependent potassium, K_s is slowly inactivating potassium, and h is the hyperpolarization-activated cation current. Full descriptions of the rate constants underlying these currents have been previously published [Hajos et al., 2004, Wang, 2002, Wang and Buzsaki, 1996]. Default current injection values, I_{inj}, for basket, O-LM, and MSG were 0 pA, -10 pA, and 21 pA, respectively.

Simulations were run in GENESIS 2.3 [Bower and Beeman, 2003, Bower et al., 2002] on a Mac XServ cluster, and data were analyzed in Matlab R2011a. The complete GENESIS code is available on ModelDB, accession number 142104.

6.2.3 Network Properties

The CA3 network properties were specified in terms of synaptic strengths, synaptic time constants, and synaptic connectivity. Synaptic currents were implemented with the standard double-exponential mechanism, using the GENESIS *synchan* object [Bower

and Beeman, 2003] (details above). Pyramidal cells formed AMPA synapses, while all interneurons formed $GABA_A$ synapses. Table 6-1 lists synaptic strengths, specifying the maximal conductance of a given synaptic connection. These values were based on experimentally measured unitary excitatory/inhibitory postsynaptic potential values [Traub and Miles, 1991, Traub et al., 1999a], where available, as well as on previous models [Hajos et al., 2004, Neymotin et al., 2011, Taxidis et al., 2012]. Synaptic time constants were those used in [Neymotin et al., 2011], with AMPA synapses having τ_1 = 0.05 ms and τ_2 = 5.3 ms. All GABAergic synapses had τ_1 = 0.07 and τ_2 = 9.1 ms, with the exception of synapses with presynaptic O-LM cells. In such cases, τ_1 = 0.2 and τ_2 = 20 ms (Neymotin et al. 2011). A schematic diagram of the network connectivity is shown in Figure 6-1 and in Table 6-2 we report network connectivity in terms of the number of presynaptic neurons converging on each postsynaptic neuron. Connectivity values were derived from paired recordings of presynaptic and postsynaptic cells [Traub and Miles, 1991] as well as from previous modeling studies [Hajos et al., 2004, Neymotin et al., 2011, Taxidis et al., 2012, Traub et al., 1996]. Pyramidal cells received innervation from other pyramidal cells in the basal dendrites (4th basal compartment from the soma). Basket cells innervated the soma of pyramidal cells, whereas O-LM cells innervated the distal apical dendrites (9th apical compartment from the soma).

Table 6-1. Maximal synaptic conductances (nS)

	Postsynaptic			
Presynaptic	Pyramidal	Basket	O-LM	MSG
Pyr	2.6	0.05	0.05	
Basket	9.2	0.125		
O-LM	8.3			
MSG		0.5	0.5	0.25

6.2.4 Background Activity

The background network activity was modeled by Poisson-distributed excitatory and inhibitory postsynaptic potentials. These synapses impinged on the soma of pyramidal cells and interneurons, and also on the most distal apical dendritic compartment of

Table 6-2. CA3 network connectivity expressed in terms of synaptic convergence

Presynaptic	Postsynaptic Pyramidal	Basket	O-LM	MSG
Pyr	10	20	10	
Basket	15	25		
O-LM	10			
MSG		5	5	10

pyramidal cells. The mean frequency of AMPA and GABA background events was 1000 Hz, and the maximal background synaptic conductances are provided in Table 6-3. These values were chosen to provide symmetric resting membrane potential fluctuations at -65mV with standard deviations between 1 and 2 mV (Destexhe et al. 2003).

Table 6-3. Background synaptic activity

Cell	Synapse	Section	Conductance (nS)
Pyramidal	AMPA	Soma	1.0
Pyramidal	AMPA	Dendrite	1.0
Basket	AMPA	Soma	0.03
O-LM	AMPA	Soma	0.03
Pyramidal	$GABA_A$	Soma	2.5
Pyramidal	$GABA_A$	Dendrite	2.5
Basket	$GABA_A$	Soma	0.01
O-LM	$GABA_A$	Soma	0.01

6.2.5 Circadian Modulation

To represent circadian drive, we incorporated three major inputs to the model that were subject to 24-hour modulation (Figure 6-1). These inputs were defined as a function of the 24-hour circadian time variable, T, with T = 0 h corresponding to midnight and T = 12 h to noon. Each circadian input was controlled by a circadian scaling factor (Figure 6-2B), defined below. Since circadian changes happen on much slower timescales as compared to the neural networks dynamics, a total of 16 separate simulations were run, in which T was varied as a model parameter. Each simulation produced 10 seconds of data, and the first second was discarded prior to analysis in order to remove transient effects.

The first circadian input was modulation of the medial septum. Multiunit recordings have shown that medial septum activity possesses a robust circadian rhythm, peaking at night [Yamazaki et al., 1998]. Modulation of the medial septum was achieved by scaling the tonic current injection, I_{inj}, to MSG cells: $I_{inj} = \bar{I}_{inj} S_{septal}$. In this equation, $\bar{I}_{inj}$ is the default current injection for MSG cells, as described above, $S_{septal} = (1 + C_{septal} cos(2\pi T/24)$ is the septal circadian scaling factor, and C_{septal} = 0.25 is the septal circadian scaling coefficient. This input caused maximal septal activity to peak when T = 0 h. In our model, we focused specifically on septal GABAergic input because, as mentioned above, previous studies have shown little cholinergic effect on SPK rates in vivo [Buzsaki, 1986, Lee et al., 1994, Suzuki and Smith, 1988b].

Second, melatonin, a primary systemic output of the circadian system, is released nightly by the pineal gland. In the hippocampus, melatonin has an excitatory effect and decreases the strength of GABAergic inhibition [Wan et al., 1999]. To account for the effects of melatonin, all GABAergic maximal synaptic conductances (including background synapses) were multiplied by the scaling factor $S_{mel} = 1 + C_{mel} cos(2\pi(T - 12)/24)$, producing maximum attenuation of GABA at night. C_{mel}=0.10 with the exception of Figure 6-2E, where C_{mel} is varied across a range of parameters (described below).

Finally, a variety of other factors can also influence CA3 activity, including 24-hour variation of CA3 pyramidal neuron calcium currents [Kole et al., 2001], adenosine release [Liu et al., 2000], and neuromodulatory effects. As a simplifying assumption, we represented the combined effects of these additional circadian inputs by sinusoidal modulation of pyramidal cell current injection. Experimental studies suggest that 24-hour modulation of CA3 pyramidal cell firing activity peaks during the day [Brunel and de Montigny, 1987] and, therefore, pyramidal current injection was modulated as follows: $I_{inj} = \bar{I}_{inj} S_{pyr}$, where $\bar{I}_{inj}$ is the default current injection for pyramidal cells, as described above; $S_{pyr} = (1 + C_{pyr} cos(2\pi(T - 12)/24)$; and C_{pyr} = 0.25. Values of the

septal, melatonin, and pyramidal circadian scalings factors as a function of time of day are summarized in Figure 6-2B.

The default strengths of the circadian scaling coefficients C_{septal}, C_{mel} and C_{pyr} were based on experimental studies where available. Specifically, C_{mel} = 0.10 was chosen to produce an approximately 20% change in $GABA_A$ currents, consistent with that observed upon application of physiological levels of melatonin in slice [Wan et al., 1999]. C_{pyr} was constrained so that pyramidal cell firing peaked during the day, in order to ensure agreement with experimental measurements [Brunel and de Montigny, 1987], although we note that this experimentally measured daytime peak showed a seasonal dependence as well. C_{septal} was chosen such that interneurons were entrained to septal circadian drive. Thus, while C_{mel} was constrained by direct experimental measurement, C_{pyr} and C_{septal} were adjusted as parameters to enable the model to reproduce functional activity.

6.2.6 Sensitivity Analysis

To evaluate the sensitivity of our modeling results to variation in the relative strengths of circadian inputs, we swept melatonin and septal circadian inputs through a range of values. The strength of the melatonin circadian input was varied by sweeping C_{mel} between 0.05 and 0.18. The strength of medial septal innervation was varied by randomly disabling MSG cells, so as to simulate injury to the septum. The percentage of remaining MSG cells, $fMSG$, was varied between 0 and 100%. All other parameters were held at their default values. For each (C_{mel}, $fMSG$) pair of values, a set of simulations were run in which circadian time T was varied and the resulting firing rate data were fit to a sinusoid with 24-hour period to estimate acrophase. For some iterations of the simulation, instances arose when sinusoids could not be reliably fit to the data. Generally, these instances corresponded to situations wherein the relationship between firing rate and time was either non-sinusoidal or of very low amplitude. Therefore, we rejected fits for which the mean squared error (MSE) was

greater than 33% of the datas variance and for which the amplitude of the sinusoidal oscillation was less than 3% of the mean firing rate.

We also investigated the sensitivity of the model to changes in its internal network connectivity. Drastic network changes could alter the firing activity patterns produced by the network. Subtler network changes could affect how 24-hour rhythms propagated throughout the network. However, in most cases, the network was stable for changes in convergence values by 5 neurons. We also found that increasing the parameters C_{pyr} and C_{septal}, which we tuned as free parameters, could often counteract the effects on network 24-hour rhythms of decreased network convergence, and vice versa.

6.3 Results

As described in the computer model received three major circadian inputs. Examples of neural firing and circadian scaling factor inputs are shown in Figure 6-2A, B. When all three circadian inputs were included, pyramidal, O-LM, and basket cell firing rates oscillated in phase, peaking at noon (Figure 6-2C). To represent injury, we explored the effects of removing one of the circadian inputs, specifically, the input from MSG cells. This caused basket cell firing acrophase to shift to the night, while pyramidals still peaked at noon (Figure 6-2D). Pyramidal cell oscillations also showed an increase in amplitude, resulting in a clear phase misalignment with basket cells. O-LM cells still peaked weakly at noon, but they too could exhibit a weak nighttime peak with increased melatonin drive. To further investigate the origins of the basket cell phase shift, we systematically varied the strengths of both septal and melatonin inputs (Figure 6-2E). When the septal input was sufficiently stronger than the melatonin drive, basket cell firing peaked during the day and, when the converse was true, it peaked during the night. Increasing the amplitude of the pyramidal cell circadian drive elevated the boundary region vertically (not shown). In general, in order for the basket cell phase shift to occur, the septal circadian input must dominate in the healthy state and then be sufficiently damaged such that the boundary between these two phase-regimes

is crossed. The thinness of the boundary region implies sensitivity to small changes in circadian drive; in some cases even an $\approx$ 20% reduction in septal innervation was sufficient to produce a phase shift, an amount that is comparable with cell loss reported in other parahippocampal regions [Gorter et al., 2003]. These results show that phase shifting of hippocampal neural activity can emerge following a change in the balance of circadian inputs. As we shall discuss, this phase shifting of neural firing rates might have direct relevance for explaining the phase shift in experimentally measured SPKs, and might also be relevant for the determining the daily timing of epileptic seizures.

6.4 Discussion

6.4.1 Generality of the Computer Model to Alternative Sources of Circadian Perturbation

While our MRI characterization focused specifically on changes in the medial septum, our computer model displayed a phase shift in the circadian rhythm of basket cell firing due to changes in the melatonin circadian input (Figure 6-2E) as well. Such a phase shift could also be observed for changes in the strength of the pyramidal circadian input (not shown). Therefore, the mechanism for producing a phase shift by altering the relative balance of circadian drive appears general and independent of the nature of the specific circadian drivers involved. Our MRI structural characterization of the medial septum suggests that damage to the septum is one source for producing altered circadian drive. Damage to the septum is also supported by previous studies [Gorter et al., 2001, 2003]. However, it is possible that other circadian drivers could also be modified so as to contribute to the phase shift. For example, changes in melatonin levels have been reported in epileptics, although there is conflicting evidence as to whether melatonin is increased or decreased in the absence of seizures [Bazil et al., 2000, Hofstra and de Weerd, 2009, Schapel et al., 1995]. Likewise, damage to other nuclei under circadian influence, such as the orexin-secreting cells in the hypothalamus [Peyron et al., 1998, Selbach et al., 2004], histamine-secreting cells in

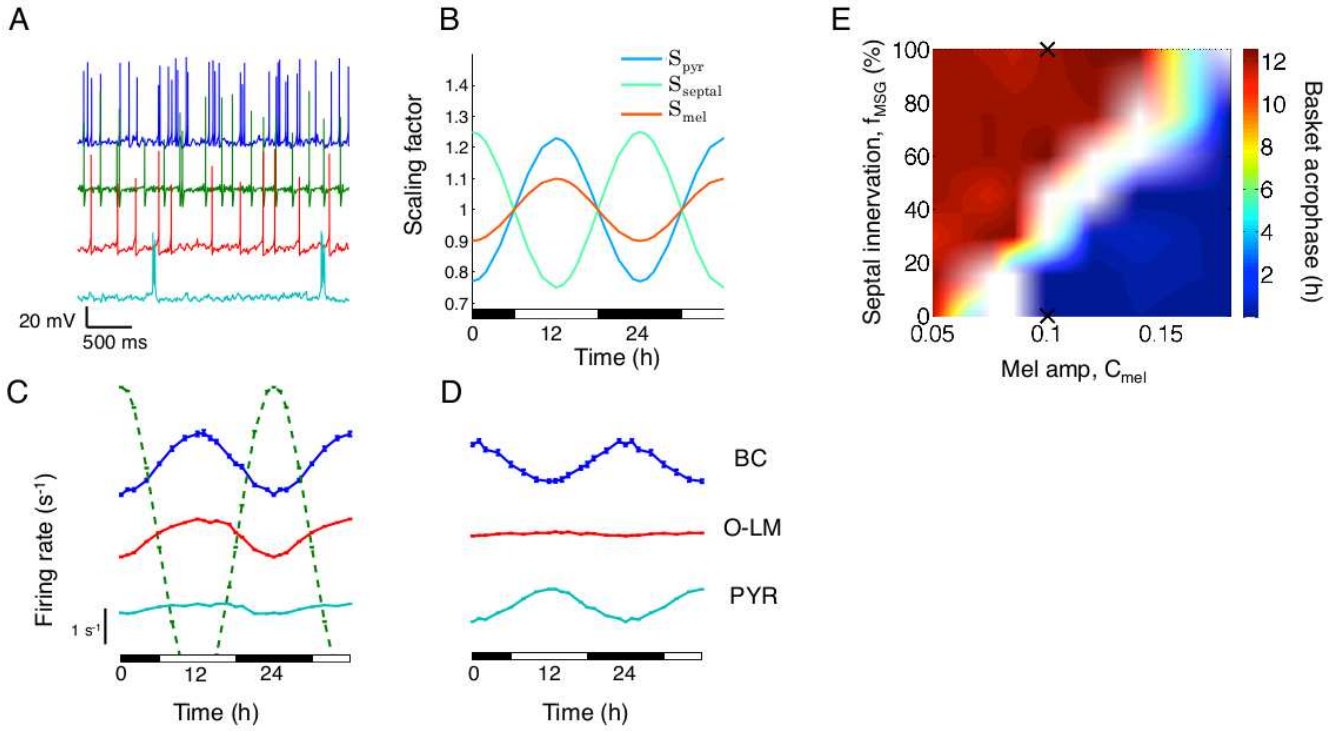

Figure 6-2. Damage to the medial septum can produce a circadian phase shift by altering the balance of circadian input. (A) Voltage traces showing examples of neural activity produced by the model. Cell types from top to bottom are BC, MSG, O-LM, and PYR and are colored blue, green, red, and cyan, respectively. (B) Three circadian inputs were included: circadian modulation of pyramidal cell current injection, circadian modulation of medial septal GABAergic cell current injection, and nightly attenuation of $GABA_A$ synaptic transmission by melatonin. Each input was simulated by adjusting its respective scaling factor, Spyr, Sseptal, and Smel (see Materials and Methods). (C,D) Simulations of neural activity before (C) and after (D) the complete removal of medial septum input show a 1800 phase shift in basket cell circadian rhythms. MSG cells are indicated by dotted green line. (E) Basket cell firing acrophase is a function of the percentage of septal innervation, fMSG, and the melatonin circadian scaling coefficient, C_{mel} (see Materials and Methods). Crosses mark simulation configurations in C,D; regions where sinusoids cannot be reliably fitted for phase estimation are shaded white. For a phase shift to occur, medial septal input must be sufficiently damaged such that the white boundary region is crossed. Error bars mean $\pm$ SEM. BC = basket cells; MSG = medial septal GABAergic interneurons; O-LM = stratum oriens interneurons projecting into the lacunosum moleculare; PYR = pyramidal neurons.

the tuberomammillary nuclei [Yanovsky and Haas, 1998], or serotonin-producing cells of the raphe nuclei [Assaf and Miller, 1978, Kubota et al., 2003], may also be relevant. In general, it is possible that any circadian input that meets the following three criteria could be relevant for influencing the SPK phase shift: 1) has the ability to influence the rate of hippocampal SPKs; 2) shows evidence of 24-hour rhythms; 3) experiences damage or alteration following SE. While the medial septum meets these criteria, other sources of circadian input may be relevant as well. It is also feasible that connectivity within the CA3 network might be altered during epileptogenesis. We investigated this possibility by changing network convergences while holding other parameters constant, and found that this could produce a phase shift under certain circumstances. For example, one such condition was a reduction in the convergence of pyramidal cells on basket cells. As pyramidal cells reached peak firing during the day, loss of their input to basket cells allowed the underlying melatonin circadian drive to promote peak firing at night, thereby producing a phase shift. Thus, loss of principal cell input to basket cells due to necrotic processes might also be a contributing factor to a phase shift. This investigation also underscores the principle that many parameter changes can lead to a phase shift via the same underlying mechanism, namely, a change in the balance of circadian drive to a given cell type.

6.4.2 Relationship Between Experimental SPK Phase Shift and Computer Modeling Results

An implicit assumption in our computer modeling work is that the phase shift in the circadian rhythm of SPKs is directly related to hippocampal neural firing activity. While the neural mechanisms of SPK initiation are not yet fully understood, recent studies have shown that SPK rates are influenced by neuron firing. In particular, an in vitro study showed that direct stimulation of individual perisomatic-targeting interneurons, but not other cell types, was sufficient to affect the probability of CA3 population bursts [Ellender et al., 2010]. Interestingly, our computer model also predicted that a phase

shift would emerge specifically in basket cells firing following loss of septal input (Figure 6-2). Basket cells were most susceptible to phase shifting because they were strongly influenced by both the septal and the melatonin circadian inputs. For example, while O-LM cells were also driven by the septal circadian input, they were less influenced by melatonin owing to their lack of recurrent GABAergic connectivity. For other values of circadian scaling coefficients (specifically increased C_{mel} and C_{septal}), we observed that phase shifts could occur for O-LM and pyramidal cells as well. Therefore, it is possible that changes in the firing patterns of other neuron types or, alternatively, changes in network properties, such as synchronization, might also contribute to the circadian phase shift.

CHAPTER 7
STRUCTURAL CHANGE IN THE CIRCADIAN SYSTEM

7.1 Background and Overview

Our modeling work has suggested that changes in the strength of circadian inputs can produce a phase shift in hippocampal 24-hour rhythms, even when the phases of the individual circadian inputs remain constant.[1] [2] Such altered circadian drive could arise from damage to circadian relay centers, as has been proposed to occur in epilepsy [Quigg, 2000].

There are a number of circadian relay centers that could be damaged so as to contribute to this phase shift. We chose specifically to examine the medial septum for signs of structural change for a number of reasons. First, it was recently proposed based on cognitive studies that the septum could be an important circadian relay center between the SCN and the hippocampus [Ruby et al., 2008]. Multiunit recordings have shown that the septum possesses a robust circadian rhythm that persists in the absence of external light/dark cues [Yamazaki et al., 1998]. Furthermore, it is well established from tracing studies that the septum, unlike the hippocampus, receives heavy innervation from the SCN [Morin et al., 1994]. In turn, the medial septum is perhaps the most critical subcortical input to the hippocampus, and lesioning studies have shown that the septum strongly influences the rate of spontaneous generation of SPKs [Buzsaki, 1986, Suzuki and Smith, 1988a]. Given that the medial septum exhibits both circadian rhythmicity and also the ability to regulate hippocampal SPKs, we proceeded to investigate anatomical changes in the medial septum using MRI structural

[1] Parts of this chapter are in press with the Journal of Neurophysiology: Stanley, D.A., Talathi, S.S., Parekh, M.B., Cordiner, D., Zhou, J., Mareci, T.H., Ditto, W.L., Carney, P.R. Local phase shift in the 24-hour rhythm of hippocampal EEG spiking activity in a rat model of temporal lobe epilepsy [Stanley et al., 2013].

[2] This work was made possible by the analysis of MRI data, collected by Dr. Mansi B. Parekh. Dr. Parekh also performed the fiber tracking analysis.

analysis. The data in this chapter were originally presented at Sleep 2012 [Stanley et al., 2012].

7.2 Methods

7.2.1 Animal Methods

General methods for animal handling and induction of the temporal lobe epilepsy (TLE) model are as described in the General Methods chapter (Chapter 4).

7.2.2 Experimental Timeline

A total of N=11 animals were used for excised MRI (3 control, 8 spontaneously seizing). Of the 8 spontaneously seizing animals used for excised MRI, N=6 also provided usable data for longitudinal in vivo imaging. Animals were monitored for at most 60 days. The experimental timeline for rats undergoing MRI is shown in Figure 7-1.

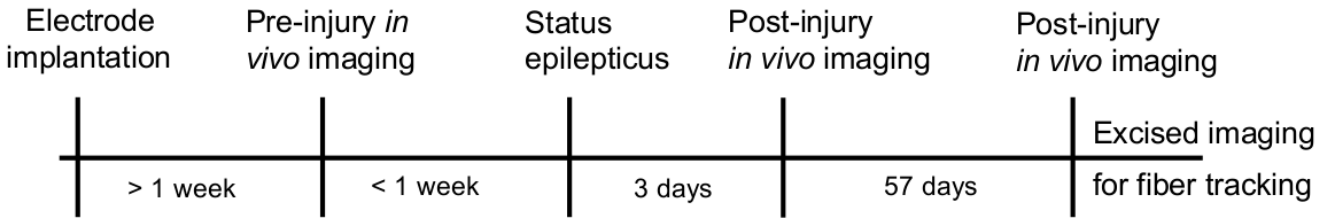

Figure 7-1. Experimental timeline for rat MRI.

7.2.3 MRI Data Collection and Analysis

For MRI, the rats were continuously video/EEG recorded for a period of 60 days post-SE. Temporal changes in the rat brains were monitored in vivo with MRI pre-SE and also at days 3 and 60 post-SE at 11.1 Tesla. The rats were initially anesthetized with 4% isoflurane in 2.0 L/min O_2 and then 4 mg/kg of xylazine was injected subcutaneously, along with 2 mL of lactated Ringer's solution (Hospira, Lake Forrest, IL) to maintain the physical condition of the rats during the extended MRI scans. Each rat was placed in a prone position, in a custom-made MRI-compatible stereotaxic frame and cradle, to allow repeatable positioning and minimize motion artifacts. In the magnet, anesthesia was maintained with 1.5 – 2.0% isoflurane in O_2 at

1 L/min. Respiration and temperature were monitored and physiological temperature was maintained using heated air flowing over the animal (SA Instruments, Stony Brook, NY). Magnetic resonance was measured using a custom-built, saddle shaped 470 MHz coil, for both excitation and detection, positioned on top of the rat's head and centered over the brain. In vivo acquisition parameters for diffusion-weighted imaging and T2 measurements have previously been published [Parekh et al., 2010]. Diffusion weighted imaging (DWI) data were collected in 27 directions with a b-value of 800 s/mm^2 and in 6 directions with a b-value of 100 s/mm^2, and were then fitted to a rank-2 tensor to calculate AD (average diffusivity) and FA (fractional anisotropy). A region of interest was manually drawn for the medial septum to quantify AD, FA, and T2 relaxation times. After the rats were imaged in vivo at the 60 days post-SE time point, they were transcardially perfused and the brains excised and stored in 10% formalin. High angular resolution diffusion imaging (HARDI) data were collected from excised brains in 46 directions with a b-value of 1000 s/mm^2 and in 6 directions with a b-value of 100 s/mm^2 [Parekh et al., 2010]. The log of the image intensity for each voxel for HARDI data was fit linearly to a rank-2 tensor model of diffusion (i.e. diffusion tensor imaging, DTI) as a function of the diffusion weighting, and the AD and FA values were calculated from the resulting tensor [Basser, 1995] for the fimbria and medial septum. For fiber tracking, the diffusion displacement probability distribution function at each voxel was estimated using the Mixture of Wisharts (MOW) approach to fit a continuous distribution of diffusion tensors [Jian et al., 2007]. This post-processing method allowed for the resolution of complex fiber structures, such as crossing and kissing fibers within a voxel. Tractography was performed on the entire imaged brain by seeding all voxels with the following parameters: 64 seeds per voxel; a step size of 0.5 of the voxel length, with a turning angle threshold of 50; and an FA threshold of 0.05 at each step. The fimbria region of interest was used to then filter out fibers that passed through the region. Fibers

that traversed the corpus callosum were excluded. All statistical tests reported are paired-samples t tests unless otherwise specified.

7.3 Results

To study anatomical changes in the medial septum, we performed a longitudinal structural characterization with high field diffusion- and T2-weighted MRI. From diffusion-weighted MRI data, we calculated measures of AD and FA, which provide information about the magnitude and directionality of molecular displacement, respectively [Pierpaoli et al., 1996]. In vivo MRI of the medial septum showed a statistically significant increase in AD and a reduction in T2 relaxometry at 60 days post-SE (Figure 7-2A). The increase in AD is suggestive of cell loss, and the reduced T2 likely reflects the sequestering of iron by microglia and astrocytes, which form scars in response to neuronal damage [Zatta, 2003]. Changes were seen at 3 days post-SE, reflecting local edema. While these changes do not reach significance, histological studies in a similar animal model have confirmed early cell loss in the septal areas following SE [Gorter et al., 2001, 2003]. Since the medial septum projects to the hippocampus primarily by way of the fimbria [Peterson et al., 1987a], we performed fiber tracking analysis of the fimbria based on excised diffusion-weighted images. This analysis revealed a statistically significant 32.29.5% reduction in fiber volume 60 days post-SE (Figure 7-2B). The changes observed in the medial septum (Figure 7-2A) imply that this loss of fiber volume can be partially accounted for by Wallerian degeneration of medial septal projections to the hippocampus [Pierpaoli et al., 2001]. These findings suggest that loss of circadian input to the hippocampus might emerge through degeneration of the medial septum.

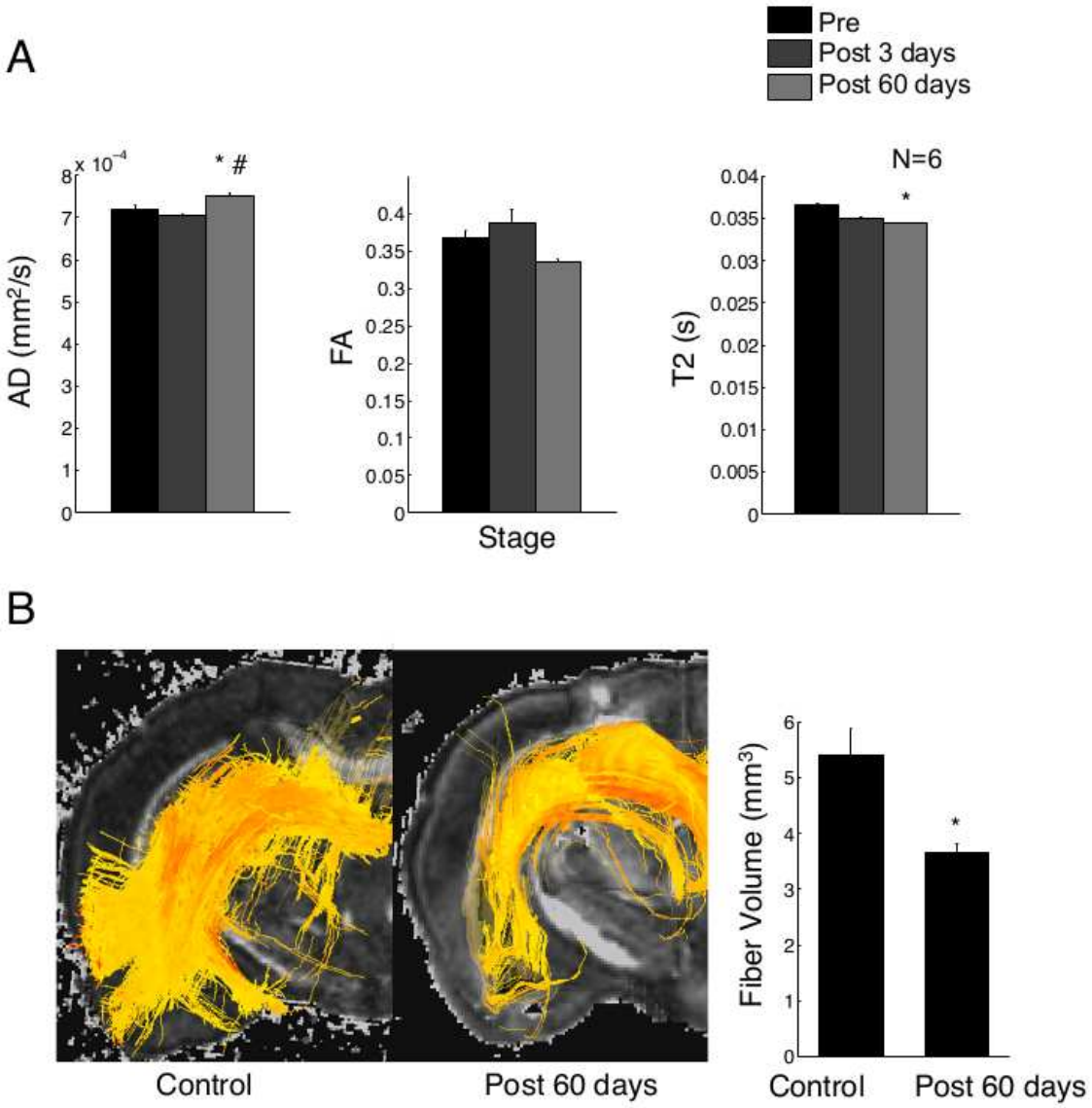

Figure 7-2. Structural changes in the medial septum and fimbria in epileptogenic animals. A, Quantified in vivo average diffusivity (AD), fractional anisotropy (FA), and T2 relaxation values for the medial septum in pre-injury, 3 days post-status epilepticus (SE), and 60 days post-SE stages for N=6 rats. Statistically significant changes in AD and T2 are indicative of neuron loss in the medial septum. *$p < 0.05$, relative to pre-injury measurement; #$p < 0.05$, relative to 3 days measurement. B, Fiber tracking of the fimbria in excised control and spontaneously seizing rat brains 60 days post-SE. A significant reduction in total fiber volume is observed in the seizing rats (N=8 rats) when compared to control rats (N=3 rats). *$p < 0.05$, unpaired t test relative to control measurement. Values are mean $\pm$ SEM.

CHAPTER 8
HIPPOCAMPAL EEG RHYTHMS: DISRUPTED 24-HOUR REGULATION

8.1 Background and Overview

In this chapter, we investigate long-term changes in the power of hippocampal EEG rhythms in rat temporal lobe epilepsy (TLE). As discussed in Section 2.3 of Chapter 2, rhythmic activity is a main feature in the hippocampal EEG. Like the spontaneous hippocampal spike (SPK) events studied in Chapter 5, EEG rhythms can serve as a marker for 24-hour regulation of hippocampal neural activity. Specifically, since EEG rhythms are well-defined and are associated with specific hippocampal cell types, they can yield additional information about neural-level mechanisms, complementary to our SPK analysis.

In our previous work, we provided evidence that the SPK 24-hour rhythm phase shift was not associated with changes in wake-sleep cycle or suprachiasmatic nucleus (SCN) rhythms. Rather, we proposed a mechanism by which circadian inputs to the hippocampus regulated the firing activity of specific groups of neurons on a 24-hour basis, and that subtle changes in these inputs could produce a phase shift in the 24-hour rhythm of cell firing activity. In our model, we observed that basket cells were particularly sensitive to circadian input, and most readily shifted their firing phase following circadian perturbation. Basket cells are known to play fundamental roles in the generation of hippocampal gamma rhythms (25 – 140 Hz) [Buzsáki and Wang, 2012, Wang and Buzsaki, 1996, Whittington et al., 2000], which leads to the prediction that these rhythms in particular might be affected in our experimental data. Additionally, in our previous work we postulated that damage to the medial septum might be partly responsible for altering hippocampal 24-hour rhythms. As discussed in Chapter 2, the medial septum is important for generation of the hippocampal theta rhythm. Previous studies have shown that hippocampal theta rhythm amplitude is reduced in epilepsy and have suggested that the septal structures responsible for pacing the theta rhythm

may be altered [Colom et al., 2006]. Therefore, based on the septum's putative role as a circadian input, we expect that theta rhythm power may also be altered as a function of the time of day [1] .

Traditionally, the phrase "EEG rhythms" can have two distinct meanings. First, EEG rhythms can refer to specific and often transient oscillations that are associated with specific cognitive activities. These oscillations may occupy different frequency ranges depending on the species and brain regions from which they are recorded [Penttonen and Buzsáki, 2003]. Hippocampal gamma and theta are examples of such oscillations. In contrast, EEG rhythms may also refer to all activity within a defined frequency bands, regardless of brain state. These frequency band are also referred to using terms such as alpha, theta, and gamma and have internationally accepted definitions [Chatrian et al., 1974]. The defined EEG frequency bands will often, but not always, correlate with the frequencies of specific neural oscillations. For example, the theta band is defined internationally as 4 – 7.5 Hz, but theta oscillations are slower in larger animals (3 – 5 Hz), such as the cat, and faster in smaller animals such as the rat (6 – 9 Hz) [Penttonen and Buzsáki, 2003].

In this chapter, our approach is to analyze long-term changes in the power of hippocampal EEG rhythms. Ideally, we would like to track changes in the amplitudes of specific EEG oscillatory events, since these can be closely related to specific types of neural activity. However, given the large volume of data required to study 24-hour rhythms, it was not possible to manually annotate every EEG event. For theta rhythms, we used a common automated routine to extract epochs of theta activity [Csicsvari et al.,

[1] Note that theta rhythm oscillations and theta state, which we analyzed in Chapter 5, are not equivalent. Theta oscillations are a phenomenon of the theta state. For example, extreme cases, such as complete medial septal lesion, will abolish theta oscillations but leave other hallmarks of the theta state still apparent, such as suppression of SPWs [Buzsaki et al., 1983, Suzuki and Smith, 1988a].

1998, 1999, 2000]. For other oscillations, however, there are not (to our knowledge) reliable automated schemes for classification. Therefore, we followed a more common approach, which was to measure the power in specific frequency bands across all data. We did, however, choose frequency bands to correspond to the known frequency ranges of rat hippocampal EEG oscillations reported in the literature [Buzsáki and Silva, 2012, Buzsáki and Wang, 2012, Penttonen and Buzsáki, 2003, Traub et al., 1999b, Whittington et al., 1997]. Specifically, we examined eight main frequency bands: delta (1 – 5 Hz), theta (5 – 10 Hz), beta (12 – 25 Hz), slow gamma (25 – 50 Hz), mid-frequency gamma (50 – 90 Hz), fast gamma (90 – 140 Hz), fast oscillations / ripples (140 – 200 Hz), and ultra-fast oscillations (200 – 500 Hz).

In the following sections, we first extract frequency band power as a function of time using power spectral density (PSD) analysis. We show that all frequency bands exhibit 24-hour oscillations. Then, we demonstrate that certain frequency bands (namely those in the gamma and beta ranges) phase shift following injury. To explain this phase shift, we introduce a phenomenological model in which there are multiple circadian inputs to the hippocampus and propose that the phase shift could be produced by changes in the relative strengths of these circadian inputs. This is supported by our identification of a form of phase–amplitude coupling, in which we show that 24-hour rhythms can be grouped into 2 categories based on phase and amplitude changes, suggesting the influence of two putative circadian input to the hippocampus. Furthermore, using principal component analysis (PCA), we show that multiple separate modes are required to capture 95% of the variance in our data. We discuss how this might indicate the existence multiple circadian inputs. Finally, motivated by our previous work and our interest in the medial septum, we provide additional characterization of 24-hour modulation of the hippocampal theta rhythm. We show specifically that the magnitude of the phase shift is reduced in the hippocampal theta state and propose that the theta state may improve functional coupling to a specific circadian input. We also

show that the phase shift and changes in hippocampal theta did not occur in rats that were injured but that did not develop TLE. Previously, we performed a similar analysis to that presented here, only using empirical mode decomposition (EMD) in place of PSD, and demonstrated similar results [Stanley et al., 2011b].

8.2 Methods

8.2.1 Animal Methods and Data Collection

Animal methods, experimental timelines, and procedures for acquisition of raw data are described in the General Methods (Chapter 4). An experimental timeline is supplied in Figure 4-1 of the General Methods. As with our previous analysis, we analyzed data exclusively from Channel 2 of Figure 4-2. Our procedures for fitting of 24-hour rhythms to cosine functions and extraction of theta epochs are also described therein. In contrast to the data used in the previous EEG chapter (Chapter 5), we now have data for N=4 seizing rats and N=2 non-seizing rats. For convenience, we will label the four seizing rats 1 – 4 and the non-seizing rats 5 – 6. The additional seizing animal, Rat 4, was not available for previous spike analysis because the spike sorting algorithm failed to classify spikes of consistent shape.

8.2.2 Extraction of Power Spectral Densities

To extract changes in EEG power as a function of time, we first divided the EEG signal into 2-second non-overlapping epochs (Figure 8-2 A). We then applied a 2-second hamming window and calculated the PSD (Figure 8-2 B). The mean powers in each of the eight frequency bands were recorded. This process was repeated for every 2-second epoch of data and yielded, for each rat, eight time series describing EEG power as a function of time for each of the eight frequency bands. In our analysis values reported are the mean PSD of a frequency band, rather than the total integrated power. This yields values in units mV^2/Hz and allows power values to be independent of the width of their chosen frequency band.

In some cases, we desired finer spectral resolution. To improve spectral resolution, rather than using the standard frequency bands listed above, we split data into many narrower frequency bands. Specifically, we sampled delta (1 – 5 Hz) and theta (5 – 10 Hz) as before, but then subsequent frequencies were divided into 19 logarithmically spaced non-overlapping bands between 10 and 500 Hz. Delta and theta frequency bands were left unchanged since these frequency bands were used for the identification of theta epochs. It is indicated in the figure captions cases for which these logarithmic frequency divisions are used.

8.2.3 Data Analysis

Subsequent smoothing of data and measurement of 24-hour rhythms is as described in the General Methods (Section 4.9), but with some important additions. First, as before, time series are smoothed using 6-hour 90% overlapping windows, yielding traces showing 24-hour variation (Figure 8-2 C, dotted trace). Detrending is performed by subtracting out baseline drift, estimated by 2-day windows (Figure 8-2 C, solid green lines). The resulting detrended time series are denoted with the symbol Δ.

Data are then separated into pre-injury (Pre), post-injury latency (Post-L) and post-injury spontaneously seizing (Post-SS) stages and cosinor analysis (see General Methods, Section 4.9) is used to extract the amplitude and phase of 24-hour oscillations (Figure 8-2 D). Zero amplitude tests are also applied to ensure that data are indeed oscillatory [Nelson et al., 1979].

Considering that our datasets were drawn from only 4 animals and, yet, contained over 23 weeks of combined data, we have in some cases assumed that data in each of the three experimental stages (Pre, Post-L, or Post-SS) were ergodic. Under this assumption, we split detrended data into non-overlapping 2-day bins, conducted cosinor analysis on each bin, and collected the output for Pre, Post-L, and Post-SS experimental stages. Output data from all rats were pooled together, providing a large number of data points. Although the data is likely not truly ergodic, especially during the latency period,

we justify this assumption because we found that data points for Post-L and Post-SS stages were quite similar, especially when compared to pre-injury data. Therefore, although the system is changing during epileptogenesis, this does not appear to exert major effects on the parameters being measured. These similarities between Post-L and Post-SS data points were apparent both with and without assuming ergodicity. We note in figure captions instances in which we assume ergodicity and use pooled data.

8.2.4 Analysis of Correlation Between Phase and Amplitude

Our extraction of 24-hour rhythms and subsequent cosinor analysis yielded measurements for both the phase and the amplitude of 24-hour rhythms. This analysis was conducted for each frequency band in our initial spectral decomposition. In addition to quantifying how these values changed as a function of injury, we also sought to understand how change in amplitude and phase were correlated across animals. Specifically, for a single rat in the Post-L stage, we constructed vectors $P = [\phi_1 ... \phi_M]$ and $A = [A_1 ... A_M]$. These stored, respectively, the phase and amplitude estimates for each of the M frequency bands. We used the correlation coefficient between these two vectors as an estimate for phase–amplitude correlation. This was performed for both Post-L and Post-SS stages for all 4 rats. We describe results for this analysis applied to the full set of M=21 logarithmically spaced frequency bands (described above). However, results were obtained using the set of M=8 default frequency bands.

8.2.5 Principal Component Analysis

Principal component analysis (PCA) was applied in order to investigate the dimensionality of the data. Data from each frequency band were detrended, as described above, and normalized to a standard deviation of 1.0 and mean of zero. We shall refer to such data from the i^{th} frequency band as $x_i(t)$. We then calculated the covariance matrix using $X_{i,j} =< (x_i(t))(x_j(t)) >$. PCA was applied by finding eigenvalues and eigenvectors of the covariance matrix, such that $X * \boldsymbol{\mu}_i = \lambda_i \boldsymbol{\mu}_i$, where λ_i is the i_{th} eigenvalue, $\boldsymbol{\mu}_i$ is the i^{th} (column) eigenvector, and $*$ denotes matrix

multiplication. For visualization purposes, PCA analysis was applied to data from the full set of M=21 logarithmically spaced frequency bands. Similar results were obtained for the M=8 default frequency bands. Eigenvectors and eigenvalues were sorted in order of descending eigenvalue.

The i^{th} mode, defined as the projection of data along the i^{th} eigenvector, was calculated as $y_i(t) = \mathbf{x(t)} * \boldsymbol{\mu}_i$, where $\mathbf{x(t)}$ is a row vector $[x_1(t), x_2(t), ...x_N(t)]$. We estimated the fractional contribution σ_K^2 of the first K modes to the total variance of all frequency bands by

$$\sigma_K^2 = \sum_{i=1}^{K} \lambda_i / \sigma \tag{8–1}$$

In this equation, $\sigma = \sum_i \lambda_i$ is the total variance across all frequency bands.

8.2.6 Statistics

All statistical tests reported are Wilcoxon rank sum tests, unless otherwise specified. Significance is considered to be $p<0.05$. Error bars represent 95% confidence intervals.

8.3 Results

8.3.1 Phase Shift in 24-Hour Modulation of Beta and Gamma Frequency Rhythms

To begin our analysis, we first used an ideal notch filter to split the raw data into eight frequency bands. This provided a visualization of the intrinsic rhythmic activity in the EEG signal. This is illustrated in Figure 8-1. In particular, theta band activity is apparent and is detected by the theta epoch detection algorithm (indicated in red).

Secondly, we illustrate our procedure for tracking of long-term changes in EEG. In Figure 8-2 A–C shows an example PSD and demonstrates how long-term changes in the beta frequency band (12 – 25 Hz) power are extracted and smoothed (see Methods). The resulting time series exhibits clear 24-hour modulation. Figure 8-2 D

shows how this band exhibits a phase shift following injury, similar to our findings for EEG SPKs.

While Figure 8-2 provides an example of the phase shift for a single frequency band, our complete characterization included all frequency bands for all rats, (Figure 8-3). In particular, we found that 24-hour oscillations were ubiquitous for all frequency bands. Lower frequency rhythms (delta, theta) were entrained such that their amplitudes peaked near noon, while higher frequency rhythms peaked close to midnight. This was the case throughout all experimental stages (Pre, Post-L, and Post-SS). In the middle frequency ranges, generally beta and/or gamma, a phase shift appeared following injury, in which the peak shifted from noon to midnight. Sample data from Rat 1 are shown in Figure 8-3 A,B. In particular, it is clear that 24-hour rhythms can be clustered into two groups: those that peak during the day and those that peak during the night (dotted red line). Additionally, we observed that the phase shift appeared very early in the latency stage, almost immediately following status epilepticus (SE) injury for all rats (Appendix B, Figures B-1 – B-4).

Statistics were conducted on the phase shift for all animals. Figure 8-3 C shows that the phase shift was significant for beta, slow gamma, and mid-frequency gamma frequency bands. Statistics are as follows: beta ($p = 0.001$ and $p = 2.3 * 10^{-5}$ for latency and spontaneously seizing stages, respectively), slow gamma ($p = 0.0016$ and $p = 3.1 * 10^{-5}$), and mid-frequency gamma ($p = 0.01$ and $p = 0.0055$).

We also analyzed changes in the amplitudes of cosine fits following injury. We found statistically significant reductions in amplitude that occurred exclusively for the low frequency bands, delta, theta, and beta (Figure 8-3 D). Statistics are as follows: delta ($p = 0.17$ and $p = 0.0047$ for spontaneously seizing), theta ($p = 0.0036$ and $p = 0.0088$), and beta ($p = 0.0049$ and $p = 0.048$).

8.3.2 Imbalanced Circadian Input as a Driver for the Phase Shift

We have thus far observed the following: 24-hour modulation of low frequency rhythms peaked during the day, 24-hour modulation of high frequency rhythms peaked at night, and middle frequency rhythms shifted from peaking during the day to peaking at night. Furthermore, low frequency rhythms exhibited a statistically significant reduction in the amplitude of their 24-hour modulation following injury. Here we will discuss these findings and propose a simple phenomenological model.

While the hippocampus clearly possesses 24-hour rhythms, it likely does not receive direct projections from the SCN. Rather, a number of indirect pathways for relaying circadian input have been proposed [Gerstner and Yin, 2010]. In this study, we have observed that 24-hour rhythms can be grouped into two categories: those that peak during the day and those that peak during the night. We propose that these might correspond to two separate circadian inputs (Figure 8-4). If this is the case, then the phase shift might be explained by a transfer in control from the "*Day*" input to the "*Night*" input. This is supported by the observation that the low frequency rhythms, which corresponded to the daytime peak, showed a reduction in their amplitude of 24-hour modulation. Such a theory is in line with our previous modeling work (Chapter 6; Stanley et al. [2011a, 2013]), which suggests that the phase shift might result from subtle imbalances in circadian input. In subsequent sections, we shall refer to these two putative circadian inputs as *Day* and *Night*.

8.3.3 Phase–Amplitude Relationship of 24-Hour Rhythms

The phenomenological model described above proposes that there are two main circadian inputs to the hippocampus, each with unique phases (daytime and nighttime peaks) and amplitudes. Therefore, we expect there to be some relationship between phase and amplitude in the 24-hour rhythms recorded experimentally. Figure 8-6 A,B displays amplitude and phase data from all 4 rats. To show that our results are not dependent on the choice of frequency bands, as opposed to using the traditional EEG

frequency bands, we now split data into 19 logarithmically spaced frequency bands, plus theta and delta.[2] In this data, we observed a pattern whereby frequency bands possessing a daytime peak in power generally exhibited a decrease in amplitude of their 24-hour modulation post-injury. The converse was true for nighttime peaking frequency bands, which showed an apparent increase in their amplitude post-injury. There are some exceptions to this trend, notably the high frequencies of Rat 1 and the entire latency period of Rat 4.[3] To quantify this trend, we examined the correlation coefficient between the phase and amplitude changes (see Methods, Section 8.2.4) and found a positive correlation across all 4 rats. That is, a higher $T_{\Delta PSDmax}$ (meaning an activity peak closer to 24:00) corresponded to stronger 24-hour rhythms post-injury. In contrast, lower $T_{\Delta PSDmax}$ (values generally did not drop below noon) corresponded to reduced amplitude 24-hour rhythms. This was the case during both latency and spontaneously seizing stages for all 4 rats, with correlation values ranging between 0.33 and 0.85 and average values close to 0.5. Together, these findings suggest that there are two main circadian inputs to the hippocampus, and that their strength is differentially modulated, with one increasing and the other decreasing following injury.[4]

[2] Similar results were obtained using traditional frequency bands.

[3] The fact that the latency period of Rat 4 showed a uniform reduction in the amplitude of 24-hour modulation across all frequency bands might relate to the fact that Rat 4 exhibited a relatively short latency period and that all 24-hour rhythms appeared to be temporarily reduced following SE. The amplitude recovered and the trend re-appeared for the spontaneously seizing stage of epileptogenesis. See Appendix B, Figure B-4.

[4] We note that, while high frequency bands did show a relatively consistent increase in power following injury in each animal (Figure 8-6 B) this did not reach significance when data were pooled and averaged across all animals (see Figure 8-3 for description).

8.3.4 24-Hour Rhythms are Multidimensional

In this section, we examine correlation relations amongst the various frequency bands' 24-hour rhythms using PCA. PCA is a dimensionality reduction technique that identifies a set of linearly uncorrelated variables that provide a reduced description of a multidimensional signal. These variables describe motion in a vector space of reduced dimension (given by principal component eigenvectors), with each variable defining an uncorrelated mode of the original signal. As we shall discuss, such uncorrelated modes may reveal information about the underlying circadian inputs to the system.

Our PCA analysis (Figure 8-5) revealed that a total of 3 modes were required to capture 95% of the signal variance (Figure. 8-5 A). These include a mode that peaks during the night and contributes to oscillations of the high frequency bands, a mode that peaks during the day and contributes to low frequency bands, and a diffuse mode that exhibits a slight peak in the evening hours (Figure 8-5 B,C). All three principal modes for all rats passed the zero amplitude test [Nelson et al., 1979]. [5] It is important to emphasize that we chose to analyze a single stage of epileptogenesis, rather than the whole dataset, in order to ensure that the data were relatively stationary. We chose the spontaneously seizing stage because it was the longest and thus provided the most data.

These results state that the EEG 24-hour rhythms can be largely reconstructed by the linear summation of three uncorrelated modes. The existence of multiple uncorrelated modes supports the notion of multiple circadian inputs, since, abstractly,

[5] It is significant that these modes be 24-hour sinusoidal rhythms because different EEG rhythms are generated by specific underlying mechanisms, and their power is modulated by many non-circadian factors that operate on a variety of timescales. Dependent on our choice of filtering techniques, these modulations will also appear in our signals alongside 24-hour oscillations. Since there is no reason to expect that these other factors should be correlated, they may appear as additional dimensions in our data. Therefore, it is important to confirm that the modes are 24-hour rhythms.

we would expect rhythms produced by multiple independent oscillators would be less correlated than rhythms produced by input from a single oscillator, such as the SCN. One interpretation is that these uncorrelated modes may correspond to specific circadian inputs, such as those depicted in Figure 8-4. Specifically, the fact that the first two modes concentrate their contributions to the high and low frequency bands, respectively, supports the organization of *Day* and *Night* drivers that we have predicted.

We note that this result is non-trivial because, based on Figure 8-3, we might have expected PCA to reveal that a single 24-hour rhythmic mode was sufficient to capture 95% of the signal variance. Such a single mode could produce day and night peaking 24-hour rhythms simply by inverting the sign of eigenvector entries where needed. Such a finding would instead suggest the presence of a single dominant circadian input.

8.3.5 Altered 24-Hour Modulation of Theta Rhythm Power

While we have proposed abstract entities for the circadian inputs shown in Figure 8-4, a number of studies have suggested specific entities that might be their physiological correlates. These are summarized in Chapter 3, Section 3.6. In particular, our previous work suggested that circadian input via the medial septum might become impaired and contribute to the phase shifting of hippocampal SPKs. This was supported by both a detailed computer model (Chapter 6) and an MRI study that suggested damage to the medial septum post-injury (Chapter 7).

The medial septum is firmly established through *in vivo* studies to be critical for the generation of hippocampal theta[Lee et al., 1994, Petsche et al., 1962]. Given its importance, our hypothesis that the medial septum is impaired would be falsified by a lack of alteration to the theta rhythm. On the contrary, while changes in hippocampal theta rhythm may indicate the possibility of medial septum damage, changes to the hippocampus or other structures could also produce similar effects Colom et al. [2006]. Preliminary analysis of the theta frequency band suggested that its 24-hour modulation was reduced (Figure 8-3 D). Here, we will investigate theta rhythms in more detail.

We used a standard technique, described in Chapter 4, to extract epochs of theta rhythm activity based on the ratio of power in theta and delta frequency bands. In Figure 8-7 A, we investigated the power in the theta frequency specifically during epochs of theta activity. We found that theta power was significantly reduced at all times of the day. This is in agreement with findings in a similar epilepsy model [Colom et al., 2006] and may reflect damage to the underlying theta generating structures. The greatest reduction in theta power occured near noon, and the implications of this will be addressed in the discussion. Figure 8-7 B shows a statistically significant reduction in the 24-hour modulation of hippocampal theta rhythms. [6] Therefore, in addition to the theta rhythm itself being reduced, its 24-hour modulation is also impaired.

In Figure 8-8, we split data into theta and non-theta states and repeated our characterization of EEG phase (as in Figures 8-2 and 8-3). We observed that the phase shift still appeared for beta and gamma frequency rhythms in both the theta and non-theta states; however, the phase shift was more pronounced in the non-theta states. Specifically, post-injury the beta and gamma bands peaked significantly earlier in the day in the theta state, as compared to non-theta state (Figure 8-8 B,C). In terms of our phenomenological model (Figure 8-4), this might suggest that, in the theta state, the circadian inputs promoting daytime activity peak were relatively enhanced.

8.3.6 24-Hour Rhythms in Non-Seizing Rats

Finally, for non-seizing rats (Rats 5 and 6), we repeated the major facets of our characterization above. This is summarized in Figure 8-9. Detrended PSD data for selected frequency bands are shown and, quantifying the phase of this activity, we observed that the phase shift magnitude was much reduced for non-seizing animals (Figure 8-9 A,B). The changes in phase did not reach statistical significance, nor did

[6] This is also visible in Figure 8-7 A, but less clearly because data were not detrended.

the changes in amplitude (Figure 8-9 C,D). Finally, the theta rhythm profile showed consistent patterns pre- and post-injury (Figure 8-9 E,F). Together, these results suggest that the changes in 24-hour modulation and hippocampal theta are associated with epileptogenesis and are not merely an epiphenomenon of injury.

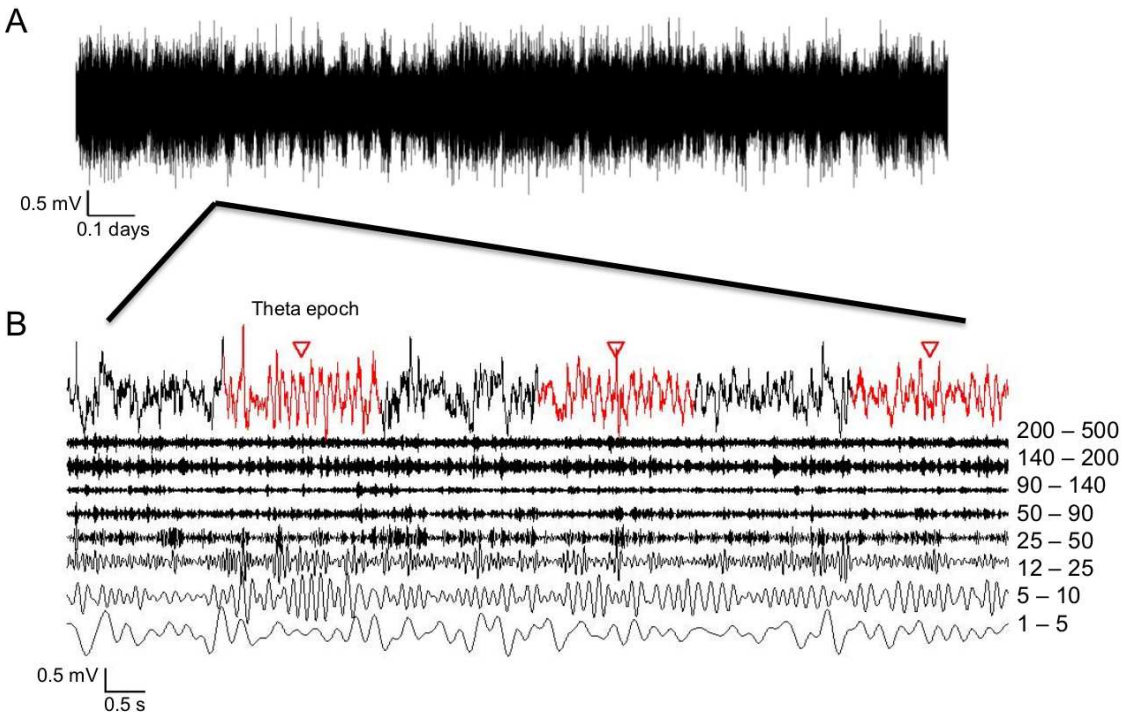

Figure 8-1. Frequency content of raw EEG data. A, Two days of continuous raw EEG data taken from the pre-injury stage. B, Top trace shows 12 seconds of raw data. Bottom eight traces show decomposition of raw data into frequency bands (indicated in Hz). The amplitude of the top two frequency bands has been magnified by a factor of 5 for improved visualization. Arrows indicate 2-second epochs of data detected as theta-state based on the theta/delta power ratio method. Data were separated into frequency bands using an ideal (noncausal) filter.

8.4 Discussion

Our EEG studies have produced the following findings. First, we have shown that the power of hippocampal EEG rhythms is modulated on a 24-hour cycle. Secondly, these rhythms are altered in epilepsy, with beta and gamma frequency rhythms exhibiting a phase shift and delta, beta, and theta frequency rhythms exhibiting

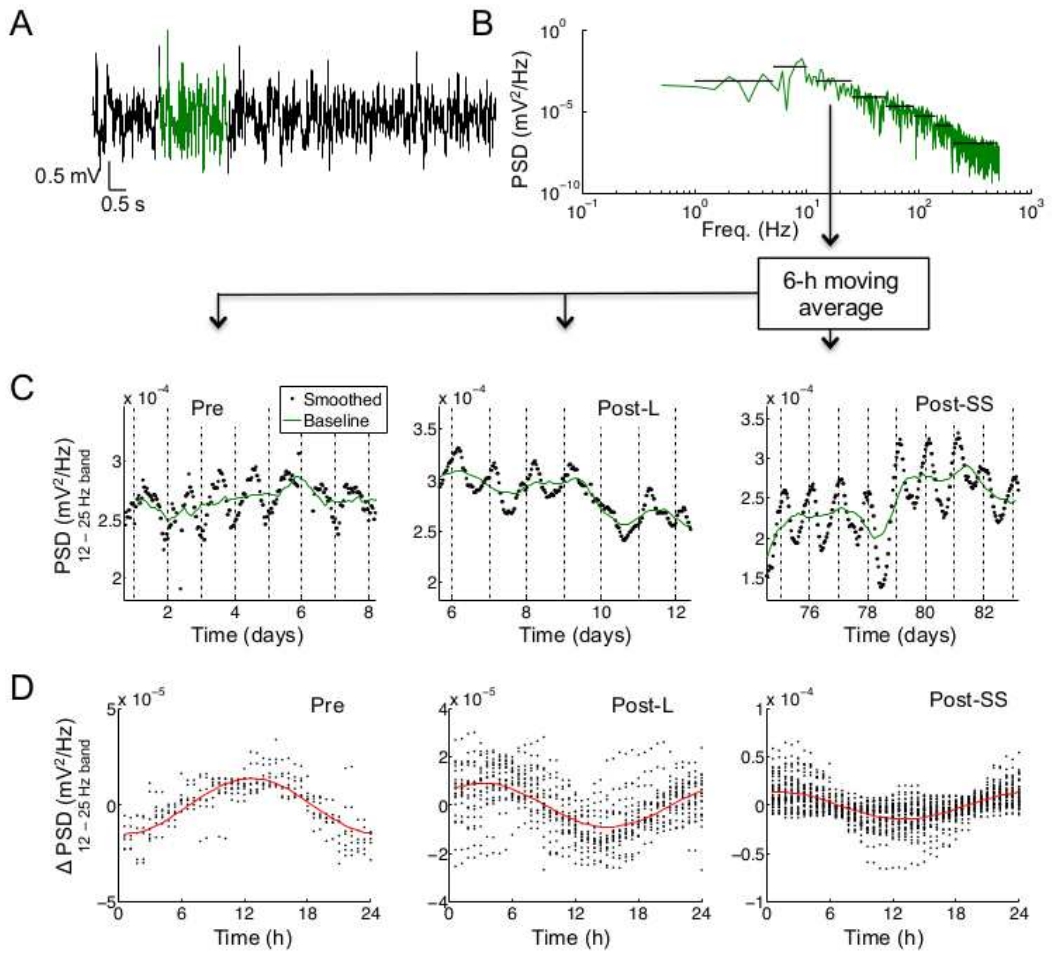

Figure 8-2. Long-term tracking of power spectral density (PSD) reveals a phase shift following injury. A, A 12-second sample of raw data taken from the pre-injury stage. A 2-second epoch of data is highlighted in green. B, PSD of the green 2-second epoch of data. Eight horizontal bars indicate the mean power in each of the frequency bands used in our analysis. The horizontal position of the bar denotes the frequency range of the band. C, Long term changes in the beta-range frequency band (12 – 25 Hz) power were estimated for the entire dataset and smoothed by 6-hour 90% overlapping sliding windows (dotted). Additionally, baseline drift (solid green) is shown as estimated using a 2-day sliding window. Data are shown for each of the three experimental stages: pre-injury (Pre), post-injury latency (Post-L) and post-injury spontaneously seizing (Post-SS). D, The baseline drift was subtracted out and the resulting detrended time series was expressed in a single 24-hour window (modulo 24). Cosine fits are shown in red. A phase shift of ≈180 degrees is visible between Pre and Post-L stages and Pre and Post-SS stages for this particular frequency band. All data shown is from Rat 1.

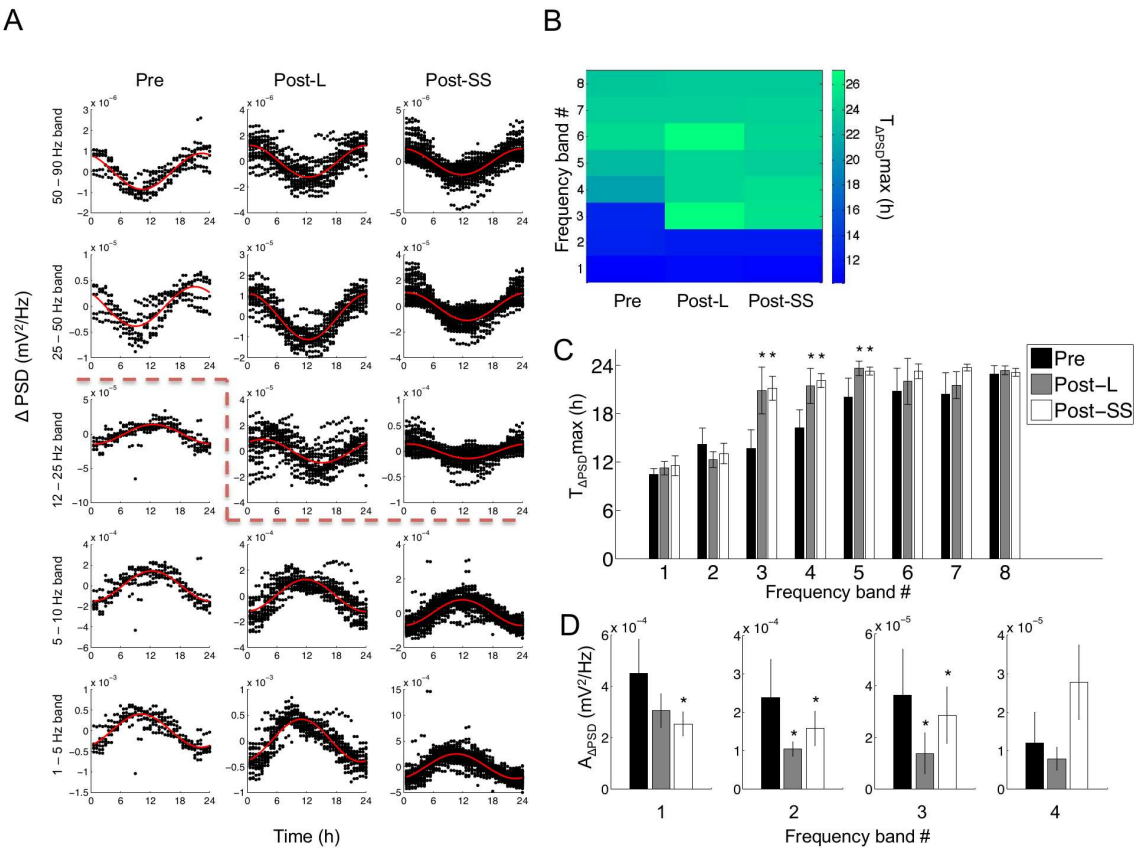

Figure 8-3. Phase and amplitude relationship amongst frequency bands. A) Cosine fits to detrended PSD data (ΔPSD) for selected frequency bands for Rat 1. Modulation of EEG rhythms in the theta and delta frequency bands is entrained to peak near noon, while the gamma frequency bands peak near midnight. The beta frequency band exhibited a phase shift, from peaking during the day to peaking at night. Red dotted line illustrates division between day and night peaking rhythms. Data are from Rat 1. Other rats showed phase shifts also occupying gamma frequency bands. B) Time of maximum ΔPSD ($T_{\Delta PSDmax}$), as extracted from cosine fits for all frequency bands. Frequency bands are as defined in Figure 8-1. C) Examination of the phase shift across all rats revealed that the phase shift was statistically significant for beta (12 – 25 Hz), slow gamma (25 – 50 Hz), and mid-frequency gamma (50 – 90 Hz) frequency bands. D) Examination of the amplitude of cosine fits showed that the magnitude of 24-hour modulation in delta, theta, and beta frequency bands reduced following injury. Certain higher frequency bands showed an increase in amplitude post-injury, but these did not reach significance and are not shown due to space limitations. * $p < 0.05$ by Wilcoxin rank sum test on pooled data (N=16, 20, and 55 2-day bins for Pre, Post-L, and Post-SS data, respectively). Pre, Post-L, and Post-SS refer to pre-injury, post-injury latency, and post-injury spontaneously seizing stages of epileptogenesis, respectively.

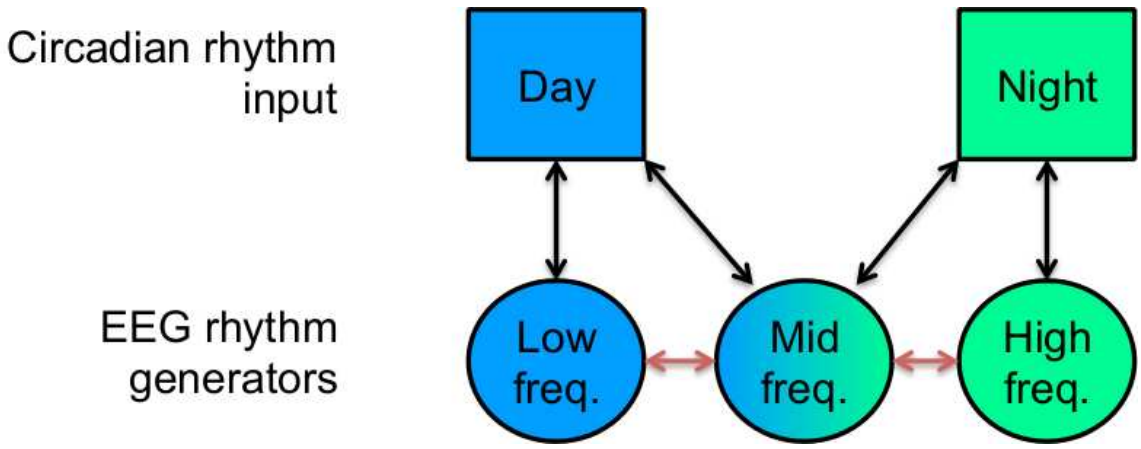

Figure 8-4. Altered circadian input as a mechanism for the 24-hour rhythm phase shift. The observation that EEG rhythms could be clearly divided into two groups, those that peak during the day and those that peak at night, suggests that these rhythms are driven by two main circadian inputs to the hippocampus. We hypothesized that reduction in the strength of the day input might produce a phase shift by promoting a transfer in control to the night circadian input. Red arrows indicate the possibility that 24-hour modulation of the middle frequency may be transmitted indirectly through coupling to other EEG rhythm generators, rather than by direct input from circadian relay centers.

a reduction in their amplitude of 24-hour modulation. Through analysis of data dimensionality and also phase–amplitude relationships, we have provided evidence that there are two main circadian inputs to the hippocampus and have suggested that their strength is altered following injury. Finally, we have shown that 24-hour regulation of theta rhythms is also altered in epilepsy and that the theta state appears to promote activity to peak earlier in the day. In this section, we will discuss these results in relation to previous literature, propose a specific physiological mechanism that could explain these findings, and suggest future studies.

8.4.1 Relationship to Previous Circadian Literature

There have been few previous investigations on 24-hour rhythms of hippocampal neural activity in epilepsy. Our previous work in this area showed that another EEG feature, hippocampal SPKs, also exhibited a phase shift (Chapters 5–7; Stanley et al. [2013]). In this previous study, we acknowledged the possibility that the appearance of

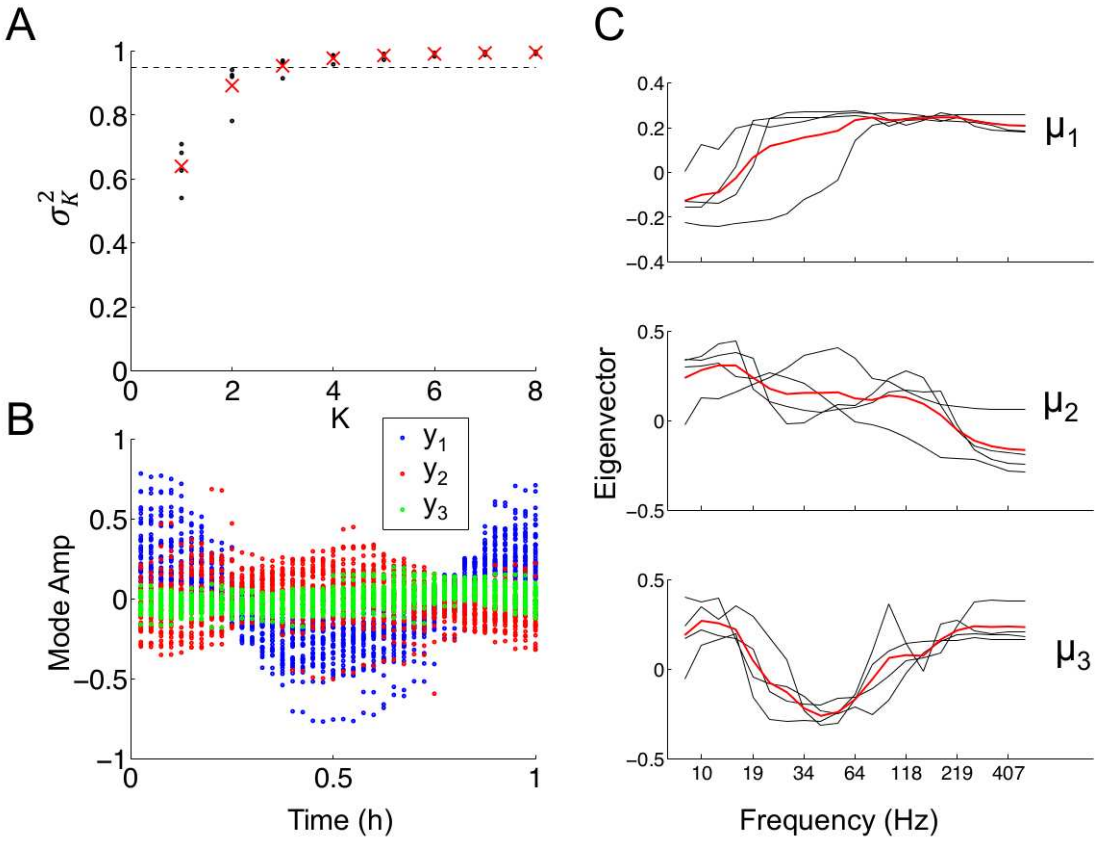

Figure 8-5. Principal component analysis of EEG frequency bands suggests multiple circadian inputs. A) Principal component analysis (PCA) was applied to the detrended time series for each rat (Appendix B, Figure B-1 – B-4). σ_K^2 represents the fractional contribution of the first K modes to the total variance in all frequency bands (see Methods). The first three modes are sufficient to capture 95% of the variance (dotted line). B) The three principal modes, $y_1(t)$ ... $y_3(t)$, which represent data viewed in the eigenvector space. The first of these modes peaks at midnight, the second at noon, and the third is distributed. C) The eigenvectors associated with each of the three principal modes show consistent patterns, with μ_1 contributing primarily to high frequency bands, μ_2 to low frequency bands, and μ_3 to all but the middle frequency bands. In (A,C) population means (red) are shown alongside values from individual rats (black). Data from an example rat (Rat 1) is shown in (B). PCA was calculated specifically using data from the spontaneously seizing stage, which was chosen because it was the longest of the three experimental stages.

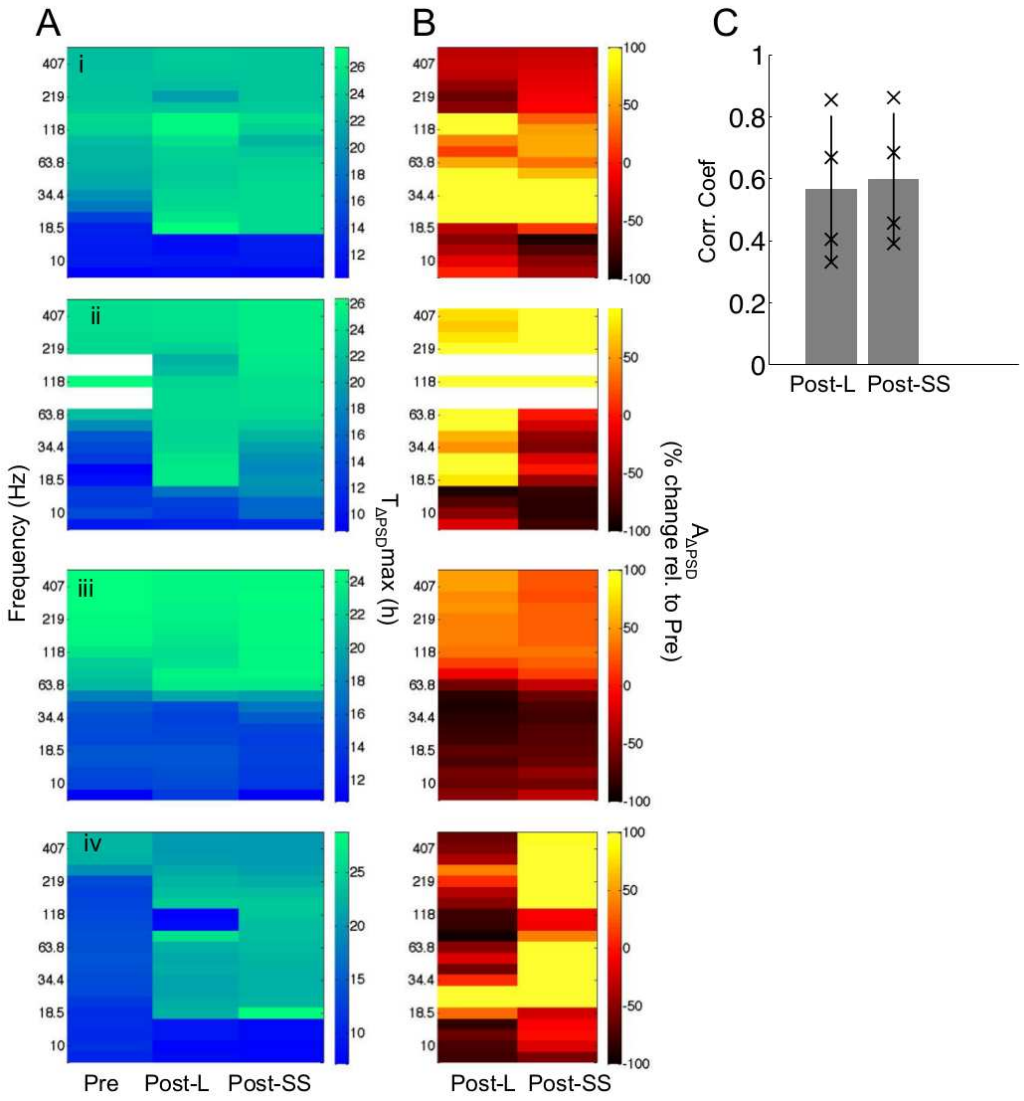

Figure 8-6. Post-injury changes in amplitude are coupled to phase A) Time of maximum ΔPSD ($T_{\Delta PSDmax}$, as extracted from cosine fits) for Rats 1-4 (i–iv). B) Percent change in amplitude of PSD 24-hour modulation ($A_{\Delta PSD}$, as extracted from cosine fits), relative to pre-injury period. We observed that for regions where $A_{\Delta PSD}$ decreased following injury, the corresponding regions of the phase plots (A) showed rhythms were generally entrained to a noon-time peak. Similarly, regions where $A_{\Delta PSD}$ increased following injury appeared associated with midnight $T_{\Delta PSDmax}$ in (A). C) We quantified this correlation by measuring the correlation coefficient between amplitude change and phase for all four rats and for the two different stages of epileptogenesis. A positive correlation was shown for all rats (crosses), with mean values $>$0.5 (bars). White shading indicates data for which circadian fits could not be reliably obtained (zero amplitude test failure).

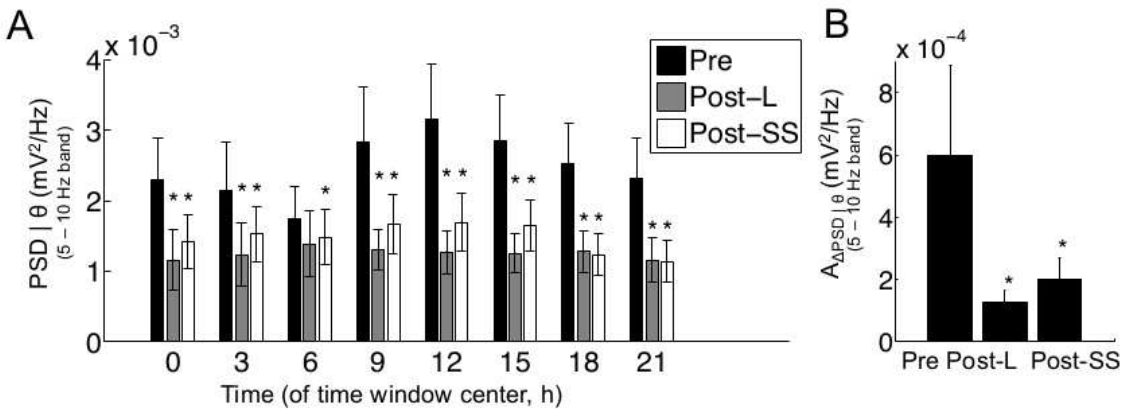

Figure 8-7. Altered daily modulation of hippocampal theta power following injury A) We measured mean theta PSD during eight 3-hour time windows throughout the day. We observed a statistically significant reduction in theta that was greatest close to noon. * $p < 0.05$ by Wilcoxin rank sum test on pooled data (Statistics based on at least N=29, 39, and 93 3-hour time windows for Pre, Post-L, Post-SS data, respectively. N for each time windows varied due to gaps in data). B) Amplitude of the 24-hour rhythm in the theta frequency band, as estimated from cosine fits. A statistically significant reduction was found post-injury. Similar results were found for the delta and beta bands. * $p < 0.05$ by Wilcoxin rank sum test on pooled data (N=16, 20, and 55 2-day bins for Pre, Post-L, and Post-SS data, respectively). For both (A) and (B), data were analyzed specifically from epochs of data identified as being theta-state, according to our theta detection algorithm (see Methods). Pre, Post-L, and Post-SS refer to pre-injury, post-injury latency, and post-injury spontaneously seizing stages of epileptogenesis, respectively.

the SPK phase shift might in fact be caused by the emergence of interital spikes rather than an actual change in circadian rhythms. Our identification herein of a secondary feature in the hippocampal EEG suggests that the phase shift is not a function of our choice of feature. Secondly, this study also proposed that subtle imbalances in circadian input strength could generate a phase shift, and this was demonstrated in a biophysical computer model. This proposed mechanism is supported by our present findings, which provide evidence for multiple circadian inputs that are differentially regulated following injury.

Other studies have also supported the notion of changes in circadian regulation in epilepsy. In particular, Matzen et al. [2012] used single- and paired-pulse response

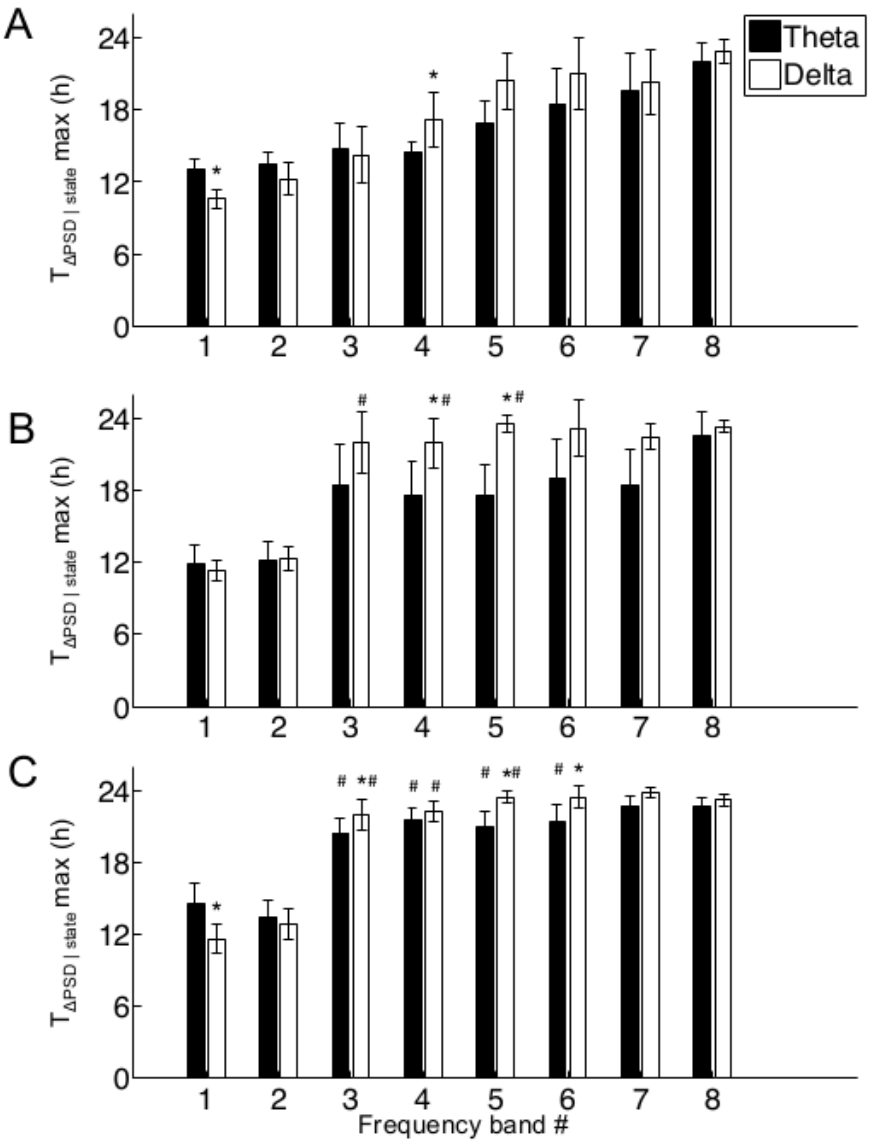

Figure 8-8. Phase shift is enhanced in non-theta states. Two-second epochs of data were classified as either theta or non-theta using a standard classification method (see Methods). Then, the time of maximum ΔPSD was calculated as in Figure 8-3 C for each of the theta and non-theta datasets $T_{\Delta PSD|stage}$. A-C) pre-injury (Pre), post-injury latency (Post-L) and post-injury spontaneously seizing (Post-SS) stages are shown, respectively. As with the case when theta and non-theta epochs were pooled together (Figure 8-3 C), a phase shift was observed in the middle frequency ranges. However, the shift in phase for the theta state data was significantly less than that for non-theta. Frequency bands 1 – 8 are as defined in Figure 8-1. *,# $p < 0.05$ by Wilcoxin rank sum test on pooled data (N=16, 20, and 55 2-day bins for Pre, Post-L, Post-SS data, respectively). # indicates significance relative to pre-injury data point and * indicates non-theta datapoint is significantly different from corresponding theta data.

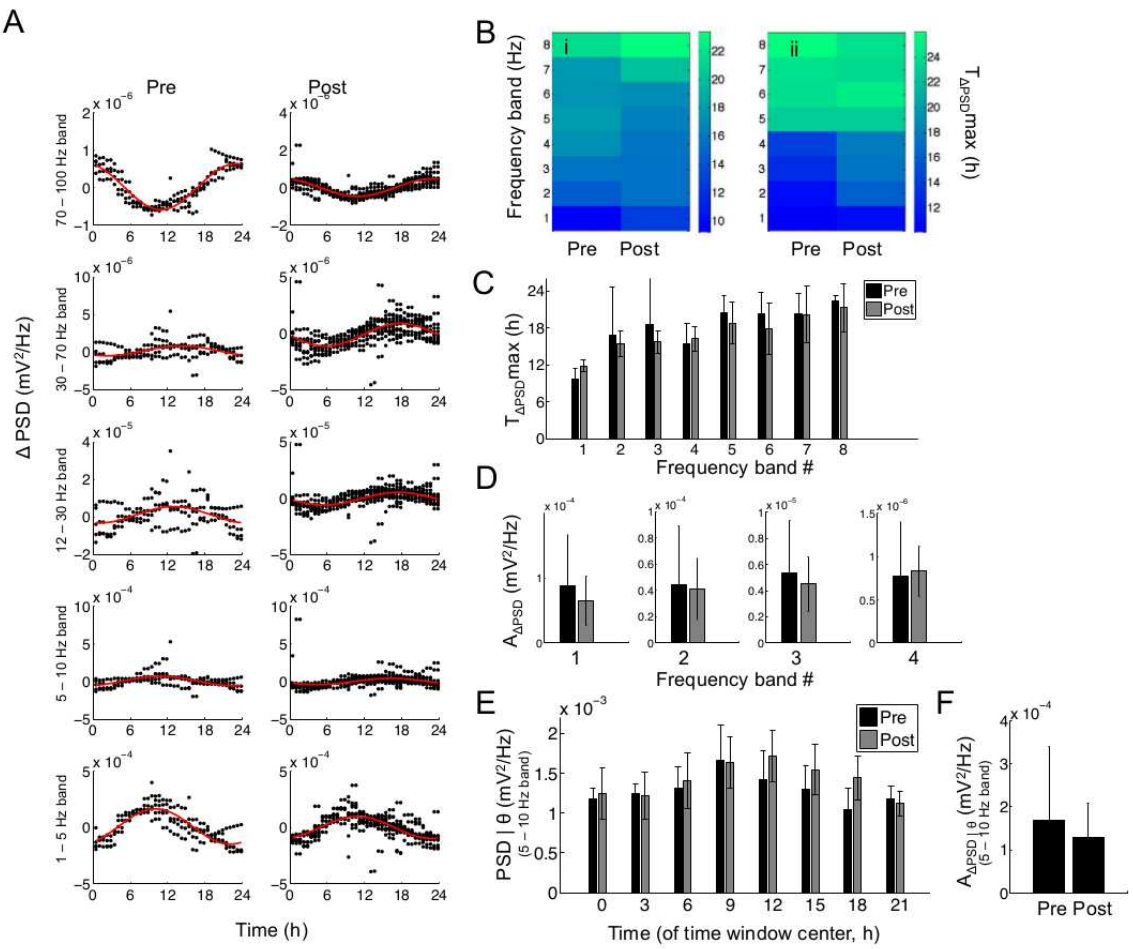

Figure 8-9. Analysis of phase and amplitude changes for non-seizing rats. A) Cosine fits to detrended PSD data for selected frequency bands for Rat 6. B) Time of maximum ΔPSD ($T_{\Delta PSDmax}$), as extracted from cosine fits for Rats 5-6 (i–ii). C) Examination of phase data across both non-seizing rats revealed no significant change in phase post injury. Frequency bands as in Figure 8-3 C. D) Likewise, amplitude data across did not reveal any significant change. E) As in Figure 8-7 A, mean theta PSD was measured during eight 3-hour time windows throughout the day. There was no significant reduction in theta, and the distribution maintained its peak near noon following injury. F) The amplitude of the 24-hour rhythm in the theta frequency band was estimated based on cosine fits. Unlike for the case of seizing rats (Figure 8-7 B), we did not observe a significant reduction post-injury. For both (E) and (F), data were analyzed specifically from epochs of data identified as being theta-state (see Methods). Wilcoxin rank sum tests were applied to pooled data from non-seizing rats, and significant differences between pre- and post-injury states were not observed (N=4 and 9 2-day bins for Pre and Post for panels (C), (D) and (F); Data in panel (E) obtained from at least N=6 and 16 3-hour time windows for Pre and Post. N for each time windows varied due to gaps in data). Pre, Post-L, and Post-SS refer to pre-injury, post-injury latency, and post-injury spontaneously seizing stages of epileptogenesis, respectively.

measurements to suggest that hippocampal excitation was enhanced during the day and that inhibition was enhanced at night in an animal epilepsy model. These changes, they proposed, might be caused by altered rhythms of hormone release from the hypothalamus. Additionally, as mentioned above, Chaudhury et al. [2005] conducted experiments on melatonin knock out mice and showed that 24-hour modulation of hippocampal activity was altered, but not eliminated. This suggests that, in addition to melatonin, other hippocampal inputs were contributing to the generation of 24-hour rhythms.

8.4.2 Interpretation of Results

8.4.2.1 Changes in 24-Hour Regulation of Hippocampal Theta

Hippocampal theta activity was previously investigated in a pilocarpine status epilepticus animal model by Colom et al. [2006]. Confirming their observations, we have shown a reduction in the amplitude of hippocampal theta power following injury. Furthermore, quantifying these changes as a function of the time of day, we found that the greatest reduction in hippocampal theta power occurred close to noon.

Abstractly, there are two general mechanisms that might account for the reduction of theta power at noon. First, assume that 24-hour rhythms of theta power are driven by a circadian input that peaks at noon and that promotes increased theta activity power. Then, loss of this input could produce a reduction in theta that is greatest at noon. Alternatively, assume that 24-hour rhythms of theta power are driven by a circadian input that is *inhibited* at noon and that this input acts to diminish theta activity power. In this case, loss of this noon-time inhibition (i.e. disinhibition) might also contribute to an increase in theta activity.

There are many candidates for circadian inputs that could influence theta rhythm power. One candidate is the medial septum, the cholingergic and GABAergic septal

outputs of which have been suggested to promote increased theta activity power.[7] Thus, assuming the medial septal input peaks at noon, damage to this input could explain the noon-time reduction in hippocampal theta.

We note that a study on 24-hour rhythms by Yamazaki et al. [1998] showed that multi-unit activity (MUA) in the medial septum peaked at night rather than during the day. However, it is difficult to translate the results of their study to ours because their data was collected continuously, regardless of behavioural state. Since behavioural states, such as wakefulness and sleep, can also influence neural activity,[8] it is difficult to distinguish 24-hour rhythms driven by behaviour from those driven by the SCN.[9] In their data, the medial septum MUA appears well correlated with wheel running activity (see Figure 2B of Yamazaki et al. [1998]). This suggests that the 24-hour rhythms they have reported may be mainly driven by behavioural activity. In contrast, our measurements of theta-activity power were performed exclusively in the theta state and, hence, should be less dependent on behaviour. If our prediction for the role of the medial septum is correct, we would expect 24-hour rhythms of medial septum activity, exclusively within the theta state, to peak during the day as opposed to during the night. Experimental measurement of septal 24-hour rhythms in such a state-dependent

[7] This is supported by both lesioning and pharmacological studies: 1) Lee et al. [1994] showed that selective cholinergic lesion of the medial septum reduces theta rhythm power. 2) Smythe et al. [1992] found that bicuculine, which attenuates GABA, was able to restore theta following septal inactivation. They argued therefore that loss of septal GABAergic input might reduce hippocampal theta by promoting hyperinhibition. 3) Buzsáki et al. [1986] showed urethane, which in general potentiates inhibitory transmitters (thus also promoting hyperinhibition) and attenuates excitatory transmitters [Hara and Harris, 2002], reduces theta power.

[8] Indeed, Hassani et al. [2009] have shown that different cells present in the medial septum each exhibit a complex array of firing patterns across wake–sleep behavioural stages.

[9] This is one motivation for investigating 24-hour rhythms in both the theta state (Figures 8-7 and 8-8) and in the full dataset (Figure 8-3).

manner would be useful for interpreting our results and may suggest how the influence of the SCN integrates with other 24-hour rhythms.

8.4.2.2 Effect of Theta State on Phase Shift

We have shown that, following injury, the peak activity in beta and gamma frequency bands was less shifted towards midnight in theta states, as compared to delta states (Figure 8-8). EEG rhythms such as theta serve the purpose of increasing functional coupling across brain regions [Buzsaki, 2009]. A large number of structures participate in the hippocampal theta oscillation, such as the medial septum, the supramammillary region, the amygdala, and a large number of cortical structures [Buzsáki, 2002]. One interpretation of this finding is that the theta state temporarily increases the coupling between the hippocampus and the putative circadian input responsible for generating the *Day* rhythm (Figure 8-4), thereby encouraging a peak in activity that is earlier in the day. An alternate interpretation, is that, since there are differences between theta and non-theta gamma [Leung, 1998, Traub and Miles, 1991], the difference in peak times could simply be the result of the circadian system differentially regulating these two types of gamma.

8.4.3 Underlying Physiological Mechanisms

Based on the analysis of EEG signals, we have provided evidence that there are two main circadian inputs to the hippocampus. This raises a central question: what are the physiological correlates of these two circadian inputs? There are a great many candidate circadian inputs to the hippocampus, summarized in Chapter 3, Section 3.6. However, in addition to simply providing a 24-hour rhythmic signal to the hippocampus, the circadian input in question must also A) have the ability to modulate EEG rhythms and B) become altered during epileptogenesis. While this places some restrictions on which inputs could be relevant, damage associated with SE is widespread and many brain regions become altered [Parekh et al., 2010].

The medial septum, given its rich interaction with hippocampal dynamics, meets the criteria of being able to modulate hippocampal EEG rhythms. A number of studies have also suggested that it may be damaged or altered during epileptogenesis. Concerning its influence on neural rhythms, the medial septum has been investigated in a number of empirical studies. It is firmly established *in vivo* that the medial septum is critical for the generation of hippocampal theta[Lee et al., 1994, Petsche et al., 1962]. *In vivo* studies have also suggested that both septal lesion and pharmacological modulation via atropine, a cholinergic antagonist, can influence hippocampal beta and gamma oscillations (20 – 50 Hz) [Leung, 1998]. GABAergic septal activity has also been shown to influence gamma frequency rhythms by *in vivo* pharmacological modulation via muscimol, a GABA agonist [Ma and Leung, 1999]. From a wiring perspective, the medial septum is a major source of cholinergic input and this projects widely through the hippocampus. Furthermore, GABAergic input from the medial septum appears to specifically target hippocampal interneurons, and therefore should play a critical role in the generation and regulation of EEG rhythms [Freund and Antal, 1988]. These targets include both O-LM cells, which are associated with hippocampal theta [Hajos et al., 2004, Wang, 2002], and basket cells, which are associated with gamma [Buzsáki and Wang, 2012].

In addition to our prior MRI studies, other investigations have provided structural and functional evidence for medial septum alteration. Using histology, Gorter et al. [2001, 2003] reported cell loss in the medial septum early following SE. Additionally, Colom et al. [2006] reported altered firing of medial septal neurons during epileptogenesis, with rhythmic fast firing neurons (putative GABAergic and glutamatergic) increasing their firing rate. They suggested this increased firing rate could be related to both destruction of septal GABAergic neurons and also degeneration of inhibitory septo-hippocampal projections. Changes to the medial septum might also explain the observed theta rhythm

alterations and, as we have previously discussed at length, the observed changes in hippocampal SPK 24-hour rhythms.

Figure 8-6 also shows that hippocampal 24-hour rhythms in high frequency bands increase in amplitude following injury. While a decrease in a 24-hour oscillation can be explained simply by loss or damage to the corresponding input, it is more difficult to explain how an increase in 24-hour rhythms might arise. Changes in melatonin 24-hour rhythms have been investigated in a number of studies and, while evidence is mixed, some have suggested that its release can be enhanced in the epileptic state [Hofstra and de Weerd, 2009, Quigg, 2000]. Melatonin also has well established mechanistic roles within the hippocampus, attenuating $GABA_A$ mediated currents [Wan et al., 1999] and increasing overall excitability [Musshoff and Speckmann, 2003, Musshoff et al., 2002].

8.4.4 Alternative Mechanisms

Here we discuss a possible alternative mechanism to that proposed in Figure 8-4. Instead of the phase shift being produced by a transfer in control of circadian drivers, the phase shift could simply appear because of our choice of using fixed frequency bands in our analysis. Specifically, if an EEG rhythm that is normally entrained to peak during the night is altered post-injury such that it enters a lower frequency band, this could produce the appearance of a phase shift. Thus, adaptive techniques, such as empirical mode decomposition, which do not require pre-specified frequency divisions might be useful in future analysis. However, as we can see for some animals in Figure 8-6, particularly Rats 2 and 4, the phase shift can occupy a very wide range of frequency bands. It is unlikely that an EEG rhythm's frequency would shift so drastically following injury, making this explanation not viable for these animals.

8.4.5 Future Work

Based on this study, we can identify three areas where future work is needed. First, additional signal analysis work is needed to further characterize changes in

24-hour rhythms. Specifically, since gamma rhythms are not continuously occurring events but, rather, transient phenomena, it is presently not possible to say whether the 24-hour frequency band modulation we witnessed is due to changes in the amplitude of each gamma event or due to changes in how often they occur. Ideally, future studies employing automated tracking techniques would track both the amplitude of these oscillations and also their rate of occurrence, similar to our approach here for studying theta. Secondly, our datasets contain accompanying video recordings. Since behavioural states can influence brain rhythms, it would be ideal to classify data according to behavioural state and remove this variable from our analysis. Finally, we should look at the 24-hour modulation of measurements of coherence and cross-frequency coupling. This will be useful for identifying whether 24-hour modulation of middle frequency rhythms is driven by coupling to other EEG rhythms (red arrows, Figure 8-4) or by direct circadian input (black arrows, Figure 8-4). Such studies could be accompanied by the generation of detailed septo-hippocampal models that can be used to study how various circadian inputs would modulate EEG rhythms. Finally, to identify the physiological identity of the specific circadian inputs, we propose obtaining additional chronic EEG recordings under conditions of either medial septal lesion and pinealectomy.

8.5 Closing Remarks

In summary, we have shown that there emerges a phase shift in the 24-hour modulation of EEG rhythms in the beta and gamma frequency bands. We have also provided evidence that there are multiple circadian inputs to the hippocampus and that these change in strength following epileptogenic injury. Additionally, we have provided a detailed characterization of the changes that occur to theta oscillations. These findings support the prediction of our prior modeling work, which predicted that a phase shift could emerge as a result of changes in the relative strengths of hippocampal circadian

inputs. Additionally, it is also consistent with our proposal that the medial septum might be a circadian relay center that is altered to underlie the phase shift.

CHAPTER 9
DISCUSSION AND CONCLUSIONS

9.1 Overview

In this dissertation, we have studied hippocampal 24-hour rhythms and have characterized their alteration in temporal lobe epilepsy (TLE).[1] We characterized that two primary markers of the hippocampal EEG, spikes (SPKs) and beta and gamma frequency rhythms exhibit a phase shift following epilepsy-inducing injury. These changes appear to be directly associated with epilepsy, as rats that received injury but did not develop spontaneous seizures did not exhibit these symptoms. To investigate the underlying mechanisms, we constructed a detailed model of the septo-hippocampal neural network, and characterized how subtle changes in the relative strengths of circadian inputs could lead to a phase shift. This model predicted that there are at least two circadian inputs driving hippocampal 24-hour rhythms. Through additional analysis of EEG rhythms, we demonstrated functional evidence for two main circadian inputs based on both dimensionality analysis and on the characterization of phase–amplitude relationships. Finally, we investigated structural changes in the medial septum, a putative circadian input, and showed that it showed signs of injury in epileptic animals. We propose that circadian input via the medial septum might be altered so as to contribute to the observed hippocampal 24-hour rhythm disruptions.

In this chapter, we will discuss implications of our findings in relation to broader epilepsy and circadian research.

[1] Parts of this chapter are in press with the Journal of Neurophysiology: Stanley, D.A., Talathi, S.S., Parekh, M.B., Cordiner, D., Zhou, J., Mareci, T.H., Ditto, W.L., Carney, P.R. Local phase shift in the 24-hour rhythm of hippocampal EEG spiking activity in a rat model of temporal lobe epilepsy [Stanley et al., 2013].

9.2 Implications of Altered Circadian Rhythms

9.2.1 Cognitive Impairment

Circadian alteration may contribute to epilepsy-associated cognitive symptoms. For example, circadian rhythms have been shown to affect memory formation [Gerstner and Yin, 2010], and there is evidence that processes such as long-term potentiation (LTP) are regulated on a 24-hour cycle [Chaudhury et al., 2005]. Hippocampal sharp waves are important for LTP [Buzsaki, 1996, Selbach et al., 2004] and theta and gamma waves play central roles in memory encoding [Colgin and Moser, 2010]. Thus, it is possible that the phase misalignment of hippocampal activities investigated in this study here might be relevant for memory impairment in epilepsy.

9.2.2 Emergence of Seizures

It is traditionally thought that processes such as neuron loss and subsequent circuit rewiring contribute to the emergence of seizures by creating excitatory-inhibitory imbalances [Briggs and Galanopoulou, 2011, Dudek and Spitz, 1997, El-Hassar et al., 2007, Sloviter, 2005]. It is possible that altered circadian regulation could facilitate the creation of such excitatory-inhibitory imbalances. Our modeling work showed that reduced septal circadian input can produce a phase misalignment in the 24-hour rhythms of pyramidal cells and basket cells (Figure 6-2C,D); we propose that this creates an optimal time window for seizure occurrence. A description of this phenomenon, and how it might interact with other epileptogenic processes to trigger the emergence of seizures, is provided in Figure 9-1. Specifically, the phase shift appears during the latency period resulting from structural damage associated with SE (Figure 9-1,i-ii). Although the optimal time window exists during the latency period, cell death and other changes resulting from SE suppress firing such that excitation is still balanced by inhibition (Figure 9-1,iii). Over time, epileptogenic processes restore mean firing activity to pre-seizure levels (dotted line), but they cannot restore the correct balance of circadian drive (Figure 9-1,iv). Thus, even if the daily mean firing rate of excitatory and

inhibitory cells does not exceed pre-seizure levels, the presence of the phase shift will still promote a temporary, yet potentially potent, excitatory-inhibitory imbalance during the optimal time window (Figure 9-1,v).

The presence of this optimal time window may reflect the 24-hour rhythm of epileptic seizures, which are observed to cluster in the afternoon in both rodent and human TLE [Hofstra and de Weerd, 2009, Loddenkemper et al., 2011, Quigg, 2000]. Previously it has been hypothesized that the 24-hour rhythm of epileptic seizures results from passive entrainment to the 24-hour rhythms of neuromodulators [Quigg, 2000]. However, the findings of a phase shift support the notion that the 24-hour rhythm of seizures may be actively driven by abnormal circadian regulation that promotes periods of excitatory-inhibitory imbalance throughout the day.

An additional property of the mechanisms underlying 24-hour seizure rhythms can be discerned based on cross-species comparison. Specifically, although rodents and humans with TLE have peak seizure occurrence in the afternoon, they have opposing activity patterns (nocturnal vs. diurnal), thus indicating that daily rhythms of seizures are not driven directly by sleep or wake activity. Rather, the underlying mechanism must be phase-conserved across these species. Twenty-four hour rhythms of medial septum firing activity, to our knowledge, have not yet been quantified in humans; however, melatonin is known to be phase-conserved [Quigg, 2000]. Whether the underlying mechanism is passive entrainment, as has been previously proposed, or an active response to a phase shift, we predict that the phases of the oscillations involved should be conserved across species.

9.3 Closing Remarks

Based on a number of large datasets, we have conducted a thorough analysis of 24-hour rhythms of hippocampal neural activity in TLE. While we hope that our investigations have made a significant contribution to the field of research on circadian rhythms and epilepsy, we believe there are many exciting opportunities for discovery in

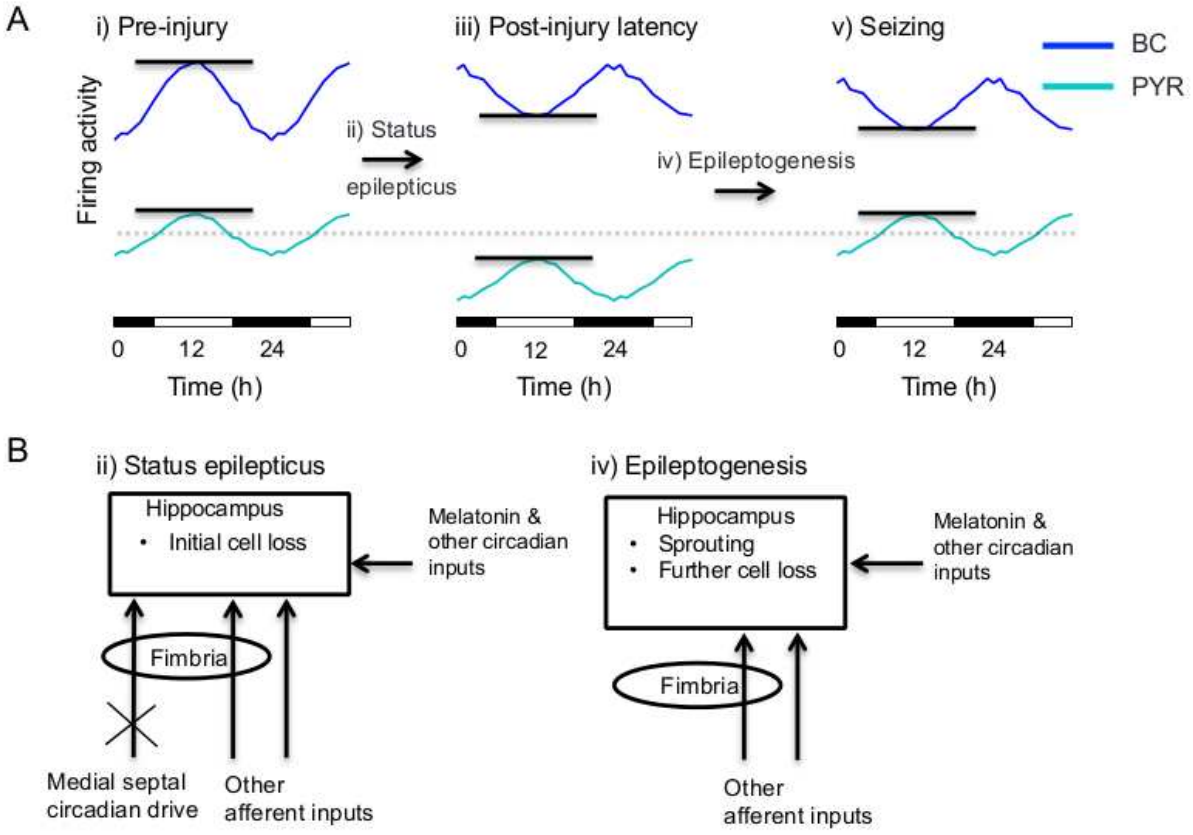

Figure 9-1. Schematic of circadian changes during epileptogenesis and their proposed influence on epileptic seizures. (A, B) Functional and structural changes during epileptogenesis, respectively. Pyramidal (PYR) and basket cell (BC) firing rates are shown and key events are numbered. Dotted line indicates the pre-injury average firing rate for pyramidal cells. Solid lines serve as a guide to the eye for changes in the ratio of excitation to inhibition. Key events (i-v) during epileptogenesis are: i) Prior to injury, PYR and BC activity are balanced throughout the day. ii) Injury from status epilepticus (SE) attenuates circadian input to the hippocampus from regions such as the medial septum, creating an imbalance in circadian drive. iii) This produces a phase shift in the firing of basket cell activity. Additional damage caused by SE, such as hippocampal cell loss (B, ii), alters the average daily firing activity and sets epileptogenic processes in motion. iv) Epileptogenic processes, including further cell loss, sprouting, and other homeostatic mechanisms, drive the emergence of spontaneous seizures. v) These processes act in part to restore the daily average levels of excitatory and inhibitory activity (dotted line). However, they do not restore the correct balance of circadian input and, thus, the phase shift persists. The circadian phase shift produces a time window during which the ratio of excitation to inhibition is increased, increasing the likelihood of seizures.

this area. For example, our analysis focused on a single channel in a dataset containing a total of 32 electrodes, meaning we are only using a small fraction of the total available data. Given that these electrodes are bilaterally spaced throughout the hippocampus and dentate gyrus, future work investigating 24-hour regulation of spatial coupling is possible. Additionally, with the development of new techniques for automated extraction of neural features, it will be possible to investigate more specific neural features, including individual episodes of gamma and beta oscillations.

Finally, this dissertation may serve as a testament to the potential of the “big data” movement within the realm of neuroscience. Ironically, through the use of signal processing, data analysis, and modeling techniques, we have managed to advance the field of research in a largely experimental domain without conducting a single new animal experiment. As the quantity, quality, and richness, of data that single experimentalists can collect continues to grow, we are hopeful for increased collaboration between experimentalists and theoreticians in neuroscience.

APPENDIX A
COMPLETE EEG SPK DATA

This appendix expands on the data presented in Chapter 5, and shows the data for all animals used to obtain statistics for SKP 24-hour rhythms. Figure A-1 shows extracted 24-hour rhythms for all N=3 seizing rats used to generate statistics in Figure 5-2D. Likewise, Figure A-2 shows extracted 24-hour rhythms for all N=3 seizing rats used to generate statistics in Figure 5-2F.

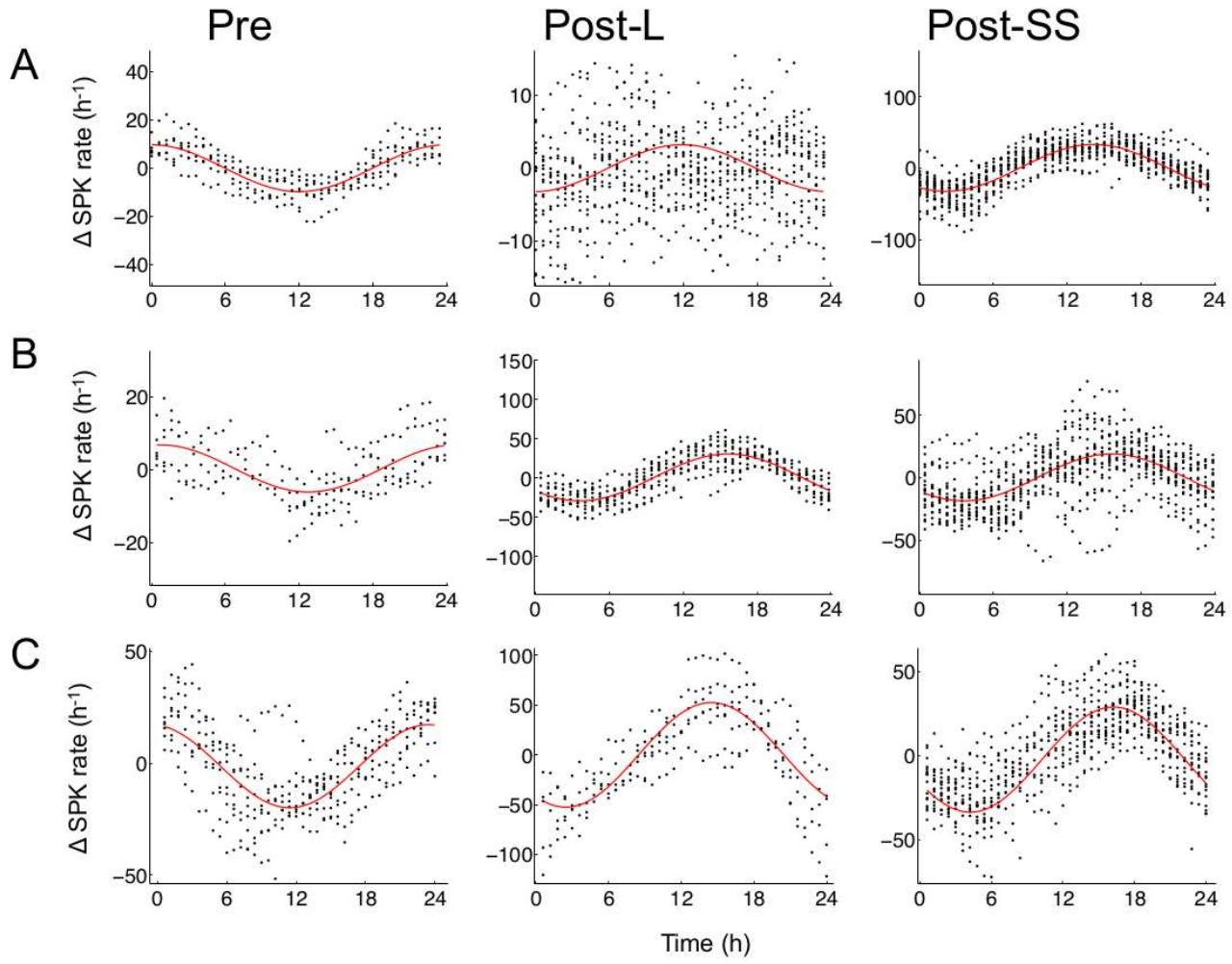

Figure A-1. (A-C),Shown are the 24-hour rhythms of SPK activity for all rats that developed spontaneous seizures. Rat shown in (C) corresponds to example animal shown in Figure 5-2C

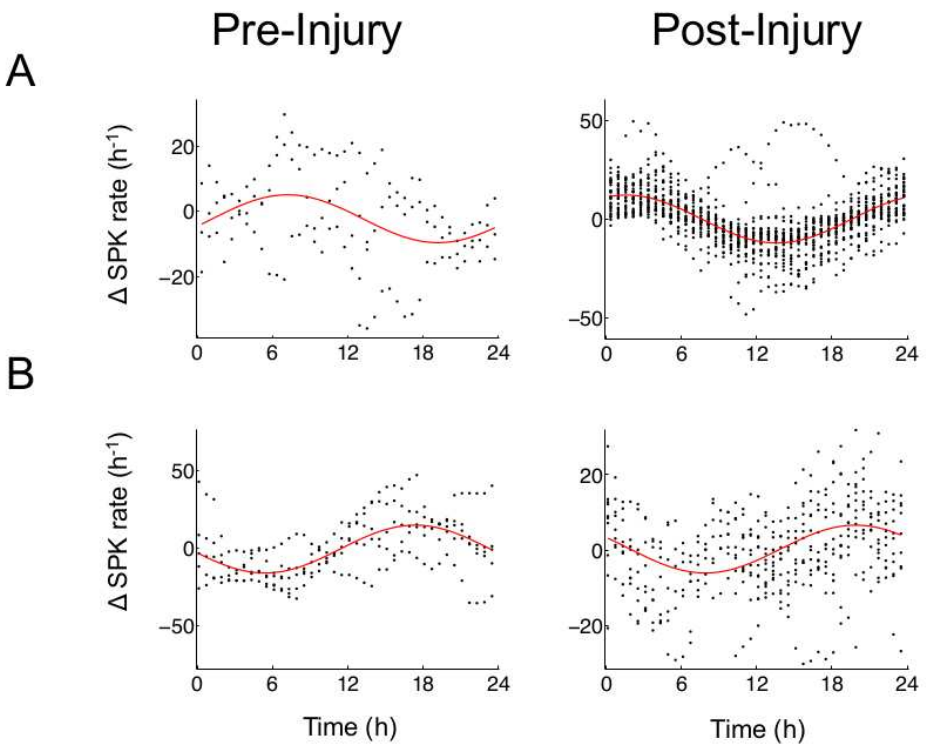

Figure A-2. (A,B) Shown are the 24-hour rhythms of SPK activity for the two rats that did not develope spontaneous seizures. Rat shown in (A) corresponds to example animal shown in Figure 5-2E.

APPENDIX B
COMPLETE EEG RHYTHM DATA

This appendix provides two sets of figures. The first set (Figure B-1 to B-6) shows the detrended EEG PSD time series that were used in the analysis in Chapter 8. They also provide continuous estimates of the time of day that PSD activity is maximal ($T_{\Delta PSDmax}$). The second set shows detrended EEG PSD time series condensed into single 24-hour time windows and fit to sinusoids.

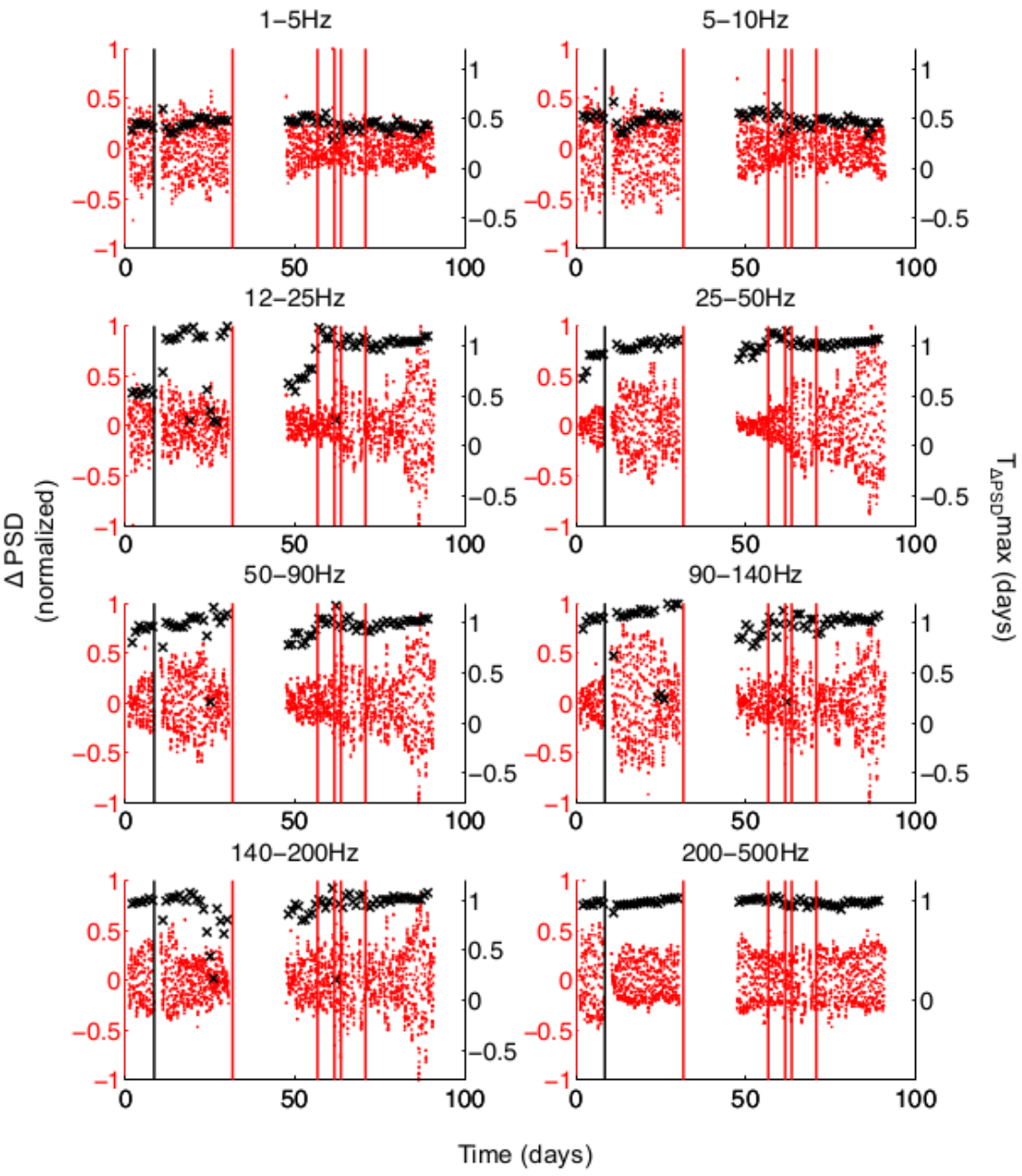

Figure B-1. Detrended PSD data (ΔPSD) is shown for all frequency bands for Rat 1. Time of maximum ΔPSD ($T_{\Delta PSDmax}$) was estimated for sliding 2-day windows (50% overlapping), providing a rolling estimate of phase. Black vertical line indicates time of induction of status epilepticus (SE) and red vertical lines indicate seizure timings.

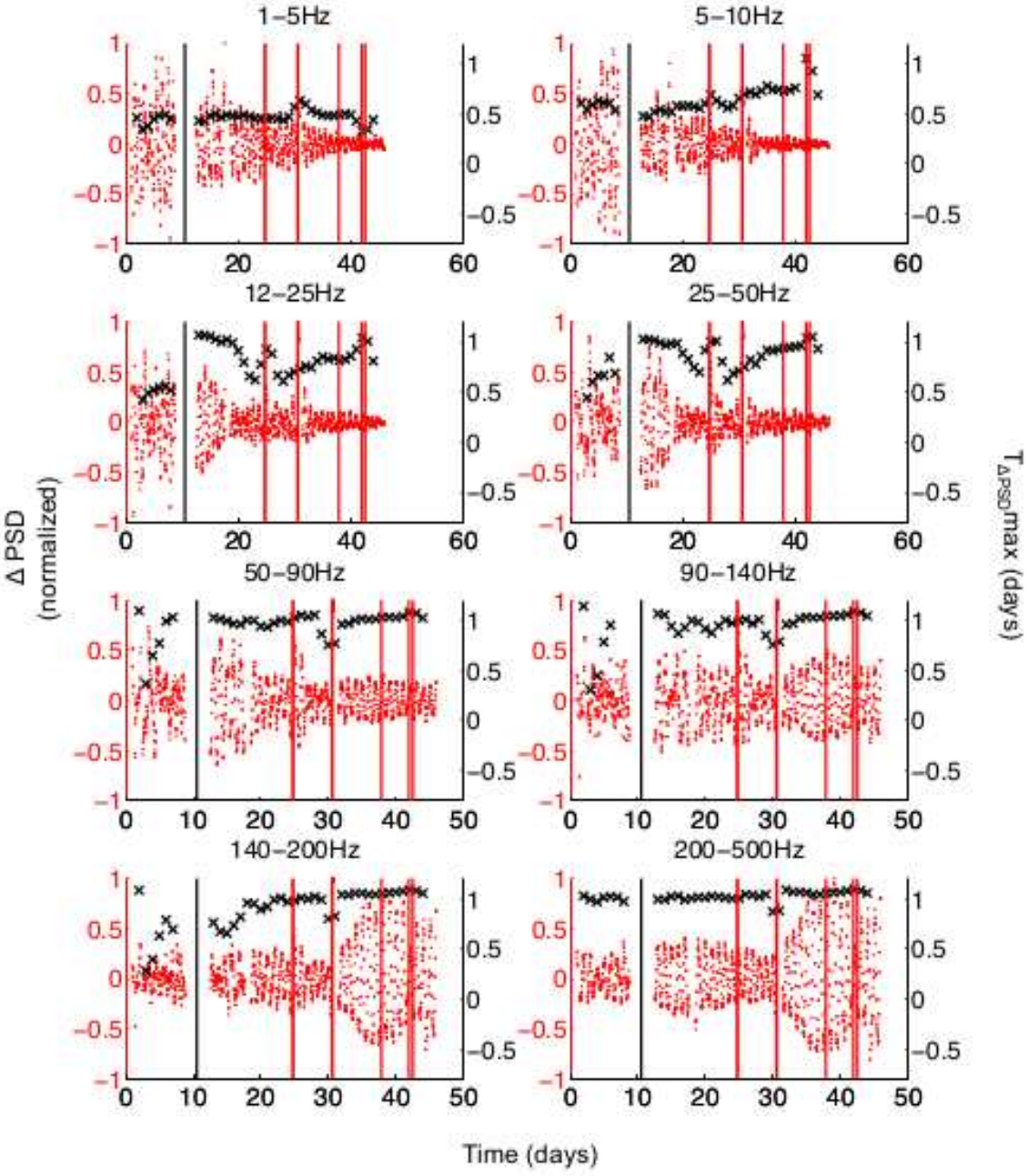

Figure B-2. Rat 2 data, as in Figure B-1.

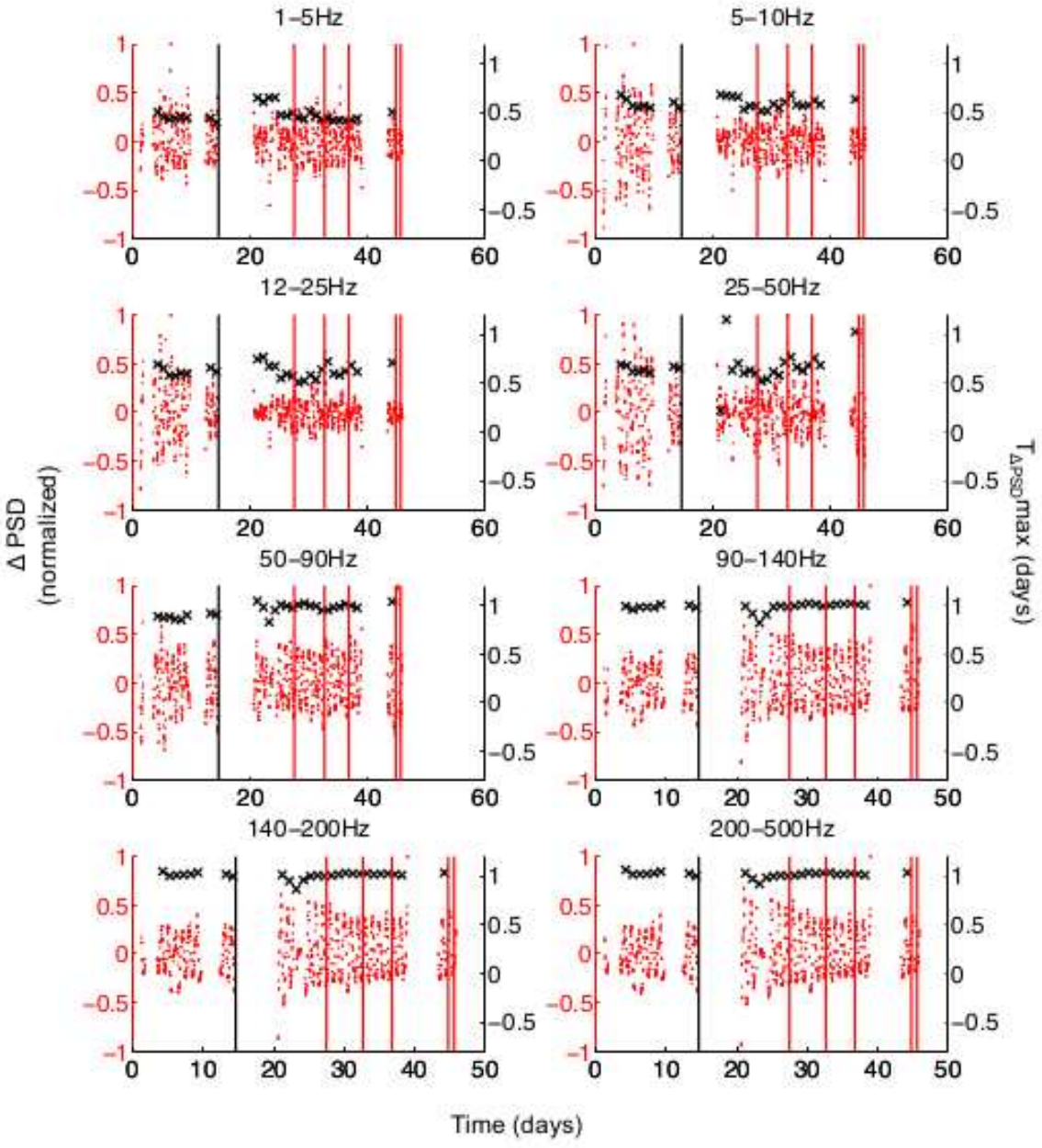

Figure B-3. Rat 3 data, as in Figure B-1.

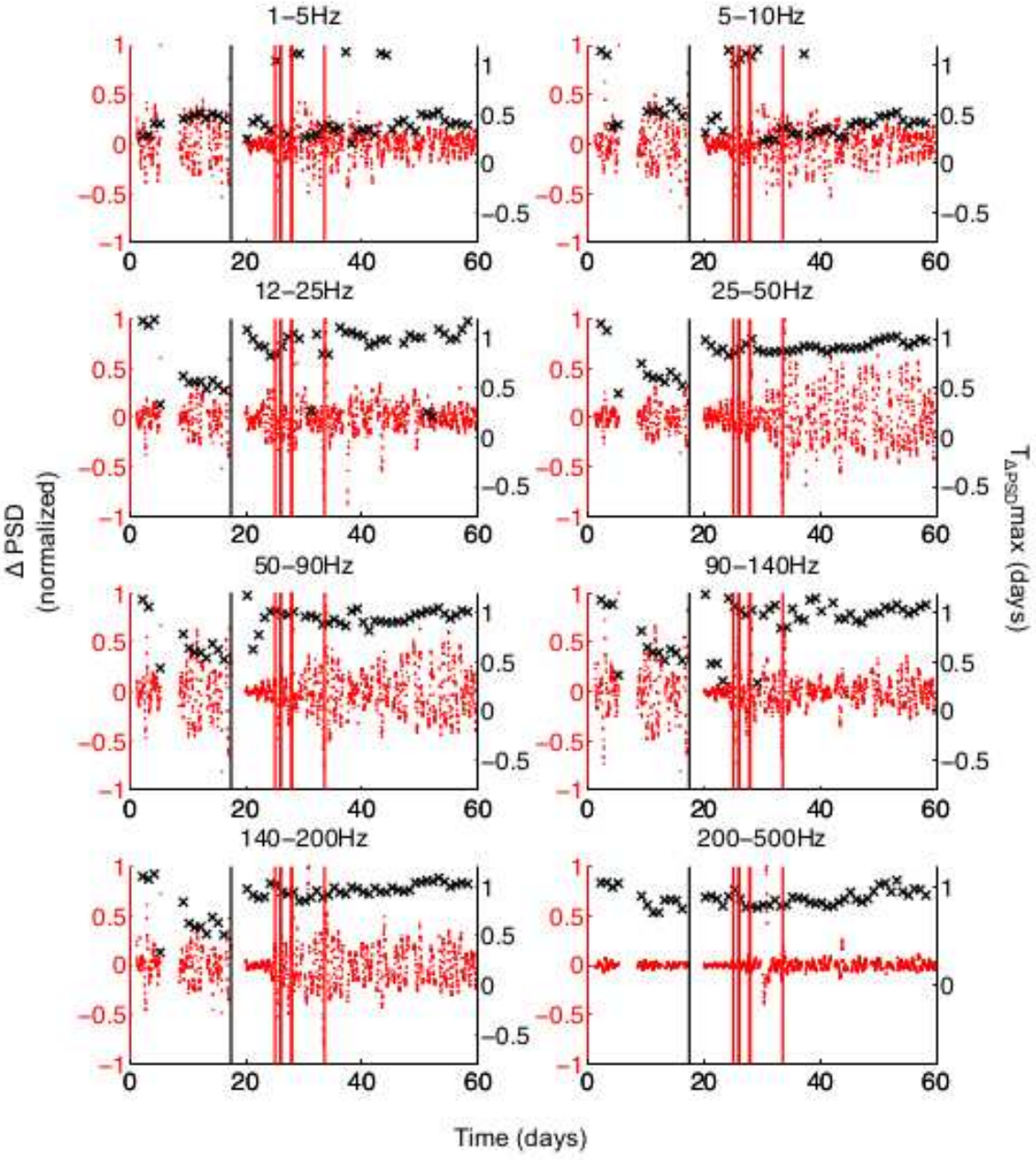

Figure B-4. Rat 4 data, as in Figure B-1.

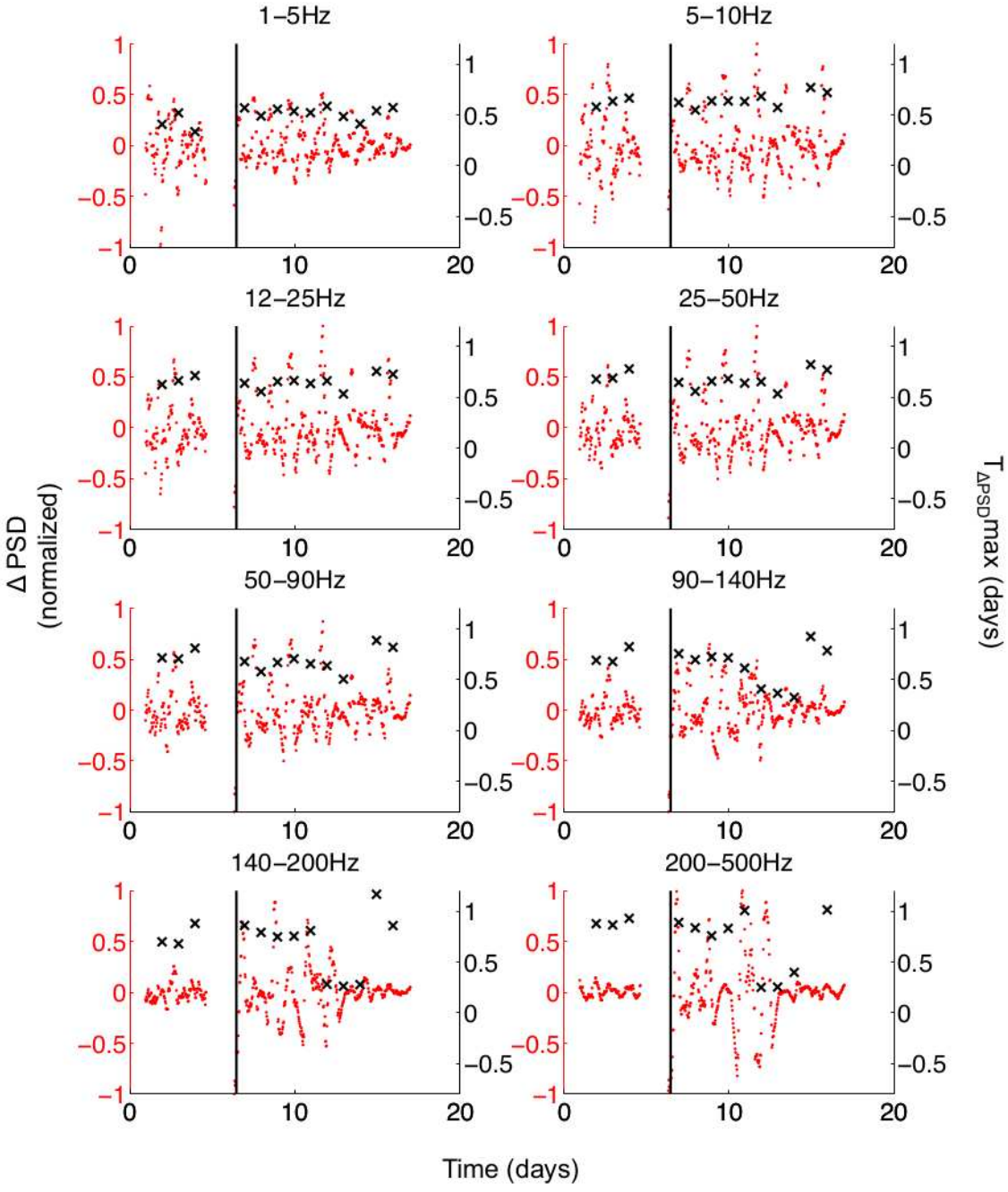

Figure B-5. Rat 5 data, as in Figure B-1. This is a non-seizing animal.

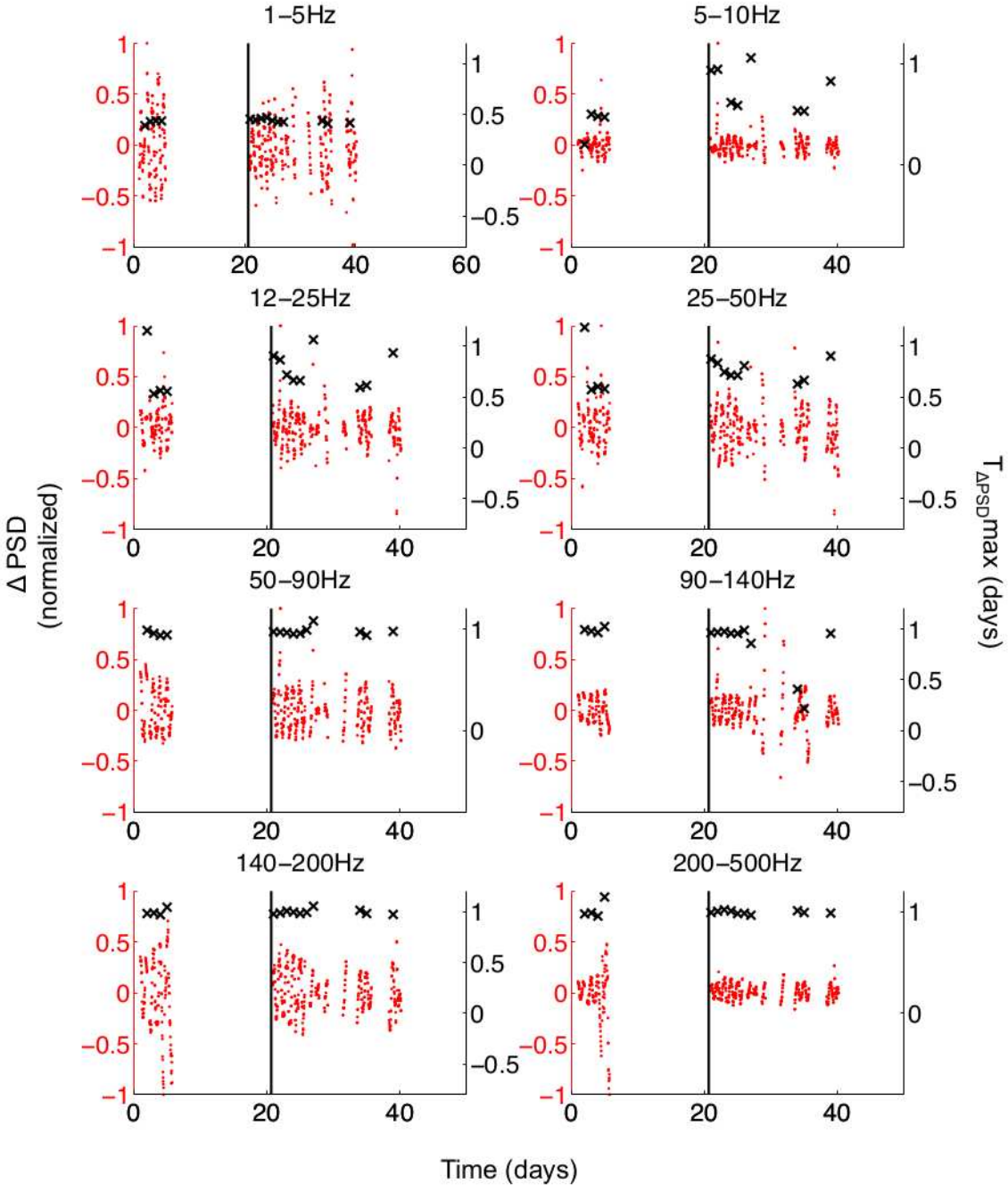

Figure B-6. Rat 6 data, as in Figure B-1. This is a non-seizing animal.

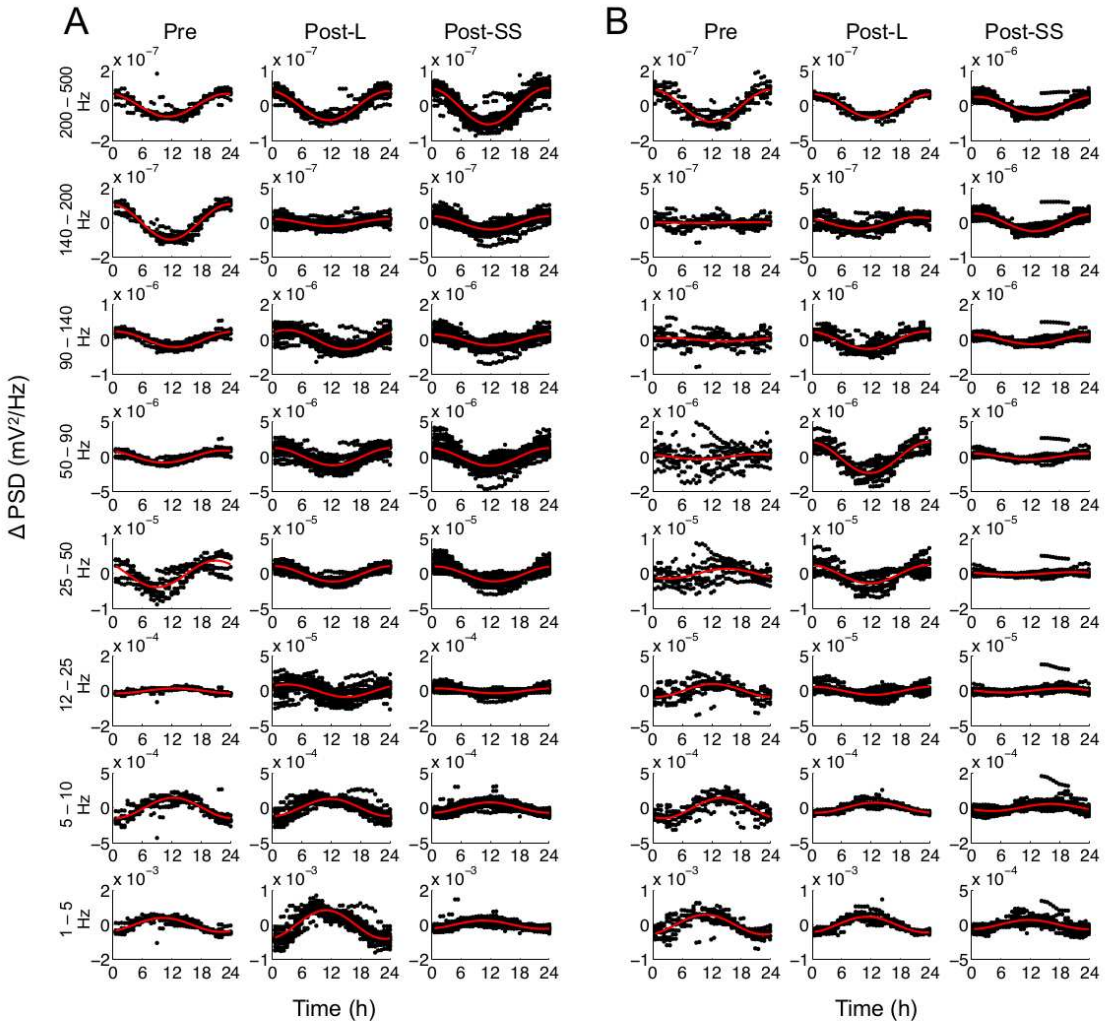

Figure B-7. (A,B) Sinusoidal fits (red) on detrended data for Rats 1 and 2. Data has been condensed into 24-hour time windows (modulo 24).

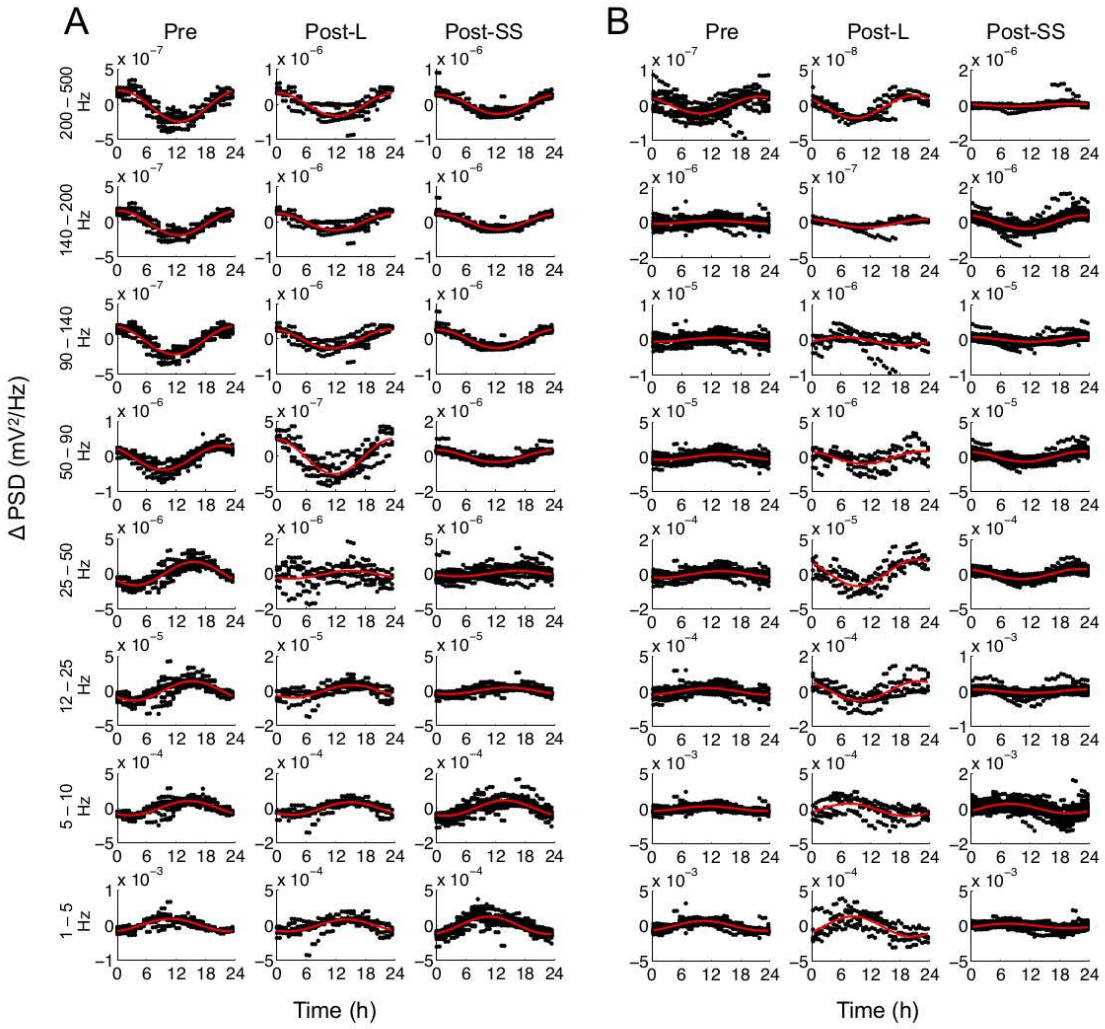

Figure B-8. (A,B) Sinusoidal fits (red) on detrended data for Rats 3 and 4. Data has been condensed into 24-hour time windows (modulo 24).

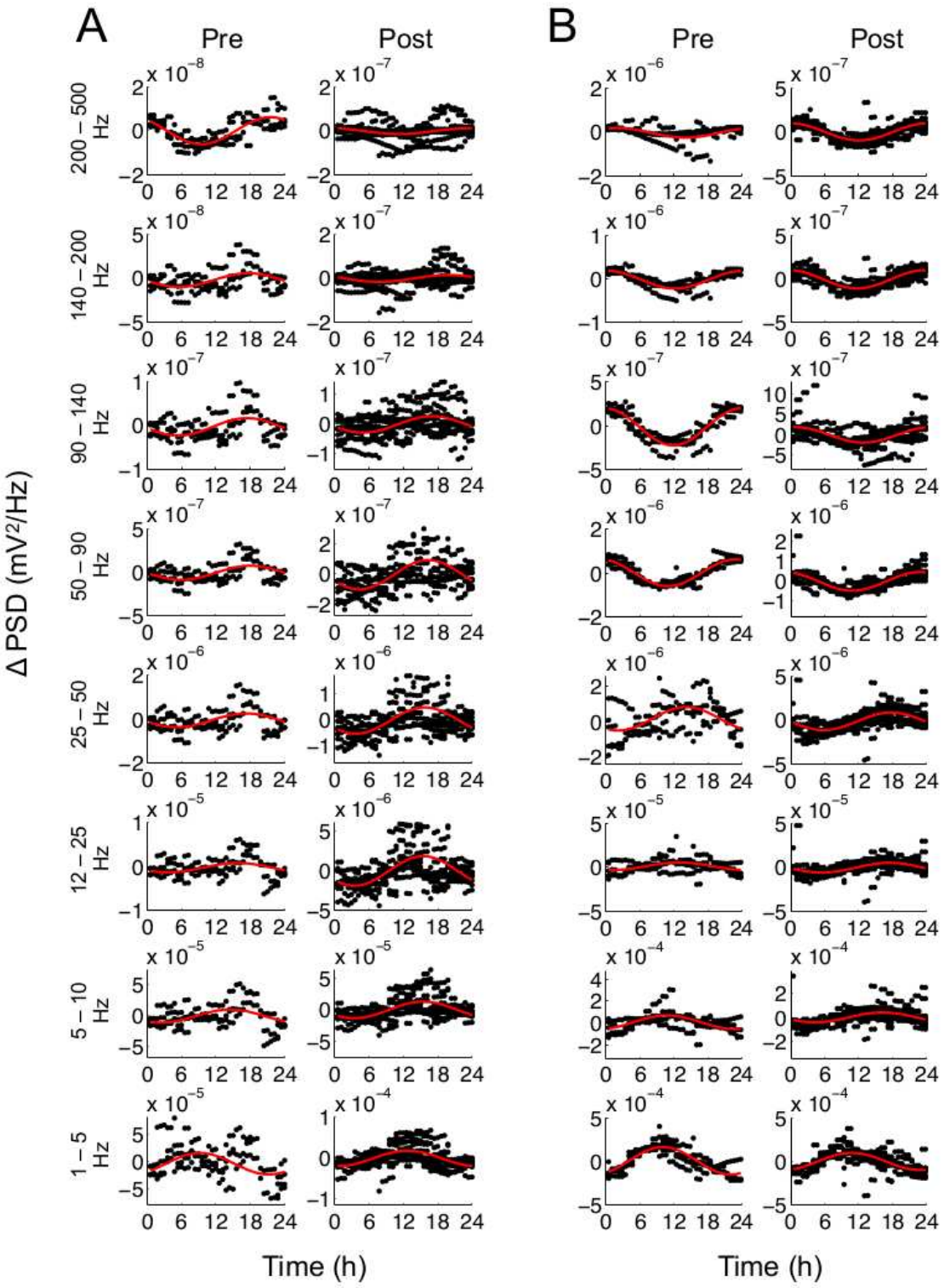

Figure B-9. (A,B) Sinusoidal fits (red) on detrended data for Rats 5 and 6. Data has been condensed into 24-hour time windows (modulo 24). These are non-seizing animals.

REFERENCES

E. Abrahamson, R. Leak, and R. Moore. The suprachiasmatic nucleus projects to posterior hypothalamic arousal systems. *Neuroreport*, 12(2):435–440, 2001.

H. Agren, M. Koulu, J. M. Saavedra, W. Z. Potter, M. Linnoila, et al. Circadian covariation of norepinephrine and serotonin in the locus coeruleus and dorsal raphe nucleus in the rat. *Brain research*, 397(2):353–358, 1986.

F. Angeleri, J. Majkowski, G. Cacchio, A. Sobieszek, S. D'acunto, R. Gesuita, A. Bachleda, G. Polonara, L. Krolicki, M. Signorino, et al. Posttraumatic epilepsy risk factors: One-year prospective study after head injury. *Epilepsia*, 40(9):1222–1230, 1999.

V. Aroniadou-Anderjaska, B. Fritsch, F. Qashu, and M. F. Braga. Pathology and pathophysiology of the amygdala in epileptogenesis and epilepsy. *Epilepsy research*, 78(2):102–116, 2008.

S. Y. Assaf and J. J. Miller. The role of a raphe serotonin system in the control of septal unit activity and hippocampal desynchronization. *Neuroscience*, 3(6):539–50, 1978.

G. Aston-Jones, S. Chen, Y. Zhu, and M. L. Oshinsky. A neural circuit for circadian regulation of arousal. *Nature neuroscience*, 4(7):732–738, 2001.

E. C. Azmitia and M. Segal. An autoradiographic analysis of the differential ascending projections of the dorsal and median raphe nuclei in the rat. *Journal of Comparative Neurology*, 179(3):641–667, 1978.

D. Baker, G. Church, J. Collins, D. Endy, J. Jacobson, J. Keasling, P. Modrich, C. Smolke, and R. Weiss. Engineering life: building a fab for biology. *Scientific American*, 294(6): 44–51, 2006.

A. R. Barnard and P. M. Nolan. When clocks go bad: neurobehavioural consequences of disrupted circadian timing. *PLoS Genetics*, 4(5):e1000040, 2008.

C. A. Barnes, B. L. McNaughton, G. V. Goddard, R. M. Douglas, and R. Adamec. Circadian rhythm of synaptic excitability in rat and monkey central nervous system. *Science*, 197(4298):91–2, 1977.

P. J. Basser. Inferring microstructural features and the physiological state of tissues from diffusion-weighted images. *NMR Biomed*, 8(7-8):333–44, 1995.

J. F. Bastlund, P. Jennum, P. Mohapel, S. Penschuck, and W. P. Watson. Spontaneous epileptic rats show changes in sleep architecture and hypothalamic pathology. *Epilepsia*, 46(6):934–8, 2005.

C. W. Bazil, D. Short, D. Crispin, and W. Zheng. Patients with intractable epilepsy have low melatonin, which increases following seizures. *Neurology*, 55(11):1746–8, 2000.

D. G. Beersma and M. Gordijn. Circadian control of the sleep–wake cycle. *Physiology & behavior*, 90(2):190–195, 2007.

C. E. Begley, M. Famulari, J. F. Annegers, D. R. Lairson, T. F. Reynolds, S. Coan, S. Dubinsky, M. E. Newmark, C. Leibson, E. So, et al. The cost of epilepsy in the united states: An estimate from population-based clinical and survey data. *Epilepsia*, 41(3):342–351, 2000.

M. D. Belle, C. O. Diekman, D. B. Forger, and H. D. Piggins. Daily electrical silencing in the mammalian circadian clock. *Science Signaling*, 326(5950):281, 2009.

M. A. Belluscio, K. Mizuseki, R. Schmidt, R. Kempter, and G. Buzsaki. Cross-frequency phase-phase coupling between and oscillations in the hippocampus. *J Neurosci*, 32 (2):423–35, 2012.

E. H. Bertram. Temporal lobe epilepsy: where do the seizures really begin? *Epilepsy & behavior*, 14(1):32–37, 2009.

C. Biervert, B. C. Schroeder, C. Kubisch, S. F. Berkovic, P. Propping, T. J. Jentsch, and O. K. Steinlein. A potassium channel mutation in neonatal human epilepsy. *Science*, 279(5349):403–406, 1998.

J. Bower and D. Beeman. *The book of GENESIS: Exploring realistic neural models with the GEneral NEural SImulation System*. Springer-Verlag, New York, NY, 2003.

J. Bower, D. Beeman, and M. Hucka. *The genesis simulation system*, volume 2. 2002.

A. Bragin, J. Engel, C. L. Wilson, I. Fried, and G. W. Mathern. Hippocampal and entorhinal cortex high-frequency oscillations (100–500 hz) in human epileptic brain and in kainic acid-treated rats with chronic seizures. *Epilepsia*, 40(2):127–137, 1999.

S. W. Briggs and A. S. Galanopoulou. Altered gaba signaling in early life epilepsies. *Neural Plast*, 2011:527605, 2011.

S. Brunel and C. de Montigny. Diurnal rhythms in the responsiveness of hippocampal pyramidal neurons to serotonin, norepinephrine, gamma-aminobutyric acid and acetylcholine. *Brain Res Bull*, 18(2):205–12, 1987.

G. Buzsaki. Hippocampal sharp waves: their origin and significance. *Brain Res*, 398(2): 242–52, 1986.

G. Buzsaki. The hippocampo-neocortical dialogue. *Cereb Cortex*, 6(2):81–92, 1996.

G. Buzsáki. Theta oscillations in the hippocampus. *Neuron*, 33(3):325–340, 2002.

G. Buzsaki. *Rhythms of the Brain*. Oxford University Press, USA, 2009.

G. Buzsáki and F. L. d. Silva. High frequency oscillations in the intact brain. *Progress in Neurobiology*, 98(3):241–249, 2012.

G. Buzsáki and X.-J. Wang. Mechanisms of gamma oscillations. *Annual review of neuroscience*, 35:203–225, 2012.

G. Buzsaki, L. W. Leung, and C. H. Vanderwolf. Cellular bases of hippocampal eeg in the behaving rat. *Brain Res*, 287(2):139–71, 1983.

G. Buzsáki, J. Czopf, I. Kondakor, and L. Kellenyi. Laminar distribution of hippocampal rhythmic slow activity (rsa) in the behaving rat: current-source density analysis, effects of urethane and atropine. *Brain research*, 365(1):125–137, 1986.

G. Buzsaki, M. Hsu, C. Slamka, F. H. Gage, and Z. Horváth. Emergence and propagation of interictal spikes in the subcortically denervated hippocampus. *Hippocampus*, 1(2):163–80, 1991.

T. Cambras, J. R. Weller, M. Anglès-Pujoràs, M. L. Lee, A. Christopher, A. Díez-Noguera, J. M. Krueger, and O. Horacio. Circadian desynchronization of core body temperature and sleep stages in the rat. *Proceedings of the National Academy of Sciences*, 104(18):7634–7639, 2007.

M. A. Carskadon, S. E. Labyak, C. Acebo, and R. Seifer. Intrinsic circadian period of adolescent humans measured in conditions of forced desynchrony. *Neuroscience letters*, 260(2):129–132, 1999.

L. J. Cauller, Z. Boulos, and G. V. Goddard. Circadian rhythms in hippocampal responsiveness to perforant path stimulation and their relation to behavioral state. *Brain Res*, 329(1-2):117–30, 1985.

D. J. Chalmers. Facing up to the problem of consciousness. *Journal of consciousness studies*, 2(3):200–219, 1995.

G. Chatrian, L. Bergamini, M. Dondey, D. Klass, M. Lennox-Buchthal, and I. Petersen. A glossary of terms most commonly used by clinical electroencephalographers. *Electroencephalogr Clin Neurophysiol*, 37(5):538–548, 1974.

D. Chaudhury, L. M. Wang, and C. S. Colwell. Circadian regulation of hippocampal long-term potentiation. *J Biol Rhythms*, 20(3):225–36, 2005.

H. Cho, X. Zhao, M. Hatori, T. Y. Ruth, G. D. Barish, M. T. Lam, L.-W. Chong, L. DiTacchio, A. R. Atkins, C. K. Glass, et al. Regulation of circadian behaviour and metabolism by rev-erb-[agr] and rev-erb-[bgr]. *Nature*, 485(7396):123–127, 2012.

K. Cho. Chronic 'jet lag' produces temporal lobe atrophy and spatial cognitive deficits. *Nat Neurosci*, 4(6):567–8, 2001.

K. Cho, A. Ennaceur, J. C. Cole, and C. K. Suh. Chronic jet lag produces cognitive deficits. *J Neurosci*, 20(6):1–5, 2000.

L. L. Colgin and E. I. Moser. Gamma oscillations in the hippocampus. *Physiology*, 25(5): 319–329, 2010.

L. V. Colom, A. García-Hernández, M. T. Castañeda, M. G. Perez-Cordova, and E. R. Garrido-Sanabria. Septo-hippocampal networks in chronically epileptic rats: potential antiepileptic effects of theta rhythm generation. *Journal of neurophysiology*, 95(6): 3645–3653, 2006.

F. Crick and C. Koch. A framework for consciousness. *Nature neuroscience*, 6(2): 119–126, 2003.

J. Csicsvari, H. Hirase, A. Czurko, and G. Buzsaki. Reliability and state dependence of pyramidal cell-interneuron synapses in the hippocampus: an ensemble approach in the behaving rat. *Neuron*, 21(1):179–89, 1998.

J. Csicsvari, H. Hirase, A. Czurkó, A. Mamiya, and G. Buzsáki. Oscillatory coupling of hippocampal pyramidal cells and interneurons in the behaving rat. *The Journal of neuroscience*, 19(1):274–287, 1999.

J. Csicsvari, H. Hirase, A. Mamiya, G. Buzsáki, et al. Ensemble patterns of hippocampal ca3-ca1 neurons during sharp wave-associated population events. *Neuron*, 28(2):585, 2000.

F. L. Da Silva, M. Witter, P. Boeijinga, and A. Lohman. Anatomic organization and physiology of the limbic cortex. *Physiological reviews*, 70(2):453–511, 1990.

R. C. Dana and J. L. Martinez. Effect of adrenalectomy on the circadian rhythm of ltp. *Brain research*, 308(2):392–395, 1984.

S. Deurveilher, K. Semba, et al. Indirect projections from the suprachiasmatic nucleus to major arousal-promoting cell groups in rat: implications for the circadian control of behavioural state. *Neuroscience*, 130(1):165–183, 2005.

F. E. Dudek and M. Spitz. Hypothetical mechanisms for the cellular and neurophysiologic basis of secondary epileptogenesis: proposed role of synaptic reorganization. *J Clin Neurophysiol*, 14(2):90–101, 1997.

L. El-Hassar, M. Milh, F. Wendling, N. Ferrand, M. Esclapez, and C. Bernard. Cell domain-dependent changes in the glutamatergic and gabaergic drives during epileptogenesis in the rat ca1 region. *J Physiol*, 578(Pt 1):193–211, 2007.

T. J. Ellender, W. Nissen, L. L. Colgin, E. O. Mann, and O. Paulsen. Priming of hippocampal population bursts by individual perisomatic-targeting interneurons. *J Neurosci*, 30(17):5979–91, 2010.

J. Engel. Intractable epilepsy: definition and neurobiology. *Epilepsia*, 42(s6):3–3, 2001.

M. S. Fee, P. P. Mitra, and D. Kleinfeld. Automatic sorting of multiple unit neuronal signals in the presence of anisotropic and non-gaussian variability. *J Neurosci Methods*, 69(2):175–88, 1996.

C. Fischer. *The Corpus: The Hippocratic Writings*. Kaplan, 2008.

J. A. F. Fisher. *A Treatise on Electricity: And the Construction and Management of Electrical and Mechanical Torpedoes*. Griffin, Great Britain, 1871.

T. F. Freund and M. Antal. Gaba-containing neurons in the septum control inhibitory interneurons in the hippocampus. *Nature*, 336(6195):170–3, 1988.

A. H. Friedman and C. A. Walker. Circadian rhythms in rat mid-brain and caudate nucleus biogenic amine levels. *The Journal of physiology*, 197(1):77–85, 1968.

A. H. Friedman and C. A. Walker. Rat brain amines, blood histamine and glucose levels in relationship to circadian changes in sleep induced by pentobarbitone sodium. *The Journal of Physiology*, 202(1):133–146, 1969.

F. H. Gage, A. Björklund, and U. Stenevi. Reinnervation of the partially deafferented hippocampus by compensatory collateral sprouting from spared cholinergic and noradrenergic afferents. *Brain Research*, 268(1):27–37, 1983.

J. R. Gerstner and J. C. Yin. Circadian rhythms and memory formation. *Nat Rev Neurosci*, 11(8):577–88, 2010.

W. Gerstner and R. Naud. How good are neuron models? *Science*, 326(5951):379–380, 2009.

J. A. Gorter, E. A. van Vliet, E. Aronica, and F. H. Lopes da Silva. Progression of spontaneous seizures after status epilepticus is associated with mossy fibre sprouting and extensive bilateral loss of hilar parvalbumin and somatostatin-immunoreactive neurons. *Eur J Neurosci*, 13(4):657–69, 2001.

J. A. Gorter, P. M. Gonçalves Pereira, E. A. van Vliet, E. Aronica, F. H. Lopes da Silva, and P. J. Lucassen. Neuronal cell death in a rat model for mesial temporal lobe epilepsy is induced by the initial status epilepticus and not by later repeated spontaneous seizures. *Epilepsia*, 44(5):647–58, 2003.

R. Goutagny, J. Jackson, and S. Williams. Self-generated theta oscillations in the hippocampus. *Nature neuroscience*, 12(12):1491–1493, 2009.

W. R. Gowers and E. B. Schlesinger. *Epilepsy and other chronic convulsive diseases: their causes, symptoms and treatment*. Wood's Library of standard medical authors. William Wood and Co., New York, 1885.

C. Guilding and H. D. Piggins. Challenging the omnipotence of the suprachiasmatic timekeeper: are circadian oscillators present throughout the mammalian brain? *European Journal of Neuroscience*, 25(11):3195–3216, 2007.

M. Hajos, W. E. Hoffmann, G. Orbán, T. Kiss, and P. Erdi. Modulation of septo-hippocampal theta activity by gabaa receptors: an experimental and computational approach. *Neuroscience*, 126(3):599–610, 2004.

K. Hara and R. A. Harris. The anesthetic mechanism of urethane: the effects on neurotransmitter-gated ion channels. *Anesthesia & Analgesia*, 94(2):313–318, 2002.

J. H. Haring and J. N. Davis. Differential distribution of locus coeruleus projections to the hippocampal formation: anatomical and biochemical evidence. *Brain research*, 325 (1):366–369, 1985.

K. M. Harris and T. J. Teyler. Age differences in a circadian influence on hippocamapl ltp. *Brain research*, 261(1):69–73, 1983.

O. K. Hassani, M. G. Lee, P. Henny, and B. E. Jones. Discharge profiles of identified gabaergic in comparison to cholinergic and putative glutamatergic basal forebrain neurons across the sleep–wake cycle. *The Journal of Neuroscience*, 29(38): 11828–11840, 2009.

M. E. Hasselmo. What is the function of hippocampal theta rhythm?linking behavioral data to phasic properties of field potential and unit recording data. *Hippocampus*, 15 (7):936–949, 2005.

M. H. Hastings, A. B. Reddy, and E. S. Maywood. A clockwork web: circadian timing in brain and periphery, in health and disease. *Nat Rev Neurosci*, 4(8):649–61, 2003.

W. A. Hauser and D. C. Hesdorffer. *Epilepsy: frequency, causes, and consequences*. Epilepsy Foundation of America New York, NY, USA, 1990.

M. L. Hines, T. Morse, M. Migliore, N. T. Carnevale, and G. M. Shepherd. Modeldb: A database to support computational neuroscience. *J Comput Neurosci*, 17(1):7–11, 2004.

P. F. Hingston, L. C. Barone, and Z. Michalewicz. *Design by Evolution: Advances in evolutionary design*. Springer, 2008.

D. Hirtz, D. Thurman, K. Gwinn-Hardy, M. Mohamed, A. Chaudhuri, and R. Zalutsky. How common are the common neurologic disorders? *Neurology*, 68(5):326–337, 2007.

E. C. Y. Ho. *If you want to be slow you have to be fast: Control of slow population activities by fast-spiking interneurons via network multistability*. PhD thesis, University of Toronto, 2011.

A. L. Hodgkin and A. F. Huxley. A quantitative description of membrane current and its application to conduction and excitation in nerve. *J Physiol*, 117(4):500–44, 1952.

W. A. Hofstra and A. W. de Weerd. How to assess circadian rhythm in humans: a review of literature. *Epilepsy Behav*, 13(3):438–44, 2008.

W. A. Hofstra and A. W. de Weerd. The circadian rhythm and its interaction with human epilepsy: a review of literature. *Sleep Med Rev*, 13(6):413–20, 2009.

W. A. Hofstra, M. C. Gordijn, J. C. v. H.-v. d. Poel, J. v. d. Palen, and A. W. De Weerd. Chronotypes and subjective sleep parameters in epilepsy patients: a large questionnaire study. *Chronobiology international*, 27(6):1271–1286, 2010.

ILEA. Proposal for revised clinical and electroencephalographic classification of epileptic seizures. *Epilepsia*, 22(4):489–501, 1981.

ILEA. Proposal for revised classification of epilepsies and epileptic syndromes. *Epilepsia*, 30(4):389–399, 1989.

S. T. Inouye. Does the ventromedial hypothalamic nucleus contain a self-sustained circadian oscillator associated with periodic feedings? *Brain Res*, 279(1-2):53–63, 1983.

S. T. Inouye and H. Kawamura. Persistence of circadian rhythmicity in a mammalian hypothalamic island containing the suprachiasmatic nucleus. *Proc Natl Acad Sci U S A*, 76(11):5962–6, 1979.

B. Jian, B. C. Vemuri, E. Ozarslan, P. R. Carney, and T. H. Mareci. A novel tensor distribution model for the diffusion-weighted mr signal. *Neuroimage*, 37(1):164–76, 2007.

H. Kang and E. M. Schuman. Long-lasting neurotrophin-induced enhancement of synaptic transmission in the adult hippocampus. *Science*, 267(5204):1658–1662, 1995.

C. H. Ko and J. S. Takahashi. Molecular components of the mammalian circadian clock. *Human molecular genetics*, 15(suppl 2):R271–R277, 2006.

M. H. Kole, J. M. Koolhaas, P. G. Luiten, and E. Fuchs. High-voltage-activated ca2+ currents and the excitability of pyramidal neurons in the hippocampal ca3 subfield in rats depend on corticosterone and time of day. *Neurosci Lett*, 307(1):53–6, 2001.

R. Kramis, C. H. Vanderwolf, and B. H. Bland. Two types of hippocampal rhythmical slow activity in both the rabbit and the rat: relations to behavior and effects of atropine, diethyl ether, urethane, and pentobarbital. *Exp Neurol*, 49(1 Pt 1):58–85, 1975.

D. Kubota, L. L. Colgin, M. Casale, F. A. Brucher, and G. Lynch. Endogenous waves in hippocampal slices. *J Neurophysiol*, 89(1):81–9, 2003.

R. Kurzweil. *The singularity is near: When humans transcend biology*. Penguin books, 2005.

P. Kwan and M. J. Brodie. Early identification of refractory epilepsy. *New England Journal of Medicine*, 342(5):314–319, 2000.

M. G. Lee, J. J. Chrobak, A. Sik, R. G. Wiley, and G. Buzsaki. Hippocampal theta activity following selective lesion of the septal cholinergic system. *Neuroscience*, 62(4): 1033–47, 1994.

L. S. Leung. Generation of theta and gamma rhythms in the hippocampus. *Neuroscience & Biobehavioral Reviews*, 22(2):275–290, 1998.

L. W. Leung. Hippocampal interictal spikes induced by kindling: relations to behavior and eeg. *Behav Brain Res*, 31(1):75–84, 1988.

D. K. Liu, R. L. Horner, and J. M. Wojtowicz. Time of day determines modulation of synaptic transmission by adenosine in the rat hippocampal slices. *Neurosci Lett*, 282 (3):200–2, 2000.

T. Loddenkemper, S. W. Lockley, J. Kaleyias, and S. V. Kothare. Chronobiology of epilepsy: diagnostic and therapeutic implications of chrono-epileptology. *J Clin Neurophysiol*, 28(2):146–53, 2011.

E. W. Lothman, E. H. Bertram, J. W. Bekenstein, and J. B. Perlin. Self-sustaining limbic status epilepticus induced by 'continuous' hippocampal stimulation: electrographic and behavioral characteristics. *Epilepsy Res*, 3(2):107–19, 1989.

E. W. Lothman, E. H. Bertram, J. Kapur, and J. L. Stringer. Recurrent spontaneous hippocampal seizures in the rat as a chronic sequela to limbic status epilepticus. *Epilepsy Res*, 6(2):110–8, 1990.

J. Ma and L.-W. S. Leung. Medial septum mediates the increase in post-ictal behaviors and hippocampal gamma waves after an electrically induced seizure. *Brain research*, 833(1):51–57, 1999.

B. A. Malow, R. Kushwaha, X. Lin, K. J. Morton, and M. S. Aldrich. Relationship of interictal epileptiform discharges to sleep depth in partial epilepsy. *Electroencephalography and clinical neurophysiology*, 102(1):20–26, 1997.

J. Matzen, K. Buchheim, and M. Holtkamp. Circadian dentate gyrus excitability in a rat model of temporal lobe epilepsy. *Exp Neurol*, 234(1):105–11, 2012.

M. H. Meisler, J. A. Kearney, et al. Sodium channel mutations in epilepsy and other neurological disorders. *Journal of Clinical Investigation*, 115(8):2010, 2005.

M. Migliore, T. M. Morse, A. P. Davison, L. Marenco, G. M. Shepherd, and M. L. Hines. Modeldb: making models publicly accessible to support computational neuroscience. *Neuroinformatics*, 1(1):135–9, 2003.

T. Mochizuki, A. Yamatodani, K. Okakura, A. Horii, N. Inagaki, and H. Wada. Circadian rhythm of histamine release from the hypothalamus of freely moving rats. *Physiology & behavior*, 51(2):391–394, 1992.

R. Mongeau, P. Blier, and C. De Montigny. The serotonergic and noradrenergic systems of the hippocampus: their interactions and the effects of antidepressant treatments. *Brain Research Reviews*, 23(3):145–195, 1997.

L. P. Morin, N. Goodless-Sanchez, L. Smale, and R. Y. Moore. Projections of the suprachiasmatic nuclei, subparaventricular zone and retrochiasmatic area in the golden hamster. *Neuroscience*, 61(2):391–410, 1994.

J. Morris. *Fisher's Face*. Faber & Faber, 2010.

R. G. Munn and D. K. Bilkey. The firing rate of hippocampal ca1 place cells is modulated with a circadian period. *Hippocampus*, 22(6):1325–37, 2012.

U. Musshoff and E. J. Speckmann. Diurnal actions of melatonin on epileptic activity in hippocampal slices of rats. *Life Sci*, 73(20):2603–10, 2003.

U. Musshoff, D. Riewenherm, E. Berger, J. D. Fauteck, and E. J. Speckmann. Melatonin receptors in rat hippocampus: molecular and functional investigations. *Hippocampus*, 12(2):165–73, 2002.

G. S. Nares. *Seamanship*. James Griffin and Co., 1868.

W. Nelson, Y. L. Tong, J. K. Lee, and F. Halberg. Methods for cosinor-rhythmometry. *Chronobiologia*, 6(4):305–23, 1979.

S. A. Neymotin, M. T. Lazarewicz, M. Sherif, D. Contreras, L. H. Finkel, and W. W. Lytton. Ketamine disrupts modulation of in a computer model of hippocampus. *J Neurosci*, 31(32):11733–43, 2011.

S. Ohdo. Chronotherapeutic strategy: rhythm monitoring, manipulation and disruption. *Advanced drug delivery reviews*, 62(9):859–875, 2010.

J. O'Keefe and M. L. Recce. Phase relationship between hippocampal place units and the eeg theta rhythm. *Hippocampus*, 3(3):317–330, 1993.

M. Ozcan, B. Yilmaz, and D. O. Carpenter. Effects of melatonin on synaptic transmission and long-term potentiation in two areas of mouse hippocampus. *Brain research*, 1111 (1):90–94, 2006.

P. Panula, U. Pirvola, S. Auvinen, and M. Airaksinen. Histamine-immunoreactive nerve fibers in the rat brain. *Neuroscience*, 28(3):585–610, 1989.

M. B. Parekh, P. R. Carney, H. Sepulveda, W. Norman, M. King, and T. H. Mareci. Early mr diffusion and relaxation changes in the parahippocampal gyrus precede the onset of spontaneous seizures in an animal model of chronic limbic epilepsy. *Exp Neurol*, 224(1):258–70, 2010.

D. A. Pasquier and F. Reinoso-Suarez. The topographic organization of hypothalamic and brain stem projections to the hippocampus. *Brain Research Bulletin*, 3(4): 373–389, 1978.

M. Penttonen and G. Buzsáki. Natural logarithmic relationship between brain oscillators. *Thalamus & Related Systems*, 2(2):145–152, 2003.

G. M. Peterson, L. R. Williams, S. Varon, and F. H. Gage. Loss of gabaergic neurons in medial septum after fimbria-fornix transection. *Neurosci Lett*, 76(2):140–4, 1987a.

G. M. Peterson, L. R. Williams, S. Varon, and F. H. Gage. Loss of gabaergic neurons in medial septum after fimbria-fornix transection. *Neuroscience letters*, 76(2):140–144, 1987b.

H. Petsche, C. Stumpf, and G. Gogolak. The significance of the rabbit's septum as a relay station between the midbrain and the hippocampus i. the control of hippocampus arousal activity by the septum cells. *Electroencephalography and clinical neurophysiology*, 14(2):202–211, 1962.

C. Peyron, D. K. Tighe, A. N. van den Pol, L. de Lecea, H. C. Heller, J. G. Sutcliffe, and T. S. Kilduff. Neurons containing hypocretin (orexin) project to multiple neuronal systems. *J Neurosci*, 18(23):9996–10015, 1998.

C. Pierpaoli, P. Jezzard, P. J. Basser, A. Barnett, and G. Di Chiro. Diffusion tensor mr imaging of the human brain. *Radiology*, 201(3):637–48, 1996.

C. Pierpaoli, A. Barnett, S. Pajevic, R. Chen, L. R. Penix, A. Virta, and P. Basser. Water diffusion changes in wallerian degeneration and their dependence on white matter architecture. *Neuroimage*, 13(6 Pt 1):1174–85, 2001.

L. Pinato, Z. Ferreira, R. Markus, and M. Nogueira. Bimodal daily variation in the serotonin content in the raphe nuclei of rats. *Biological Rhythm Research*, 35(3): 245–257, 2004.

M. Quigg. Circadian rhythms: interactions with seizures and epilepsy. *Epilepsy Res*, 42 (1):43–55, 2000.

M. Quigg and M. Straume. Dual epileptic foci in a single patient express distinct temporal patterns dependent on limbic versus nonlimbic brain location. *Annals of neurology*, 48(1):117–120, 2000.

M. Quigg, M. Straume, M. Menaker, and E. H. Bertam. Temporal distribution of partial seizures: comparison of an animal model with human partial epilepsy. *Annals of neurology*, 43(6):748–755, 1998.

M. Quigg, H. Clayburn, M. Straume, M. Menaker, and E. H. Bertram. Hypothalamic neuronal loss and altered circadian rhythm of temperature in a rat model of mesial temporal lobe epilepsy. *Epilepsia*, 40(12):1688–96, 1999.

M. Quigg, H. Clayburn, M. Straume, M. Menaker, and E. H. Bertram. Effects of circadian regulation and rest-activity state on spontaneous seizures in a rat model of limbic epilepsy. *Epilepsia*, 41(5):502–9, 2000.

M. Quigg, M. Straume, T. Smith, M. Menaker, and E. H. Bertram. Seizures induce phase shifts of rat circadian rhythms. *Brain Res*, 913(2):165–9, 2001.

R. J. Racine. Modification of seizure activity by electrical stimulation. ii. motor seizure. *Electroencephalogr Clin Neurophysiol*, 32(3):281–94, 1972.

A. V. Raghavan, J. M. Horowitz, and C. A. Fuller. Diurnal modulation of long-term potentiation in the hamster hippocampal slice. *Brain research*, 833(2):311–314, 1999.

W. Rall. Theory of physiological properties of dendrites. *Ann N Y Acad Sci*, 96:1071–92, 1962.

M. Raza, R. E. Blair, S. Sombati, D. S. Carter, L. S. Deshpande, and R. J. DeLorenzo. Evidence that injury-induced changes in hippocampal neuronal calcium dynamics during epileptogenesis cause acquired epilepsy. *Proceedings of the National Academy of Sciences of the United States of America*, 101(50):17522–17527, 2004.

E. H. Reynolds and J. V. K. Wilson. Psychoses of epilepsy in babylon: the oldest account of the disorder. *Epilepsia*, 49(9):1488–1490, 2008.

H. G. Richter, C. Torres-Farfan, P. P. Rojas-Garcia, C. Campino, F. Torrealba, and M. Seron-Ferre. The circadian timing system: making sense of day/night gene expression. *Biological Research*, pages 11–28, 2004.

A. J. Riggs and J. E. Riggs. Epilepsy's role in the historical differentiation of religion, magic, and science. *Epilepsia*, 46(3):452–453, 2005.

N. F. Ruby, C. E. Hwang, C. Wessells, F. Fernandez, P. Zhang, R. Sapolsky, and H. C. Heller. Hippocampal-dependent learning requires a functional circadian system. *Proc Natl Acad Sci U S A*, 105(40):15593–8, 2008.

J. C. Sanchez, T. H. Mareci, W. M. Norman, J. C. Principe, W. L. Ditto, and P. R. Carney. Evolving into epilepsy: Multiscale electrophysiological analysis and imaging in an animal model. *Exp Neurol*, 198(1):31–47, 2006.

C. B. Saper, T. E. Scammell, and J. Lu. Hypothalamic regulation of sleep and circadian rhythms. *Nature*, 437(7063):1257–63, 2005.

B. Scatton, H. Simon, M. Le Moal, and S. Bischoff. Origin of dopaminergic innervation of the rat hippocampal formation. *Neuroscience letters*, 18(2):125–131, 1980.

M. J. Schaaf, R. Duurland, E. R. de Kloet, and E. Vreugdenhil. Circadian variation in bdnf mrna expression in the rat hippocampus. *Molecular brain research*, 75(2): 342–344, 2000.

G. J. Schapel, R. G. Beran, D. L. Kennaway, J. McLoughney, and C. D. Matthews. Melatonin response in active epilepsy. *Epilepsia*, 36(1):75–8, 1995.

O. Selbach, N. Doreulee, C. Bohla, K. S. Eriksson, O. A. Sergeeva, W. Poelchen, R. E. Brown, and H. L. Haas. Orexins/hypocretins cause sharp wave- and theta-related

synaptic plasticity in the hippocampus via glutamatergic, gabaergic, noradrenergic, and cholinergic signaling. *Neuroscience*, 127(2):519–28, 2004.

L. P. Shearman, S. Sriram, D. R. Weaver, E. S. Maywood, I. Chaves, B. Zheng, K. Kume, C. C. Lee, G. T. van der Horst, M. H. Hastings, et al. Interacting molecular loops in the mammalian circadian clock. *Science Signaling*, 288(5468):1013, 2000.

M. N. Shouse, A. M. da Silva, and M. Sammaritano. Circadian rhythm, sleep, and epilepsy. *J Clin Neurophysiol*, 13(1):32–50, 1996.

R. S. Sloviter. The neurobiology of temporal lobe epilepsy: too much information, not enough knowledge. *C R Biol*, 328(2):143–53, 2005.

J. W. Smythe, L. V. Colom, and B. H. Bland. The extrinsic modulation of hippocampal theta depends on the coactivation of cholinergic and gaba-ergic medial septal inputs. *Neuroscience & Biobehavioral Reviews*, 16(3):289–308, 1992.

R. J. Staba, C. L. Wilson, A. Bragin, I. Fried, and J. Engel. Quantitative analysis of high-frequency oscillations (80–500 hz) recorded in human epileptic hippocampus and entorhinal cortex. *Journal of neurophysiology*, 88(4):1743–1752, 2002.

D. Stanley, P. Carney, M. Parekh, T. Mareci, S. Talathi, and W. Ditto. Phase shift in hippocampal circadian rhythm during the latent period of epileptic rats. *BMC Neuroscience*, 12(Suppl 1):P76, 2011a.

D. Stanley, S. Talathi, X. Ni, L. Huang, Y. Lai, W. Ditto, and P. Carney. Circadian rhythms of gamma oscillations following status epilepticus: Implications for cognition. *American Epilepsy Society*, 2011b.

D. Stanley, M. Parekh, S. Talathi, W. Ditto, T. Mareci, and P. Carney. Magnet resonance diffusion changes in the hypothalamus and medial septum accompany epileptogenic phase shift in hippocampal circadian rhythms. In *SLEEP*, volume 35, pages A210–A210. Amer Acad Sleep Medicine One Westbrook Corporate Ctr, STE 920, Westchester, IL 60154 USA, 2012.

D. A. Stanley, S. S. Talathi, M. B. Parekh, D. J. Cordiner, J. Zhou, T. H. Mareci, W. L. Ditto, and P. R. Carney. Phase shift in the 24-hour rhythm of hippocampal eeg spiking activity in a rat model of temporal lobe epilepsy. *Journal of neurophysiology*, 2013.

L. S. Stewart and L. S. Leung. Temporal lobe seizures alter the amplitude and timing of rat behavioral rhythms. *Epilepsy Behav*, 4(2):153–60, 2003.

K.-F. Storch, O. Lipan, I. Leykin, N. Viswanathan, F. C. Davis, W. H. Wong, and C. J. Weitz. Extensive and divergent circadian gene expression in liver and heart. *Nature*, 417(6884):78–83, 2002.

A. Strzelczyk, J. P. Reese, R. Dodel, and H. M. Hamer. Cost of epilepsy. *Pharmacoeconomics*, 26(6):463–476, 2008.

S. S. Suzuki and G. K. Smith. Spontaneous eeg spikes in the normal hippocampus. i. behavioral correlates, laminar profiles and bilateral synchrony. *Electroencephalogr Clin Neurophysiol*, 67(4):348–59, 1987.

S. S. Suzuki and G. K. Smith. Spontaneous eeg spikes in the normal hippocampus. iv. effects of medial septum and entorhinal cortex lesions. *Electroencephalogr Clin Neurophysiol*, 70(1):73–83, 1988a.

S. S. Suzuki and G. K. Smith. Spontaneous eeg spikes in the normal hippocampus. v. effects of ether, urethane, pentobarbital, atropine, diazepam and bicuculline. *Electroencephalogr Clin Neurophysiol*, 70(1):84–95, 1988b.

S. S. Talathi, D. U. Hwang, M. L. Spano, J. Simonotto, M. D. Furman, S. M. Myers, J. T. Winters, W. L. Ditto, and P. R. Carney. Non-parametric early seizure detection in an animal model of temporal lobe epilepsy. *J Neural Eng*, 5(1):85–98, 2008.

S. S. Talathi, D. U. Hwang, W. L. Ditto, T. Mareci, H. Sepulveda, M. Spano, and P. R. Carney. Circadian control of neural excitability in an animal model of temporal lobe epilepsy. *Neurosci Lett*, 455(2):145–9, 2009.

J. Taxidis, S. Coombes, R. Mason, and M. R. Owen. Modeling sharp wave-ripple complexes through a ca3-ca1 network model with chemical synapses. *Hippocampus*, 22(5):995–1017, 2012.

R. Traub and R. Miles. *Neuronal networks of the hippocampus*. Cambridge University Press, Cambridge, MA, 1991.

R. Traub, J. Jefferys, and M. Whittington. *Fast Oscillations in Cortical Circuits*. The MIT Press, Cambridge, MA, 1999a.

R. D. Traub, R. K. Wong, R. Miles, and H. Michelson. A model of a ca3 hippocampal pyramidal neuron incorporating voltage-clamp data on intrinsic conductances. *J Neurophysiol*, 66(2):635–50, 1991.

R. D. Traub, M. A. Whittington, S. B. Colling, G. Buzsaki, and J. G. Jefferys. Analysis of gamma rhythms in the rat hippocampus in vitro and in vivo. *J Physiol*, 493 (Pt 2): 471–84, 1996.

R. D. Traub, M. A. Whittington, E. H. Buhl, J. G. Jefferys, and H. J. Faulkner. On the mechanism of the γ β frequency shift in neuronal oscillations induced in rat hippocampal slices by tetanic stimulation. *The Journal of neuroscience*, 19(3): 1088–1105, 1999b.

W. Truccolo, U. T. Eden, M. R. Fellows, J. P. Donoghue, and E. N. Brown. A point process framework for relating neural spiking activity to spiking history, neural ensemble, and extrinsic covariate effects. *Journal of neurophysiology*, 93(2): 1074–1089, 2005.

P. Valnegri, M. Khelfaoui, O. Dorseuil, S. Bassani, C. Lagneaux, A. Gianfelice, R. Benfante, J. Chelly, P. Billuart, C. Sala, et al. A circadian clock in hippocampus is regulated by interaction between oligophrenin-1 and rev-erb [alpha]. *Nature neuroscience*, 14(10):1293–1301, 2011.

G. Vandewalle, C. Schmidt, G. Albouy, V. Sterpenich, A. Darsaud, G. Rauchs, P.-Y. Berken, E. Balteau, C. Degueldre, A. Luxen, et al. Brain responses to violet, blue, and green monochromatic light exposures in humans: prominent role of blue light and the brainstem. *PLoS One*, 2(11):e1247, 2007.

R. Vertes, L. Colom, W. Fortin, and B. Bland. Brainstem sites for the carbachol elicitation of the hippocampal theta rhythm in the rat. *Experimental brain research*, 96(3): 419–429, 1993.

Q. Wan, H. Y. Man, F. Liu, J. Braunton, H. B. Niznik, S. F. Pang, G. M. Brown, and Y. T. Wang. Differential modulation of gabaa receptor function by mel1a and mel1b receptors. *Nat Neurosci*, 2(5):401–3, 1999.

L. M. Wang, J. M. Dragich, T. Kudo, I. H. Odom, D. K. Welsh, T. J. O'Dell, and C. S. Colwell. Expression of the circadian clock gene period2 in the hippocampus: possible implications for synaptic plasticity and learned behaviour. *ASN neuro*, 1(3), 2009.

X. J. Wang. Pacemaker neurons for the theta rhythm and their synchronization in the septohippocampal reciprocal loop. *J Neurophysiol*, 87(2):889–900, 2002.

X. J. Wang and G. Buzsaki. Gamma oscillation by synaptic inhibition in a hippocampal interneuronal network model. *J Neurosci*, 16(20):6402–13, 1996.

M. O. West and S. A. Deadwyler. Circadian modulation of granule cell response to perforant path synaptic input in the rat. *Neuroscience*, 5(9):1597–602, 1980.

M. Whittington, R. Traub, N. Kopell, B. Ermentrout, and E. Buhl. Inhibition-based rhythms: experimental and mathematical observations on network dynamics. *International Journal of Psychophysiology*, 38(3):315–336, 2000.

M. A. Whittington, R. D. Traub, H. J. Faulkner, I. M. Stanford, and J. G. Jefferys. Recurrent excitatory postsynaptic potentials induced by synchronized fast cortical oscillations. *Proceedings of the National Academy of Sciences*, 94(22):12198–12203, 1997.

S. Wiebe. Epidemiology of temporal lobe epilepsy. *The Canadian Journal of Neurological Sciences*, 27(1), 2000.

J. Wilson and E. Reynolds. Texts and documents. translation and analysis of a cuneiform text forming part of a babylonian treatise on epilepsy. *Medical history*, 34(2):185, 1990.

K. Wulff, S. Gatti, J. G. Wettstein, and R. G. Foster. Sleep and circadian rhythm disruption in psychiatric and neurodegenerative disease. *Nat Rev Neurosci*, 11(8): 589–99, 2010.

S. Yamazaki, M. C. Kerbeshian, C. G. Hocker, G. D. Block, and M. Menaker. Rhythmic properties of the hamster suprachiasmatic nucleus in vivo. *J Neurosci*, 18(24): 10709–23, 1998.

Y. Yanovsky and H. L. Haas. Histamine increases the bursting activity of pyramidal cells in the ca3 region of mouse hippocampus. *Neurosci Lett*, 240(2):110–2, 1998.

P. Zatta. *Metal Ions and Neurodegnerative Disorders*. World Scientific, London, UK, 2003.

BIOGRAPHICAL SKETCH

Originally from Toronto, Canada, David is the son of Janet and Leonard Stanley and has one younger brother, Geoffrey. David attended Dr. John M. Dension High School and pursued his undergraduate degree in Engineering Science at the University of Toronto. In his third year, he specialized in the physics option, and focused his bachelor's thesis on quantum dot solar cells under the supervision of Dr. Nazir P. Kherani. David graduated with honours in 2007. He then moved into the field of computational neuroscience, joining the group of Dr. Berj L. Bardakjian at the University of Toronto, and worked on characterizing mechanisms underlying synaptic noise. David completed his MASc in Electrical Engineering in 2009.

Moving to Arizona and joining the new lab of Dr. William L. Ditto, David began studying the relationship between circadian rhythms and epilepsy in 2009. He transferred from Arizona State University to the University of Florida in 2011, where he completed his doctoral research under the guidance of Dr. Paul R. Carney and Dr. Sachin S. Talathi. He received his Ph.D. from the University of Florida in the summer of 2013. Following graduation, David plans to pursue postdoctoral studies and also to continue to collaborate with his former advisors on projects related to neuronal noise, circadian rhythms and, hopefully, synthetic biology.